

EPSRC

Engineering and Physical Sciences
Research Council



University Defence Research Collaboration (UDRC)

**Engineering and Physical Sciences Research Council
& Defence Science Technology Laboratory**

**Loughborough, Surrey, Strathclyde and Cardiff (LSSC)
Consortium**

**“Signal Processing Solutions for the
Networked Battlespace”**

**Second Year Progress Report
March 2015**

Director: Professor Jonathon Chambers FEng

Deputy Director: Professor John Soraghan



Contents

Highlights for Year II	p 3
Executive Summary	pp 4-6
Acknowledgements	p 6
L-WP1 Anomaly Detection	pp 7-33
L-WP2 Handling Uncertainty & Domain Knowledge	pp 34-73
L-WP3 Source Separation & Broadband Beamforming	pp 74-92
L-WP4 MIMO and Distributed Sensing	pp 93-115
L-WP5 Efficient Implementation	pp 116-133

Highlights for Year II

- The LSSC consortium including approximately 30 academic and research staff, working in partnership with Dstl and EPSRC, is continuing to operate successfully with active engagement with Atlas Elektronik (new industrial supporter joining LSSC consortium in 2014), Mathworks, Prismtech, QinetiQ, Selex-ES, Thales, and TI.
- World-class training in algorithmic signal and information processing is being provided to the affiliated PhD students; a Dstl-DGA supported PhD student will join the Dstl Graduate Development Programme in 2015; and RAs are working closely with staff from our industrial supporters.
- Academic, research staff and PhD students are regularly working across universities and with staff from the Edinburgh-Heriot Watt consortium, and staff from other universities to grow the community of practice in the UK.
- New funding has been secured as a result of UDRC II: MarCE "Array processing exploiting sparsity for submarine hull mounted arrays" with Atlas Elektronik; CDE "Ballistic missile recognition based on micro-doppler" with BAE Systems; EPSRC "Massive MIMO wireless networks: Theory and methods" with King's College and University College London.
- New solutions have been generated for anomaly detection in shipping lanes; intrusion detection in network communications; video segmentation; model-based target tracking incorporating domain knowledge; network radar resource allocation exploiting game theory; multichannel spectral factorization; underwater acoustic data denoising exploiting sparsity; and foliage penetrating CFAR detection.
- We have launched and translated to academia and industry the first Matlab toolbox for Polynomial EigenVector Decompositions (PEVDs), downloadable via the Mathworks Link Exchange.
- Top journal outputs have been generated together with presentations at leading international conferences.

Executive Summary [March 2013]

The future battlespace will be a complex environment characterised by known and unknown threats, modern and legacy sensor systems, a congested RF spectrum, and mobile and static forces. However, it is envisioned that UK forces will have a suite of networked sensor systems available to them. This suite of sensors will be a heterogeneous mix of modern and legacy systems including a small number of highly capable but expensive systems and a larger number of less expensive but less capable systems. In addition there will be a certain amount of processing power heterogeneously distributed amongst the various sensor systems.

Within this environment, there will be a need to:

- maximize the amount of information on enemy activity by the use of the most appropriate sensors;
- transport this information to the people who need to have it;
- take due notice of the amount of communications bandwidth available;
- cope with the possibility of a high density of signals;
- cope with novel signals that are hard to detect or classify;
- reduce the work load of the operators and interact with coalition forces;
- be adaptable to cope with signals as yet unknown;
- be able to execute all the operations in the shortest possible time;

To address these requirements the following **ten research themes** were identified by the EPSRC and Dstl in the call for the UDRC consortia:

T1: Weak signal detection in high volume of clutter; T2: Signal processing in high dimension feature space; T3: Signal processing in high uncertainty; T4: Signal processing for sparse or fleeting signals; T5: Signal processing to support sparse sampling of highly non-stationary signals; T6: Extraction/separation of multiple overlapping/interwoven signals; T7: Statistical anomaly detection; T8: Distributed/decentralised signal processing; T9: Algorithms to support dramatic reduction in computation; T10: Accreditable machine learning or data-driven techniques.

The LSSC consortium therefore carefully designed a coherent programme of work on the basis of five strongly ***interlinked work packages (WPs)***, each supported by a lead industrial partner(s) from amongst: the Mathworks, Prismtech, QinetiQ, Selex-Ex, Texas Instruments, and Thales; *which in 2014 have been joined by Atlas Elektronik*; and this report details the progress in these WPs in the second year between 1st April 2014 and 31st March 2015. Our consortium comprises four internationally recognised academic-based signal processing groups and provides unique capability from across the UK in the field of signal processing; particularly in *mathematically rigorous methods for statistical anomaly detection and classification in high dimensions (AD), handling uncertainty and incorporating domain knowledge*

(HU), signal separation including beamforming and compressive sensing/sparsity (SS), MIMO and distributed sensing (MDS) and their efficient implementation (EI).

The following **connectivity matrix** therefore maps our consortium’s five primary expertise areas to the ten themes:-

Theme:	[T1]	[T2]	[T3]	[T4]	[T5]	[T6]	[T7]	[T8]	[T9]	[T10]
AD	X	X					X		X	X
HU			X		X				X	
SS	X	X		X	X	X		X	X	
MDS	X		X		X			X	X	
EI	X	X	X	X	X	X	X	X	X	X

Note: Light grey crosses emphasize that research in efficient implementation and supporting dramatic reduction in computational complexity is interwoven with all other planned technical activities.

Technical Challenges: Our activity moreover impacts upon the following technical challenges provided by Dstl, on the basis of the short descriptions provided on the UDRC website as at 25th June 2012:-

Linkage Matrix Showing Work Package to Dstl Technical Challenge Mapping

CH G	1	2	3	4	5	6	7	8	9	10	11	12	13	14	15	16	17	18	19	20	21	22	23	24	25	26	27	28	29	30	31	32	33	34	35	36	37	38			
AD		X	X	X						X				X	X		X	X	X	X						X			X	X		X	X		X	X					
HU	X	X	X			X				X	X			X		X														X		X	X						X		
SS	X						X	X				X	X	X	X														X	X	X	X							X		
MDS	X				X				X								X														X										
EI	X	X	X	X	X	X	X		X	X	X		X	X	X	X	X	X	X	X							X	X		X	X	X	X						X	X	X

Operational Update for UDRC II - LSSC Consortium

In summary, over the second year the eight postdoctoral RAs have continued their activity (Mark Barnard replaced Swati Chanda as one of the RAs at Surrey) and the affiliated PhD students have continued their studies. Overall **technical leadership and management** has been overseen by the Director and Deputy Director of the LSSC consortium. Three-monthly consortium management team (CMT) and consortium steering group (CSG) meetings have been held at all the four university sites following the same cycle as in the first year. The Director has also presented at the UDRC governance meetings held at Porton Down and contributed to the UDRC management meetings. Regular reporting (two weekly (RAs) and four weekly (PhD students)) of technical progress has been a particularly useful tool for keeping the consortium together and all such reports have been shared amongst the consortium and archived. The consortium has enjoyed the input of independent experts as part of the CSG and provided three-monthly written progress reports to Dstl. The consortium has also contributed to the summer school which will be repeated in 2015 and held at Surrey; the KTM, theme meetings and Dstl challenges.

The five work packages are each led by two senior academics and supported by a lead and other industrial supporters. An important achievement during the second year has been to increase the engagement of the industrial supporters, which was reinforced by their involvement in technical presentations at the CSG meeting in Loughborough in October 2014, and the EPOCs within Dstl – we acknowledge the hard work of staff at Dstl, particularly Paul Thomas, in facilitating their interaction – which will increase our awareness of technical campaigns.

The following five reports are structured in a common style: listing staff involved; original targets; progress and achievements; further technical detail; future work for year three, together with references and outputs.

In conclusion, we believe that despite the diversity of locations of our academic and industrial partners across the UK the LSSC consortium is clearly contributing to the goals of the UDRC and providing new signal processing solutions for the networked battlespace. We look forward to the third year.

Acknowledgements

All members of the LSSC consortium wish to express their considerable thanks to Professor Andrew Baird, Paul Thomas, Bob Elsley (now retired) and Ros Knowles Dstl and Dr Matthew Lodge EPSRC for their considerable help over the second year in operating the LSSC Consortium as part of the UDRC.

L_WP1 (AD) Automated Statistical Anomaly Detection and Classification in High Dimensions for the Networked Battlespace

1.1 Staffing

Work Package Leaders: Prof Josef Kittler (SU), Prof David Parish (LU) and Dr Yulia Hicks (CU)
Other Academics: Prof Jonathon Chambers (LU)
Research Associates: Dr Cemre Zor (SU), Dr Francisco Aparicio-Navarro (LU), Dr Ioannis Kaloskampis (CU)
Affiliated Research Stud. Pengming Feng (LU), Mr. Mahmud Abdulla Mohammad(CU)
Lead Project Partner: Mr Angus Johnson (Thales)
Other Project Partners: Mr John Griffin and Mr George Matich (Selex-ES)
Dstl contacts: Drs Gavin Pearson and Jacob Suresh, Mr. Alasdair Hunter, Mr. Jonathan Crew

1.2 Aims and Introduction

Work Package 1 (L_WP1) is concerned with the development of algorithms for automatic detection of anomalies from multidimensional, under-sampled, non-complete datasets and unreliable sources. The aim is to advance the state of the art in anomaly detection by developing anomaly detection methodology that is not only effective and computationally efficient, but can also provide insight into the nature and statistical characteristics of the detected anomalies.

The fundamental philosophy is to model normality, i.e. “normal” behaviour and “normal” data characteristics in order to provide an acceptable balance between false positive / negative detections. To ensure the models of normality are not corrupted by unreliable and ambiguous data, data quality and ambiguity measures are to be taken into account.

1.3 Data

Currently we have access to the following data sets:

- Surveillance video data (CU)
- Portsmouth harbour shipping data (Thales)
- Thermal imaging data (UDRC)
- Tank and helicopter data (DSTL)
- IEEE 802.11 network traffic dataset (LU)
- Netflow measurements from a virtual network testbed (LU)

1.4 Outline of the Research Approach

Anomaly detection is classically formulated as an outlier detection problem in statistical hypothesis testing. Our thesis is that anomaly detection in complex

systems should involve additional mechanisms that would enhance the efficiency of anomaly detection, but most importantly, allow various types of anomaly and their nuances to be identified and distinguished.

A schematic diagram of the proposed overall anomaly detection system is shown in Figure 1.1. The system is adjunct to the main operational system, which in our example is a machine perception system interpreting input sensor data in a hierarchical manner by engaging non-contextual and contextual labelling processes. (For other scenarios, such as multimodal experts, the operational system would have to be suitably adapted.) The sensor data to be interpreted first feeds into a discriminative object / primitive classification system. The output of the non-contextual decision making system is then channelled to a contextual classifier.

In a conventional approach, both non-contextual and contextual decision making systems would have associated outlier detectors, and any outlier would signal anomaly. In the proposed architecture there are additional mechanisms to gain more detailed information about the nature of anomaly. First of all, there is a classifier incongruence detector, which compares the outputs of the two decision-making systems. In normal circumstances the classifiers should mutually reinforce each other. Any incongruence between the classifier outputs could be indicative of some sort of anomaly and therefore its detection is very important. It is also important to recognise that the notion of normality applies only to scenarios where sensor data quality is comparable. Thus another important mechanism is data quality assessment, which for sensor data of degraded quality would switch off the anomaly detection system. Other important mechanisms are decision confidence gauging to avoid anomaly flagging in ambiguous situations and long term statistical data analysis and monitoring to detect model drift.

Thus, we propose a comprehensive methodology for anomaly detection, which builds on the above mechanisms and jointly reasons about the findings of the respective data analysis tools. The methodological advances in anomaly detection offered by the proposed anomaly detection system architecture will be validated on diverse applications. An example includes network anomaly detection with the aim to increase the efficiency of flagging network intrusion. Another domain is anomaly detection in surveillance videos with the objective of developing an accurate, data-driven methodology which is computationally efficient and can incorporate domain knowledge.

L_WP1 has two strands as given in Table 1.1.

1.1-1 Baseline system	1.2.-1 Contextual model inference
1.1-2 Radar SAM mode	1.2-2 Data quality modelling
1.1-3 Discriminative AD	1.2-3 Incongruence detection
1.1-4 Fusion of ADs	1.2-4 System integration
1.1-5 Advanced AD system	1.2-5 Communications network AD

Table 1.1 Two strands of L_WP1

L_WP1 relates to the other work packages in terms of the following issues:

- L_WP2: Usage of mechanisms to reduce uncertainty. Input to approaches dealing with large volumes of data or data loss.
- L_WP3: Application to non-IP, i.e. non-“Cyber” signals.
- L_WP4: Information / Data Fusion approaches.
- L_WP5: User of viable implementation strategies. Provider of exemplar algorithms for evaluation.

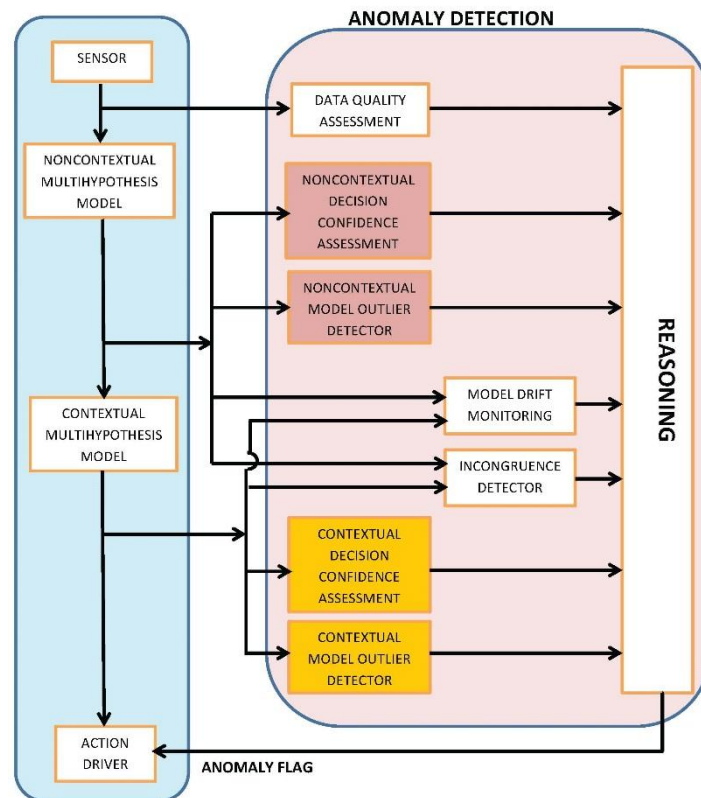


Figure 1.1 Domain Anomaly Detection System Architecture.

1.5 Overview of the Technical Progress in Year 1

The work in year 1 was concentrated on Task 1.2-3 concerned with incongruence detection and on the development of baseline systems for two applications of anomaly detection (on network and video) as part of Task 1.1-1. A summary of the contributions can be given as follows:

- A novel anomaly detection system architecture has been proposed which includes several distinct mechanisms to detect anomalous events and facilitates their characterisation. In addition to the conventional distribution outlier detection, the mechanisms include classifier incongruence detection, data quality assessment, classifier confidence gauging, model-drift detection. The outputs of these processes feed into a reasoning engine, which draws conclusions about the presence of anomaly and its nature. The details of the detection system architecture have been presented in (Kittler, et al., 2013).
- Incongruence detection as part of the novel anomaly system architecture has been investigated in detail and a novel surprise measure has been proposed. A theoretical analysis including error sensitivity of the proposed measure has been carried out for a variety of scenarios.

- As for network anomaly detection application, the focus was on developing methods to increase the efficiency of an anomaly based IDS. The initial effort to tackle the objectives of this project concentrated on the 'Data Quality Assessment'. We developed a novel approach to automatically generate labelled network traffic datasets. This approach was able to correctly label 100% of the selected instances. Work was also undertaken to automatically select a set of metrics. The resulting labelled datasets were used by a genetic algorithm based approach as part of the feature selection process for metric selection.
- A system for anomaly detection in video was developed. The core of the system is a spatial video segmentation algorithm which is based on evolving mixture models; its aim is to divide each video frame into meaningful area segments. The main contribution was an online video segmentation algorithm, which allows for consistent segmentation of consecutive video frames using an evolving mixture model. Efficient handling of computer memory and storage and automatic adjustment of the model's parameters to cater for abrupt changes between consecutive frames are the main features of the method. Our findings were presented in (Kaloskampis & Hicks, Estimating adaptive coefficients of evolving GMMs for online video segmentation, 2014).

1.6 Technical Progress in Year 2

Overview

Within the second year of the project, incongruence detection analysis, as part of Task 1.2-3, have been further developed and following the inputs from the first year, the two applications of "network anomaly detection" and "anomaly detection in video" have been improved to fulfil Tasks 1.1-1 and 1.2-2. As another application, "anomaly detection in ship behaviour in the Portsmouth area" has also been addressed and initial results have been obtained. A list of progress for the second year is given below.

- Thorough experimental analysis of the proposed incongruence measure, Δ_{avg} , has been carried out by addressing the practical issues such as the lack of knowledge about the characteristic of the underlying scenarios, e.g. label agreement, or disagreement. The marginalisation over different scenarios has been achieved by aggregating the corresponding distributions and taking their prior probability of occurrence into account, followed by integrating over all noise-free surprise values below a certain threshold. As a result the theoretical and experimental analyses, guidelines on determining an appropriate threshold for incongruence detection has been proposed.
- A new application area, anomaly detection in ship behaviour in the Portsmouth area, has been studied. Methodology has been developed for modelling shipping lanes and for detecting potential anomalies in ship behaviour exhibited in the main shipping lanes. The anomaly detection methodology is based on measuring incongruence between two detectors:

detector of ship spatial location vis-a-vis shipping lane models, and a direction of sailing detector.

- As for the network anomaly detection, the main contribution on year two has been on incorporating contextual information, user's cognitive information, and Situational Awareness (SA) into the intrusion detection process to increase the efficiency of an anomaly based Intrusion Detection System (IDS). SA involves being aware of what is happening in a particular environment and determining how new information, events and actions will impact the situation in the near future (Jones, et al., 2011). In our research, this environment refers to the networked battlespace.

According to (Kokar & Endlsey, 2012), agents need to collect information about the network from different sources, make decisions based on the current knowledge and the collected information, act according to these decisions, collect feedback from the network in response to the actions, and update the current knowledge to make better decisions. Current IDSs consider only measurable network traffic information from the protected system or signatures of known attacks during the intrusion detection process. These systems do not take into account any available high-level information (i.e. above the network operation) about the protected system such as contextual information to improve their effectiveness (Sadighian, Zargar, Fernandez, & Lemay, 2013). It is accepted by many researchers that further improvement in statistically based IDSs requires some consideration of the context or situation in which the detection is being made. This infers that some aspect of the more general environment in which the system operates is incorporated into the anomaly decision process at some point.

The problem faced is how to represent this information and then how to incorporate it into the intrusion decision process. In a similar manner to (Howard & Kanareykin, 2012), we advocate the incorporation of human cognition as part of the detection process. Incorporating this high-level information into the security systems can improve their detection effectiveness. The approach that has been considered by employing a Fuzzy Cognitive Map (FCM) (Stylios & Groumpos, 2004). An FCM provides a useful framework for network users to contribute with their knowledge, to model new and unseen situation behaviours, and to calculate the influence that each action may have in the system and in other actions.

- For the anomaly detection applications for video, the video segmentation algorithm which we proposed in the first year (Kaloskampis & Hicks, Estimating adaptive coefficients of evolving GMMs for online video segmentation, 2014) was further developed in the second year to cater for coherence in video segmentation. Moreover, having observed that there are no established criteria for evaluation of overall video segmentation (as opposed to image segmentation or video object segmentation) we proposed a set of suitable criteria and a new method for evaluating the quality of video segmentation.

Furthermore, we used our video segmentation algorithm to incorporate domain knowledge in our anomaly detection framework. Towards this effort we developed a framework which classifies road types by applying video segmentation on a video and then compare the detected segments to those usually found in certain types of roads.

One of our research goals for the second year was to combine the low-level statistical models of video features learned from our method with high-level event models (e.g. hierarchical graphical models) for the purpose of analysing complex behaviour in video. Towards this effort we developed a system for activity recognition and anomaly detection in multimedia streams featuring complex human activities. The system models human activities as temporal sequences of their constituent actions and can handle actions that occur concurrently in multiple parallel streams.

Finally, we investigated the applicability of our algorithm to several defence-related datasets, including video streams from UAVs (in collaboration with LU) and the helicopter dataset provided by Dstl.

Technical Details

Anomaly Detection Mechanisms (L_WP1.2-3)

In the second year of the project, the theoretical analysis research, which previously was focused on the incongruence detection, has further been extended and experimental analysis has been broadened.

We have previously proposed the surprise measure Δ_{avg} to be used in incongruence detection such that

$$\Delta_{\text{avg}} = \frac{1}{4} \{ |P(\mu|x) - \tilde{P}(\mu|x) + \eta_{\mu}(x) - \tilde{\eta}_{\mu}(x)| + \delta(\mu, \tilde{\mu}) | \tilde{P}(\tilde{\mu}|x) - \tilde{P}(\mu|x) + \tilde{\eta}_{\tilde{\mu}}(x) - \tilde{\eta}_{\mu}(x) | \\ + | \tilde{P}(\tilde{\mu}|x) - P(\tilde{\mu}|x) + \tilde{\eta}_{\tilde{\mu}}(x) - \eta_{\tilde{\mu}}(x) | \\ + \delta(\mu, \tilde{\mu}) | P(\mu|x) - P(\tilde{\mu}|x) + \eta_{\mu}(x) - \eta_{\tilde{\mu}}(x) | \}$$

where $\tilde{\mu} = \arg \max_{\omega} \tilde{P}(\omega|x)$ and $\mu = \arg \max_{\omega} P(\omega|x)$, i.e. the dominant hypotheses flagged by the two experts; and $\tilde{\eta}_{\omega}$ and η_{ω} are the noise terms associated with the two experts for class ω . The delta function (δ) is defined as equal to 0 if $\tilde{\mu} = \mu$ and 1 otherwise.

The experimental analysis reported in the first year was based on a variety of surprise measure probability distributions obtained for fixed input noise-free surprise values, sampled by our experimental procedure.

The distributions were acquired for the individual scenarios of classifier label agreement and disagreement, for fixed values of noise-free Δ_{avg} (Note that we will denote surprise measure distributions acquired from the corrupted P and \tilde{P} as $\tilde{\Delta}_{avg}$).

However, as we will not know the characteristics of the underlying scenarios in practice, it is more appropriate to integrate over the various distributions by taking their prior probability of occurrence into account. This is in order to produce a plot of the area under the tail of the Δ_{avg} distribution as a function of threshold, for different scenarios of classifier label agreement and disagreement.

Hence, in the initial set of new experiments, the average size of the upper tail area (% over the total area) is accumulated for a given threshold point by taking the likelihood of the distributions into consideration. In Figure 1.2 and Figure 1.3, the resulting graphs depicting upper tail area (%) versus threshold is given for three and six class problems, using noise distribution with standard deviation $\sigma = 0.05$. The graphs in the first column correspond to the case of label agreement, whereas the second column applies to disagreement. The results for different fixed noise-free surprise values are shown using different line types.

It is shown comparing Figure 1.2-a and Figure 1.3-a that for any fixed surprise threshold, the upper tail area size is greater for 3 class problems ($m = 3$) compared to 6 classes ($m = 6$) in the label agreement case.

For the case of label disagreement, let us analyse, for instance, the scenario in which noise-free $\Delta_{avg} = 0.5$ by comparing Figure 1.2-b and Figure 1.3-b. Previously, it was shown that the spread of the surprise distribution towards both ends of the $[0,1]$ range is greater for $m = 3$ than for $m = 6$. This characteristic is also reflected in the respective area under the tail curves. For example, for $\tilde{\Delta}_{avg} = 0.6$, the upper tail area is just under 0.1 for $m = 3$, whereas it is almost zero for $m = 6$.

In Figure 1.2-a and Figure 1.3-a, a threshold around 0.6 can be observed to cover more than 90% of the lower tail areas for the label agreement cases. This means that almost all scenarios, which incorporate classifier agreement in the most probable hypothesis, will be perceived as congruence. Looking at Figure 1.2-b and Figure 1.3-b to analyse the case of label disagreement, using 0.6 as a threshold can be seen to result in labelling the scenarios with noise-free $\Delta_{avg} = 0.7$ as incongruence, and scenarios with $\Delta_{avg} = 0.2$ as congruence with 90% confidence. Note that for systems requiring low false positives, it might be necessary to use a lower threshold.

In our second set of experiments, we further integrated over various scenarios, by aggregating over all noise-free surprise values below a certain threshold (in our case set to 0.4) for congruence, and above this threshold for incongruence. This process has the advantage of taking the prior distributions of noise-free values into account and marginalising over the scenarios of label agreement/disagreement.

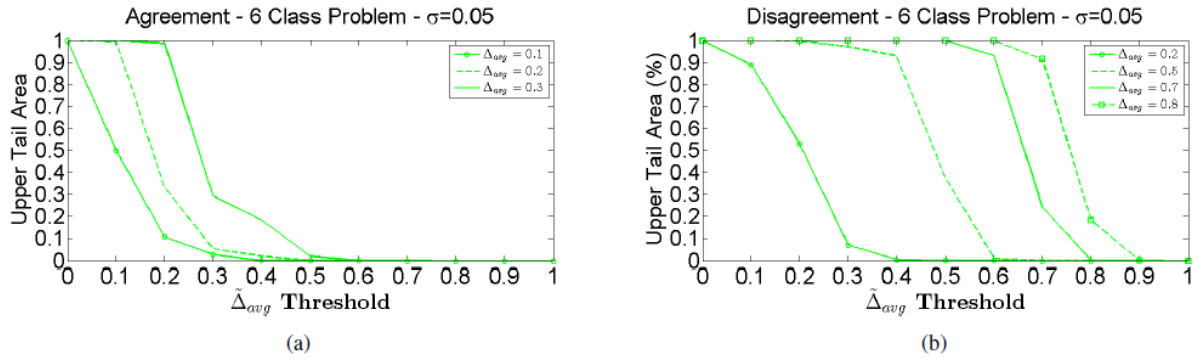


Figure 1.2 Upper tail area size versus $\tilde{\Delta}_{avg}$ threshold for different noise levels and different noise-free Δ_{avg} . Given for three class problems under the scenarios of classifier label agreement (a), and disagreement (b).

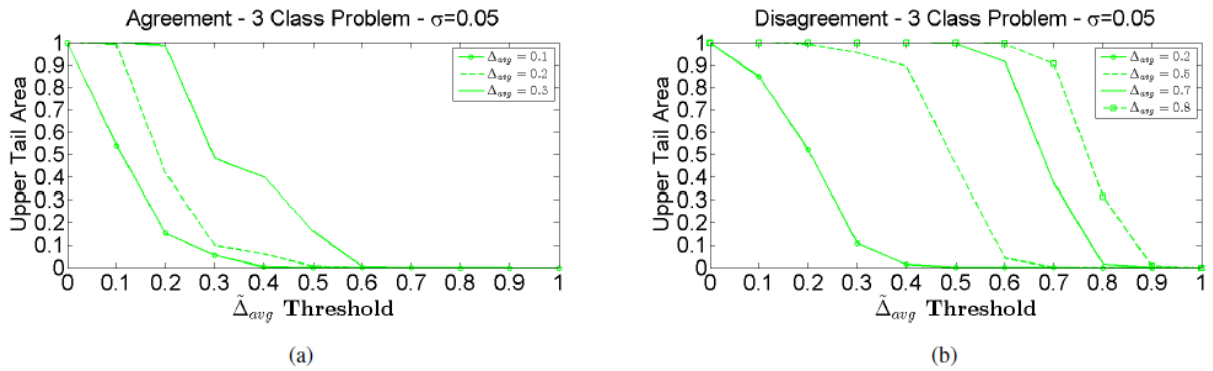


Figure 1.3 Upper tail area size versus $\tilde{\Delta}_{avg}$ threshold for different noise levels and different noise-free Δ_{avg} . Given for six class problems under the scenarios of classifier label agreement (a), and disagreement (b).

The results are shown in Figure 1.4. Figure 1.4-a indicates the confidence in the decision to accept the hypothesis that the two classifiers are congruent as a function of $\tilde{\Delta}_{avg}$. It can be observed that, for instance, a threshold of 0.4 on the proposed measure would capture both classifier congruence cases at 90% confidence. Setting the threshold to 0.6 would raise the confidence level to 100%. However, the plot in Figure 1.4-b clearly indicates that setting the threshold to yield high confidence levels for detecting classifier congruence will lead to unacceptable level of false positives, i.e. declaring incongruent classifier outputs as congruent. Thus choosing a suitable classifier incongruence detection threshold is a question of trade-off between low false positives and low false negatives.

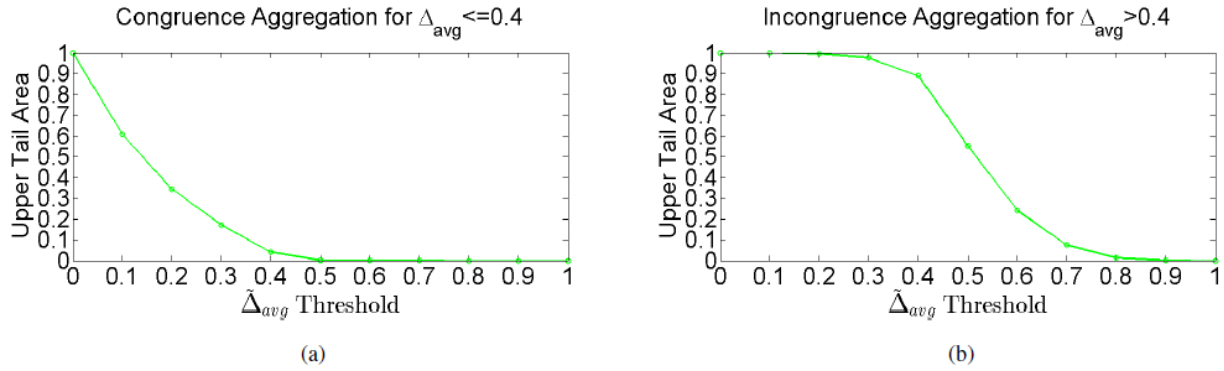


Figure 1.4 Aggregate upper tail area versus $\tilde{\Delta}_{avg}$ for $\sigma = 0.05$. Aggregated over $\Delta_{avg} \leq 0.4$ for congruence (a) and $\Delta_{avg} > 0.4$ for incongruence (b).

It is important to bear in mind that in practical applications we will not normally be able to generate the area under the tail curves for incongruence cases. The threshold selection will have to be based on such curves for classifier congruence cases only. Based on the theoretical and experimental findings, a set of practical guidelines have been developed for selecting classifier incongruence threshold in practice. These involve the following steps:

- 1) Using an anomaly-free training set of sensor data, the a posteriori probabilities, which are computed by the classifiers for various hypotheses as part of the data interpretation process, are recorded.
- 2) The adopted incongruence measure values are computed from the probabilities obtained in Step 1, and their distribution estimated.
- 3) The area under the tail of the distribution determined in Step 2 as a function of threshold on the test statistic is computed.
- 4) Using the plot derived in Step 3, a classifier incongruence hypothesis testing threshold is selected for a specified confidence level.
- 5) The incongruence testing method defined in Step 4 is evaluated for false positive and false negatives using respectively an anomaly free validation set, and a validation set with synthetically injected incongruences.

1.7 Applications

Anomaly Detection in Ship Behaviour in the Portsmouth Area

As another application of anomaly detection as part of Task 1.1-1, anomaly in ship behaviour has been studied on the data around the Portsmouth area, provided by Thales. The data consists of spatial and temporal information of the ships within the area of interest together with the ID numbers belonging to each ship. There exist the problems of missing and faulty data, resulting from deficiency in signalling of ships due to potential shortcomings such as poor weather conditions, obstructions caused by physical interferences, signal range limitations and technical transmitter/receiver issues.

As an initial step in tackling the problem, we attempted modelling of the 4 major shipping lanes, that are mainly used by transport vessels (but not ferries, for example). By creating an ordered list of all ships provided in data according to their length of route and creating the heat-maps of as few as 20 ships ranked at the middle of the list, it has been possible to define the 2 lanes of interest of out of 4. In terms of modelling, we have used Gaussian Mixture Models (GMMs) on the heat-maps obtained.

The process is continued by selecting more ships from the ordered list for modelling and measuring their likelihood of belonging to the lanes already defined. New heat-maps are created from those that are detected as *outliers* as a result of low likelihood score, and new GMMs are fit until no more peaks are found in the heat-maps. In Figure 1.5, the 5 resulting GMMs have been shown in navy colour, around the blue dots which indicate shipping positions defined by the heat-maps. Note that the model at the upper-left corner of the map does belong to ferries, and is omitted for this part of the analysis.



Figure 1.5 GMMs fit onto main shipping lanes resulting from heat-maps.

After obtaining GMMs to perform as generic classifiers trained on spatial information, we train a specific classifier on each model based on the average travel direction of the ships reporting position inside. This classifier is used for flagging routes with offset more than 45 degrees as anomalous. Note that in Figure 1.5, the measured average directions are indicated by black arrows for each of the 4 shipping lane models.

Anomaly detection is then carried out by checking the outputs (and congruence) of the generic and the specific classifiers within given test intervals. In Figure 1.6, a test route flagged as anomaly is indicated by red colour (Note that the starting point of this route is indicated by a cross). The anomaly detection methodology is to be further improved to incorporate the incongruence measure, Δ_{avg} , as a means of

measuring the congruence between the generic and specific classifiers in a more comprehensive way.

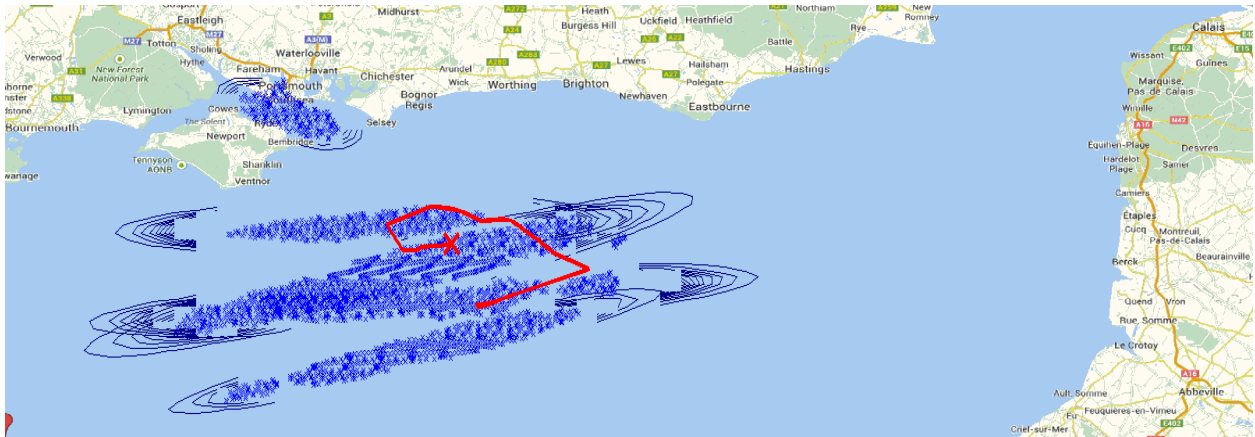


Figure 1.6 A potential anomalous ship behaviour within the main shipping lanes.

Network Anomaly Detection (L_WP1.2)

A Fuzzy Cognitive Map (FCM) is a graphical representation of the behaviour of a system, based on the knowledge of different experts, comprised of nodes and casual bidirectional connections between nodes. Each node represents casual and time-varying concepts, events, actions or goals of the system, with a fuzzy set of outcomes (Jones, et al., 2011). Each node C_i carries a weight $A_i(t)$ in the fuzzy interval $[0, 1]$, which indicates the quantitative measure of the importance that each concept has in the system, at time t . Each link is assigned a weight value e_{ij} in the fuzzy interval $[-1, 1]$, which indicates the relationship between the nodes C_i and C_j . Experts determine the effect of one concept on the others, with a fuzzy degree of weight. This knowledge is then transformed into numerical vectors associated with each concept. An FCM can be represented by an $[n \times n]$ adjacency matrix $E = |e_{ij}|$, describing the relationship between the nodes, where n is the number of nodes. The addition of k adjacency matrices can be calculated by applying the following equation over the common nodes: $E = \frac{1}{k} \sum_{n=1}^k |e_{ij}|_n$ where k is the number of experts. To calculate the influence that each of the nodes has on the other nodes, the weight value of each concept is determined at each step by aggregating the influence of the interconnected concepts on the corresponding weights, by applying the following equation: $A_i^{t+1} = f(A_i^t + \sum_{j=1, j \neq i}^n A_j^t \times e_{ij})$ where A_i^{t+1} is the value of the node C_i at step $t+1$, A_j^t is the value of the interconnected node C_j at step t , e_{ij} the weight relationship between the nodes C_i and C_j , and f an activation function.

Proposed use of FCM within IDS

Three different approaches have been proposed in which an FCM could be integrated within our anomaly based IDS. Our detection system provides three levels of belief or Basic Probability Assignment (BPA) values, for each analysed instance.

These are belief in Normal, Attack, and Uncertainty. Once these values have been generated, the BPA values are fused using Dempster-Shafer (D-S) theory of evidence. All the proposed approaches to integrate an FCM in the detection process are based on the generation or modification of the BPA values used by D-S theory. These are:

Weighted D-S Theory

D-S theory makes use of the Dempster's rule of combination to calculate the orthogonal summation of the beliefs values from two different observers into a single belief. This rule is defined as $m(N) = \frac{\sum_{X \cap Y = N} m_1(X) * m_2(Y)}{1 - \sum_{X \cap Y = \emptyset} m_1(X) * m_2(Y)} \forall N \neq \emptyset$, where $m_1(X)$ and $m_2(X)$ are the belief values in the hypothesis X , from observers/sensors 1 and 2, respectively. This rule assigns a similar level of trust to the different sensors. We have suggested that weighted D-S, which extends the D-S theory, would allow the incorporation of contextual information into the summation process via the form of individual weight values for each sensor. The problem to be addressed is how to determine these weights. Using FCM, the single weight value associated with each of the concepts could be used to define the weights used in the weighted D-S theory fusion technique. Using this approach, the modified Dempster's rule would then become: $m(N) = \frac{\sum_{X \cap Y = N} [m_1(X)]^{A_i(t)} * [m_2(Y)]^{A_j(t)}}{1 - \sum_{X \cap Y = \emptyset} [m_1(X)]^{A_i(t)} * [m_2(Y)]^{A_j(t)}} \forall N \neq \emptyset$

Composed FCM weight values

As previously explained, in FCM, each node C_i carries a weight A_i in the fuzzy interval $[0,1]$. The work in (Looney & Liang, 2003) presents a Bayesian belief network model in which the nodes carry two probability outcomes (i.e. true and false outcomes). When designing a FCM model, we can contribute to the design process by assigning an extra weight value to each node, similar to as in the Bayesian network shown in (Looney & Liang, 2003). We can extend this approach by providing two weight values (e.g. Normal and Malicious), and computing the belief in uncertainty as we currently do in our IDS. Once these three values are computed, they can be used as an extra metric in the current IDS. This extra metric, extracted from the contextual information, would be fused using the D-S theory.

BPA Adjustment

D-S theory starts by defining a frame of discernment, which is the finite set of all possible mutually exclusive outcomes about some problem domain. The power set of the frame of discernment refers to every possible mutually exclusive subset defined as a hypothesis. Each hypothesis from the power set of the frame of discernment is assigned a BPA value within the range $[0, 1]$. Our IDS generates the BPA values based on the current characteristics of the wireless network, and the measurable parameters of the network traffic. In order to incorporate contextual information from the network users, the outcome of the FCM, i.e. the weight A_i value that each node C_i carries, or the weight relationship, e_{ij} , between the nodes can be used prior to the data fusion process, to adjust the assignment of the BPA values.

These values may be used to increase or decrease the BPA values for one particular hypothesis or all the hypotheses.

Experimental results

We have carried out a series of experiments to evaluate the efficiency of one of the proposed approaches to incorporate an FCM in the intrusion detection process. Only the BPA adjustment approach has been implemented and evaluated as first step to showcase the usefulness of the proposed approach. We have developed and added a prototype FCM based contextual awareness element to the architecture of our IDS. This is implemented in the C programming language.

The experiments are based on the utilisation of the time and date in which three applications are scheduled to operate in a network. We have collected Netflow measurements gathered during 168 hours (7 days) from a virtual network testbed in the High Speed Network lab, at Loughborough University. This information is represented in Figure 1.7. The network traffic throughput has been collected to identify possible anomalies in the traffic. Three processes were scheduled to generate network traffic data; downloading a webpage (wget), securely copying a file over the network (ssh), and streaming video (VLC). Three virtual machines were set up in a testbed comprising two clients and one server.

Each application would generate a distinctive throughput value, different from the other throughput values generated by the other two applications. These applications create periodical step-like changes in the throughput values, and these changes may generate false positive alarms from the anomaly based IDS. Additionally, the events considered as anomalous are an unexpected increase in the throughput value. Therefore, the main purpose of the presented experiment is twofold. Firstly, to identify the anomalous events. Secondly, to reduce or eliminate any false positive alarms that may be generated. The network administrator has defined the date and time in which each of the applications is active.

Traffic Pattern Description				
Time	00:00:00 - 03:59:00	04:00:00 - 08:59:00	09:00:00 - 18:59:00	19:00:00 - 23:59:00
Services	video - ssh - wget	video - wget	ssh - wget	video - ssh

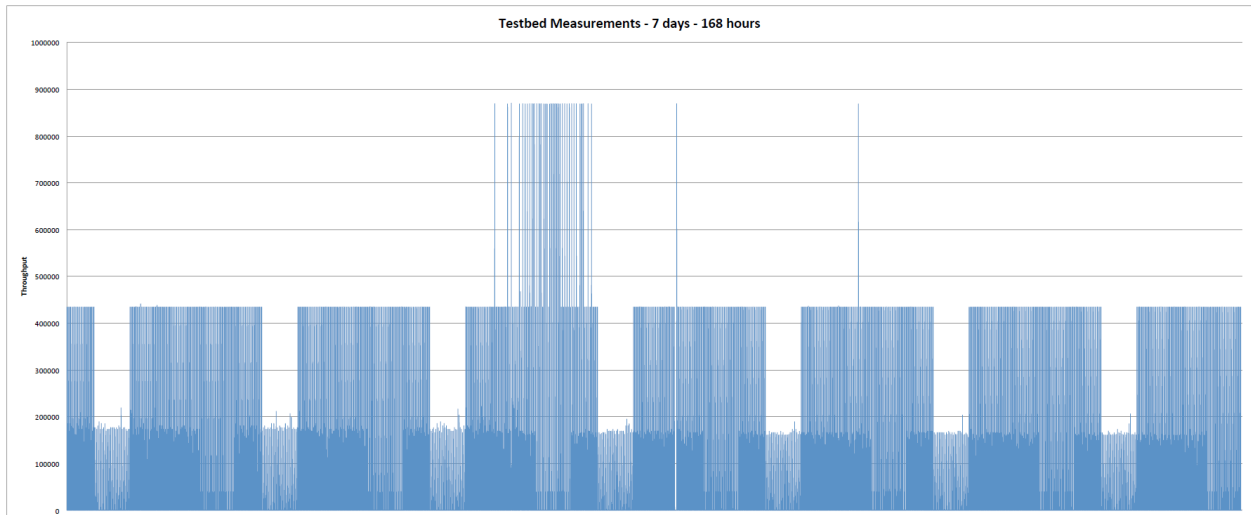


Figure 1.7. Throughput measurements – 168 hours.

Also, the network administrator has defined the expected throughput range expected for each of the applications. By doing so, the system is aware of the normality of the sudden throughput changes. Using this contextual information, the system adds percentages of correction to the assigned belief in Normal behaviour. Since the maximum BPA value assigned to the belief in Normal is 50%, the percentages of correction are 0%, 10%, 20%, 30%, 40%, and 50%. Although the detection rate is not varied by the use of the FCM, the experiments results show a considerable *improvement in the number of false positive alarms* when the FCM is used, as shown in the following table:-

False Positive Rate (%)

Window Size	No Context	10% Belief Correction	20% Belief Correction	30% Belief Correction	40% Belief Correction	50% Belief Correction
1	0,00	0,00	0,00	0,00	0,00	0,00
10	98,32	97,83	47,45	46,98	0,01	0,01
20	96,99	94,66	47,38	46,92	0,01	0,02
30	95,33	93,22	47,46	47,16	0,01	0,02
40	93,74	91,63	46,91	46,60	0,01	0,02
50	91,77	89,93	47,62	46,94	0,01	0,02

1.8 Contact with Dstl

On-going contact has been established with Jonathan Crew (Dstl) as he has been providing opinions and suggestions on our work direction. He showed interest in our current work on the FCM, how we incorporate this technique in our IDS, and how FCM improves the detection results. He also proposed different paths that we could follow that are of interest to Dstl. In particular, he proposed a number of campaigns in which he would be happy for us to work in.

Dstl Campaigns

One of these campaigns is based on incorporating D-S theory of evidence in one of Dstl's systems. Their system is composed of a number of different rule-based IDSs, variations of the public available version of Snort (www.snort.org). They have seen cases in which rules have not fired an alarm when it is believed that they should have. The main purpose of using the combined use of different rule-based IDSs is to aggregate the outcome of these IDSs and increase the detection accuracy of their detection systems. In a first instance, we have been using Snort as an example of rule-based IDSs to implement and test the required approach. In the future, we will use other publicly available rule-based IDSs such as Bro (www.bro.org) or Suricata (suricata-ids.org) to evaluate the combined use of these IDSs.

The problem with rule-based IDSs such as Snort is that these systems commonly produce absolute outcomes. Snort rules are composed of multiple elements (e.g. **alert tcp \$EXTERNAL_NET any -> \$HOME_NET \$HTTP_PORTS (msg: "SQL Ruby on rails SQL injectionattempt"; flow: established,to_server; content:"]]-"; fast_pattern:only; http_uri; pcre:"^/?\w.*?[\w.*?]\]/-smiU"; metadata:service http; reference: cve,2012-2695; reference:url, osvdb.org/show/osvdb/82403; classtype:web-application-attack; sid:23213; rev:1;).** In normal operation, rule-based IDSs trigger one alarm when all the elements in the rule are met. When an attack is identified, Snort generates a single alert of the attack. However, D-S needs belief values in order to work correctly and considers the possibility that any given input may be incorrect.

We have considered the problem of fusing the absolute outputs generated by rule-based IDSs. One of the approaches that we propose to generate beliefs from the rule-based IDSs is to identify the number of actual triggered elements in the n most likely rules. Then, the required beliefs can be computed by using the percentage of triggered/non-triggered elements for each rule. Once the beliefs have been generated, these will be sent to D-S to be fused. This approach requires the modification of the internal structure of Snort (source code) in how it evaluates the different rules and how snort compares the analysed information against the signatures. Snort has by default a number of variables used to establish thresholds and counters that control when an alarm is triggered. For instance, **alert threshold** (*the preprocessor will alert when any combination of Personally Identifiable Information PII is detected in a session. This option specifies how many need to be detected before alerting. This should be set higher than the highest individual count in your "sd pattern" rules*). Also, **count** (*this dictates how many times a PII pattern must be matched for an alert to be generated. The count is tracked across all packets in a session*). Although these variables are used only by one particular module in Snort, it is possible to make Snort trigger alarms, even if the whole rule is not met, but if the thresholds are met. Jonathan Crew was happy for us to develop this approach and acknowledged the novelty of the proposed approach.

1.10 Anomaly Detection in Video

Video segmentation algorithm

The focus of the work during the second year was to extend our work in (Kaloskampis & Hicks, Estimating adaptive coefficients of evolving GMMs for online video segmentation, 2014) to tackle the problem of spatial coherence in video segmentation. Although spatial coherence is one of the desired properties of a good segmentation the amount of research carried out towards this direction is limited.

We developed a new algorithm which deals with the problem of over-segmentation of large uniform areas in video segmentation when using an evolving mixture model. The algorithm tackles this problem at the stage of mixture merging by using a smoothness component in the energy function which controls the mixture merging process. This component imposes a penalty when neighbouring segments in the video frame have different labels and improves the spatial coherence of the mixture.

The algorithm was tested in several publicly available videos; significant improvements were noted in frames which were over-segmented by previous algorithms. We are currently testing our method using the benchmark from (Galasso, Nagaraja, Cardenas, Brox, & Schiele, 2013); preliminary results are shown in Figure 1.8. A journal article on this work is currently in preparation (Kaloskampis & Hicks, 2015).

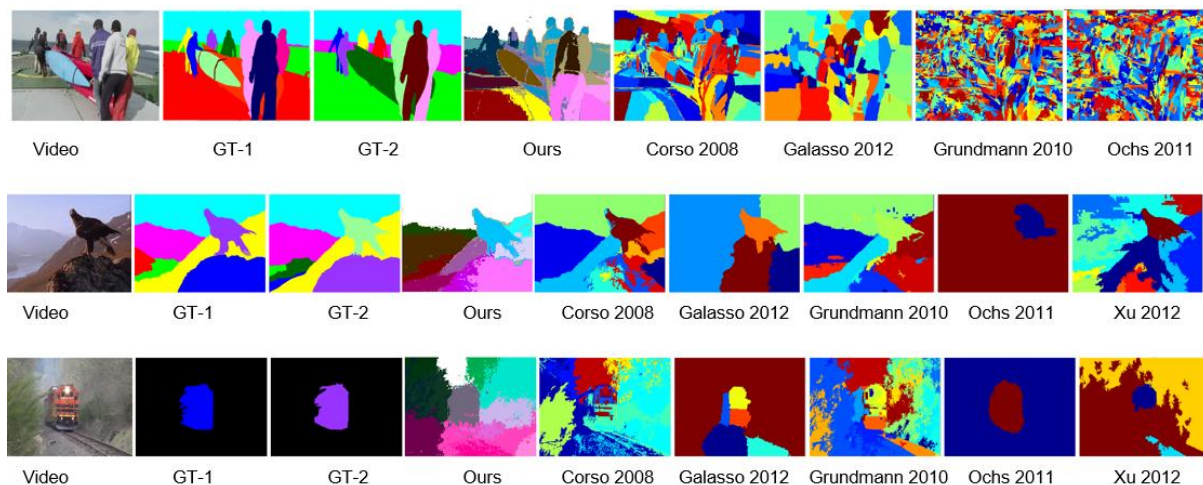


Figure 1.8 Results of our video segmentation method for the benchmark from (Galasso, Nagaraja, Cardenas, Brox, & Schiele, 2013). GT: ground truth.

Evaluation of video segmentation

In this work we developed a new method for the evaluation of the quality of video segmentation. Despite the fact that many methods have been proposed, we found that: (i) there are no established criteria for evaluation of overall video segmentation as opposed to image segmentation or video object segmentation, (ii) there is a

limited number of unsupervised evaluation methods of video segmentation and they are not designed for overall video segmentation, (iii) supervised evaluation methods of video segmentation consider the boundaries of the segmentations without taking into account region interiors.

Taking these into account, we proposed a new set of criteria for evaluation of video segmentation quality to include temporal region consistency. On the basis of the new criteria, we proposed an online method which takes into account the characteristics of both boundaries and regions. Online evaluation can be used to control the parameters of online video segmentation in real-time applications (Zhang et al., 2008). The proposed method can be used both for supervised and unsupervised evaluation.

Furthermore, we designed a test video set specifically for evaluation of the quality of video segmentation and evaluated the proposed method using both this set and segmentations of real life videos. We compared our method against a state of the art supervised evaluation method both for supervised and unsupervised evaluation. The comparison showed that our method is better at evaluation of perceptual qualities of video segmentations as well as at highlighting certain defects of video segmentations.

This work is presented in (Mohammad, Kaloskampis, & Hicks, 2015).

Road type detection using video segmentation

Vision-based road-type classification can be described as the process of specifying road types based on the video content of the scene. This task is an important step towards road scene understanding, which is required in a variety of applications, including situational awareness and fully or semi-automated driving.

Current state of the art methods tackle the problem of road type detection by selecting a number of sub-regions within each video frame as the interest regions for the driving environment and perform classification based on the features extracted within these regions. However, there is no guarantee that the sub-regions capture all key information; in fact there are specific cases in which the selected regions are not likely to contain the key information.

To overcome such issues it is necessary to take into account all regions in the frame. To achieve this issue we developed a method which first applies an online video segmentation method to each frames and then compares the detected segments to those usually found in certain types of roads. We consider a four-class problem, where the classes are motorway, off-road, trunk road, and urban road. Our method consists of two stages. The first stage is building a statistical model for each road type offline. The second stage is the online classification of new video frames. The first stage can be divided into two steps. In the first step, the training frames are segmented using an evolving Gaussian mixture model (GMM). In the second step,

we create a model for each road type from all the Gaussians taken from video sequences illustrating this road type. The classification stage can be divided into two steps. In the first step, an evolving GMM is created for the new frame. We then use the Bhattacharyya distance to find the distance between the Gaussians from the new frame and the models obtained from the first stage, which allows us to classify each of the new Gaussians as belonging to one of the road types. In the second step, the road type confidence score is calculated based on the size of the segment corresponding to each classified Gaussian. Experimental results on real-world data indicate that our method outperforms the previous state of the art method in this area in terms of classification accuracy. An overview of our results with comparison against the state-of-the-art method is given in Figure 1.9.

This work is presented in (Mohammad, Kaloskampis, & Hicks, 2015).

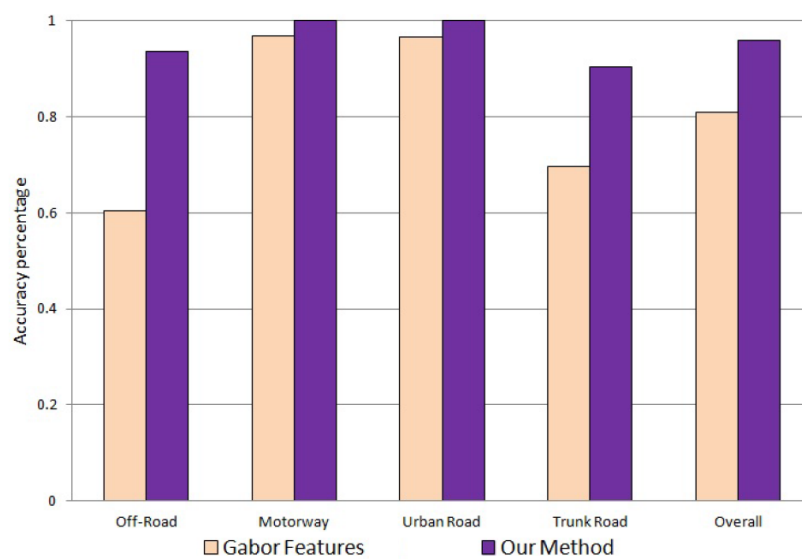


Figure 1.9 Road-type classification results. Our method is compared against the state-of-the-art method ‘Gabor features’ from (Mioulet, Breckon, Mouton, Fantoni, & Ferreira, 2013).

Activity recognition and anomaly detection in multimedia streams

In this work we present a system for activity recognition and anomaly detection in multimedia streams featuring complex human activities. The system models human activities as temporal sequences of their constituent actions and can handle actions that occur concurrently in multiple parallel streams. It operates in a supervised manner and comprises three stages, which are extraction of action sequences from data streams, feature selection and activity recognition/anomaly detection.

Previous approaches in the field of behaviour analysis from multimedia streams assume that actions constituting activities take place in a sequential manner. Therefore these methods cannot readily handle parallel streams. In fact, there is only a limited amount of research which studies activity and action concurrency. These methods have limitations which concern the number of parallel streams which they

can handle or they use models which are specified manually by human experts and therefore cannot be learned from data.

The novelty of our work is two-fold:

a. Our system features a new action sequence representation which is capable of representing prolonged, complex activities occurring in multiple streams which may result from several different sources. The new representation facilitates the use of standard models, such as HMMs to represent activities which take place in parallel, which was considered as problematic in the past.

b. We propose a new classification algorithm employed by our system which combines a feature selection facility based on the key action discovery (KAD) concept, a discriminative feature facility based on random forests (RF) and a temporal analysis facility, for which we use hierarchical hidden Markov models (HHMMs). The feature selection facility eases the classification task by removing redundant elements from the input sequences. The discriminative feature facility checks the existence or absence of the steps required for the execution of an activity, while the temporal analysis facility encodes the ordering of these steps. Note that our system can be applied as it stands to any task which involves prolonged, composite activities, as its structure and parameters are learned automatically from expert labelled data.

The proposed system offers higher accuracy in activity recognition and error detection than other leading methods in two publicly available datasets. An initial form of our system with preliminary results was presented in (Kaloskampis, Hicks, & Marshall, 2014); a journal article which presents our full system with an in-depth evaluation is currently under review (Kaloskampis, Hicks, & Marshall, 2014).

1.11 Application to defence related datasets

During the second year we applied our video segmentation algorithm to several defence related datasets, most notably the Dstl helicopter dataset and video streams from UAVs provided by Loughborough University. We have also done preliminary work on the Shiploc dataset provided by Thales.

a. The Dstl helicopter dataset provided by Dstl is a set of videos captured from an exercise which has the purpose of assessing a gunner's ability to track a helicopter. Two tasks which can be accomplished using our video segmentation algorithm are horizon detection and vehicle detection/tracking. We applied our video segmentation algorithm to the helicopter videos and sent a sample of segmented frames to Dstl.

b. The UAV video provided by Loughborough University illustrates an experiment in which a vehicle performs taxiing in a laboratory, following the yellow taxiing lines. We applied our video segmentation algorithm on this video to detect the yellow taxiing

line, which was achieved with good accuracy (Figure 1.10). We sent a sample of segmented frames to Loughborough University.

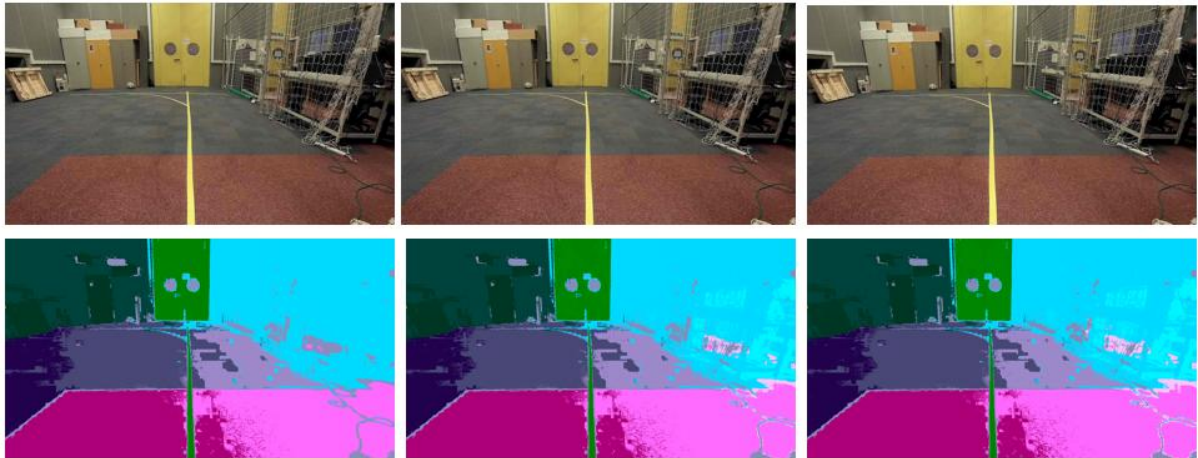


Figure 1.10 Original frames from the Loughborough UAV dataset (top row) and segmentation results (bottom row).

c. Additionally, we investigated the applicability of our anomaly detection framework (Kaloskampis, Hicks, & Marshall, 2014) to the Thales dataset. Our idea is to first build state models of usually followed routes (using, for example, continuous hidden Markov models) and then look for deviations from these routes, which could indicate anomalies. As a first step, we studied the trajectories of several ships and worked on building a set of rules to automatically distinguish between route classes.

1.12 Future Work

As a part of the anomaly detection methodology development, the plans for the third year of the project can be summarized as follows:

Anomaly Detection Mechanisms

- In the coming year the theoretical studies of incongruence will aim to consider a more realistic distribution of classifier estimation errors instead of the folded Gaussian. A strong candidate is the Poisson distribution, which can be naturally confined to the $[0,1]$ interval. At the distribution level, the study will involve a comparison of these two distributions for different scenarios (class a posteriori probability distributions). The work will then proceed with a series of experiments in which the folded Gaussian is replaced by Poisson and the impact on the distribution of incongruence measure values investigated.
- The second strand of the future theoretical work will focus on other incongruence measures, which we intend to develop from histogram similarity measures commonly used in statistics. The sensitivity of these derived classifier incongruence measures to estimation errors will then be studied experimentally, using the existing experimental set up adopted for the delta measure studies.

Applications

Anomaly Detection in Ship Behaviour

- The application work will continue with the ship behaviour anomaly detection problem. The work to date suggested a systematic method of building ship behaviour models one at a time, and using distribution outlier detection techniques to identify anomalous behaviour or a new behaviour model. In contrast to clustering, this approach does not require the number of models to be specified a priori. In a sense it is a heuristic equivalent of the Dirichlet process. The relationship of the methodology developed to the Dirichlet process model framework will be investigated, with the view of identifying any merits for its adoption in our work.

Network Anomaly Detection

- To extend the full integration of FCM in the IDS and to commence implementation of the campaigns proposed by Dstl.
- Another approach that we propose is to divide each Snort rule composed of multiple elements into rules composed of a single element. Then, using analysis tools, process the generated alarms triggered by single condition Snort rules. This method would also allow computing the percentage of triggered/non-triggered elements, and would circumvent the process of manipulating the source code of Snort. However, it will require intelligent analysis for extracting conclusions from the simplistic single condition rules.

For both proposed approaches, the next step will be integration of them in an evaluation system provided by Dstl. To do that, we have been asked to develop and install the proposed detection system in a virtual machine environment. This virtual machine environment will then be installed in one of Dstl's systems to evaluate its efficiency.

Jonathan Crew also proposed other campaigns that Loughborough University is going to implement. One of these campaigns involves the generation and use of ontologies. Ontologies are useful tools to structure and organise pieces of contextual information. We will investigate approaches to automatically generate the internal structure of these contextual information ontologies. Another of these campaigns involves the integration of statistical based IDSs into their rule-based IDSs. We will collaborate in this process. Dstl also proposed that we could write the middleware software code that connects two modules as part of the extraction of the log files and the detection systems. Finally, Jonathan Crew suggested that we could use financial information for initial evaluation of FCM, because these datasets are publicly available, these are rich in contextual information, and we can trace back the real effect that the contextual information had.

Anomaly Detection in Video

- In our future work we will develop further our evolving GMM algorithm and investigate its applicability to several defence related applications. An important application which we will study is the blind source separation problem, in collaboration with WP3-Surrey. Since the source model used by WP3-Surrey is based on GMMs (Gu, Zhang, Wang, & Xiong, 2014), the evolution of the GMM components over time can be studied using our evolving GMM algorithm. Two interesting problems, on which we can work are: (a) having an unknown number of sources; (b) the number of sources varies over time. The first problem could be potentially tackled by the automatic GMM component selection facility from (Kaloskampis & Hicks, Estimating adaptive coefficients of evolving GMMs for online video segmentation, 2014). The second could be handled by the change detection method from (Kaloskampis & Hicks, Estimating adaptive coefficients of evolving GMMs for online video segmentation, 2014).
- Another research direction which we will follow is the efficient implementation of our evolving GMM algorithm using parallel computing platforms utilising graphics processing units (GPUs). We plan to work closely with WP5 on this domain.
- We also plan to study the problem of anomaly detection in the context of defence applications. We will work on the datasets provided by Dstl (helicopter and tank videos) in collaboration with Surrey. Furthermore, we will apply our anomaly detection framework (Kaloskampis, Hicks, & Marshall, 2014) to detect anomalies in the Thales Shiploc dataset.
- We will also extend our road traffic analysis framework to detect anomalies. The extended framework will utilise ontologies to encode context information from road and airport environments. The ontologies will be combined with video segmentation to detect anomalies. An initial form of this framework is currently under development; it is designed to cater for anomalies in road environments which are related to pedestrian behaviour. We have planned collaboration with WP2-Loughborough for anomaly detection in airport environments.

1.13 Publications

Aparicio-Navarro, F. J., Kyriakopoulos, K. G., & Parish, D. J. (2014). Automatic dataset labelling and feature selection for intrusion detection systems. *MILCOM 2014*, (pp. 46–51).

F Aparicio-Navarro, F. J., Kyriakopoulos, K. G., & Parish, D. J. (2014). Empirical study of automatic dataset labelling. *ICITST 2014*, (pp. 373–379).

Kaloskampis, I., & Hicks, Y. (2014). Estimating adaptive coefficients of evolving GMMs for online video segmentation. *IEEE ISCCSP*, (pp. 554-557). Athens, Greece.

Kaloskampis, I., Hicks, Y., & Marshall, D. (2014). A framework for complex activity recognition and anomaly detection in multimedia streams. *10th International IMA Conference on Mathematics in Signal Processing*. Birmingham, UK.

Kaloskampis, I., Hicks, Y., & Marshall, D. (2014). Activity Recognition in Concurrent Multimedia Streams Using Temporal and Discriminative Analysis. *Computer Vision and Image Understanding*, under review.

Mohammad, M. A., Kaloskampis, I., & Hicks, Y. (2015). New method for evaluation of video segmentation quality. *VISAPP*. Berlin, Germany (to appear).

Mohammad, M. A., Kaloskampis, I., & Hicks, Y. (2015). Evolving GMMs for road-type classification. *IEEE ICIT*. Sevilla, Spain (to appear).

Kaloskampis, I., & Hicks, Y. (2015). Spatially coherent online video segmentation using evolving mixtures of Gaussians. In preparation.

Kittler, J., Christmas, W., de Campos, T., Windridge, D., Yan, F., Illingworth, J., et al. (2013). Domain Anomaly Detection in Machine Perception: A System Architecture and Taxonomy. *IEEE Transactions on Pattern Analysis and Machine Intelligence*.

Bibliography

Aparico-Navarro, F., Parish, D., & Kyriakopoulos, K. (2014). Automatic dataset labelling and feature selection for intrusion detection systems. *MILCOM*. Submitted.

Bueno, S., & Salmeron, J. (2009). Benchmarking main activation functions in fuzzy cognitive maps. *Expert Systems with Applications*, 36(3), 5221-5229.

Charron, C., & Hicks, Y. (2010). An evolving MoG for online image sequence segmentation. *17th IEEE International Conference on Image Processing (ICIP)*, (pp. 2189–2192).

Galasso, F., Nagaraja, N. S., Cardenas, T. J., Brox, T., & Schiele, B. (2013). A Unified Video Segmentation Benchmark: Annotation, Metrics and Analysis. *IEEE International Conference on Computer Vision (ICCV)*.

Gargiulo, F., Mazzariello, C., & Sansone, C. (2012). Automatically building datasets of labelled IP traffic traces: A self-training approach. *Applied Soft Computing*, 12(6), 1640-1649.

- Gu, F., Zhang, H., Wang, W., & Xiong, C. (2014). An expectation-maximization algorithm for blind separation of noisy mixtures using Gaussian mixture model. *IEEE Transactions on Neural Networks and Learning Systems (in press)*.
- Howard, N., & Kanareykin, S. (2012). Intention awareness in cyber security. *Proc. of the Int. Conf. on Cyber Security, Cyber Warfare and Digital Forensic (CyberSec'12)*, (pp. 6-11).
- Itti, L., & Baldi, P. (2005). A principled approach to detecting surprising events in video. *IEEE Conference on Computer Vision and Pattern Recognition (CVPR)*, (pp. 631-637).
- Jones, R., Connors, E., Mossey, M., Hyatt, J., Hansen, N., & Endsley, M. (2011). Using fuzzy cognitive mapping techniques to model situation awareness for army infantry platoon leaders. *Computational and Mathematical Organization Theory*, 17(3), 272-295.
- Kaloskampis, I., & Hicks, Y. (2014). Estimating adaptive coefficients of evolving GMMs for online video segmentation. *6th IEEE International Symposium on Communications, Control, and Signal Processing (ISCCSP 2014)*. To Appear.
- Kaloskampis, I., & Hicks, Y. (2014). Estimating adaptive coefficients of evolving GMMs for online video segmentation. *IEEE ISCCSP*, (pp. 554-557). Athens, Greece.
- Kaloskampis, I., & Hicks, Y. (2015). Spatially coherent online video segmentation using evolving mixtures of Gaussians. *In preparation*.
- Kaloskampis, I., Hicks, Y., & Marshall, D. (2011). Automatic analysis of composite activities in video sequences using key action discovery and hierarchical graphical models. *2nd IEEE Workshop on Analysis and Retrieval of Tracked Events and Motion in Imagery Streams (IEEE ARTEMIS 2011)*, (pp. 890–897).
- Kaloskampis, I., Hicks, Y., & Marshall, D. (2011). Automatic analysis of composite activities in video sequences using key action discovery and hierarchical graphical models. *2nd IEEE Workshop on Analysis and Retrieval of Tracked Events and Motion in Imagery Streams (IEEE ARTEMIS 2011)*, (pp. 890–897). Barcelona, Spain.
- Kaloskampis, I., Hicks, Y., & Marshall, D. (2014). A framework for complex activity recognition and anomaly detection in multimedia streams. *10th International IMA Conference on Mathematics in Signal Processing*. Birmingham, UK.
- Kaloskampis, I., Hicks, Y., & Marshall, D. (2014). Activity Recognition in Concurrent Multimedia Streams Using Temporal and Discriminative Analysis. *Computer Vision and Image Understanding, under review*.

- Kittler, J., Christmas, W., de Campos, T., Windridge, D., Yan, F., Illingworth, J., & Osman, M. (2013). Domain Anomaly Detection in Machine Perception: A System Architecture and Taxonomy. *IEEE Transactions on Pattern Analysis and Machine Intelligence*.
- Kokar, M. M., & Endlsey, M. R. (2012). Situation awareness and cognitive modelling. *IEEE Intelligent Systems*, 27(3), 91-96.
- Lezama, J., Alahari, K., Sivic, J., & Laptev, I. (2011). Track to the future: Spatiotemporal video segmentation with long-range motion cues. *IEEE Conference on Computer Vision and Pattern Recognition (CVPR)*.
- Looney, C., & Liang, L. (2003). Cognitive situation and threat assessments of ground battlespaces. *Information Fusion*, 4(4), 297-308.
- Military videos collection*. (2014). Retrieved from <http://www.militaryvideos.net>.
- Mioulet, L., Breckon, T., Mouton, A., Fantoni, I., & Ferreira, J. (2013). Realtime estimation of drivable image area based on monocular vision. *IEEE Symposium on Intelligent Vehicles (IV)*, (pp. 63-68).
- Mohammad, M. A., Kaloskampis, I., & Hicks, Y. (2015). Evolving GMMs for road-type classification. *IEEE ICIT*. Sevilla, Spain.
- Mohammad, M. A., Kaloskampis, I., & Hicks, Y. (2015). New method for evaluation of video segmentation quality. *International Conference on Computer Vision Theory and Applications (VISAPP)*. Berlin, Germany.
- Omnetpp*. (2014). Retrieved from <http://www.omnetpp.org>.
- Opnet*. (2014). Retrieved from <http://www.opnet.com>.
- Sadighian, A., Zargar, S., Fernandez, J., & Lemay, A. (2013). Semantic-based context-aware alert fusion for distributed Intrusion Detection System. *Proc. of the Int. Conf. on Risks and Security of Internet and Systems (CRiSIS'13)*, (pp. 1-6).
- Stylios, C. D., & Groumpos, P. P. (2004). Modeling complex systems using fuzzy cognitive maps. *IEEE Transactions on Systems, Man and Cybernetics: Systems and Humans*, 34(1), 155-162.
- University Defence Research Collaboration in Signal Processing, 'Thermal imaging videos*. (2014). Retrieved from <http://www.see.ed.ac.uk/drupal/udrc/data-centre/>.

Xiph.Org Foundation. (2013). Retrieved from <http://media.xiph.org/>.

Zabih , R., & Kolmogorov, V. (2004). Spatially coherent clustering using graph cuts.
IEEE Conference on Computer Vision and Pattern Recognition, (pp. 437-444).

L_WP2 (HU): Handling uncertainty and incorporating domain knowledge

2.1 Staffing

Work Package Leaders:	Prof. Lambotharan (LU) and Prof. Wen-Hua Chen (LU)
Other Academics:	Prof. Jonathon Chambers (NCL & LU) and Dr Alex Gong (LU)
Research Associates:	Dr Anastasia Panoui (LU), Dr Miao Yu (LU)
UDRC Research Student:	Mr Tasos Deligiannis (LU)
Affiliated Research Students:	Ms Gaia Rossetti, Mr Abdullahi Daniyan (WP 2.2) and Mr Runxiao Ding (WP 2.1)
Lead Project Partner:	Prof. Malcolm Macleod (QinetiQ)
Dstl Contacts:	Dr Marcel Hernandez, Dr Jordi Barr.

2.2. Aims and the lists of the original L_WP2 in the case for support:

Aims: To develop a generic learning framework for handling uncertainties in the measurements acquired in the networked battlespace environment. Links to L_WP1 through domain knowledge; and L_WP3 & L_WP4 in handling incomplete sensor information & achieving robustness to jamming.

This WP exploits the world model of the networked battlespace to improve performance and confidence and to reduce uncertainty to an unprecedented level. Due to the abundance of previously collected information of a battlespace and increasing availability of mobile communication and storage, rich information may be available for sensor platforms when performing signal processing as they operate in a networked battlespace. Examples for such information are digital maps about terrain and layout of the field, historical data about the site, geometric relations between platforms, and operational conditions such as weather (e.g. the influence of shadowing on optical sensors).

L_WP2.1 Reducing uncertainty by incorporating domain knowledge using Bayesian inference, adaptive signal processing and sparse sampling [PDRA2]

We will consider how to quantify the information in the world model and express it in a probabilistic statement; for example, how to synthesize the information in the prior of the world model (e.g. geometric constraints) with the prior of the state variables obtained in the previous time steps to form a combined prior probability function, and how to pool different sources of information measured via different types of sensors or provided by other resources (e.g. digital maps) for statistical inference. New signal processing algorithms offering adaptivity to operational environments will also be developed by exploiting the domain knowledge. Various parameters in these algorithms (e.g. the threshold for detection) or different types of signal processing models/algorithms will be selected based on the domain information (e.g. the change of the operation conditions when the sensor platforms move, or what decisions follow

from the signal processing results and their consequence). Historical data will be used to build up the priors in Bayesian inference for different objects of interest and different scenarios, which will reduce the reliance on real-time measurements in the battlespace. New sparse sampling measurements will be not only used to update the priors but also to confirm or reject the previous priors selected for the Bayesian learning (hypothesis tests) with the help of domain knowledge (e.g. how likely it could be that an object of interest occurs based on domain knowledge). The Bayesian inference framework will also be extended from a single to multiple sensor platforms operating in a networked environment, by fusing all the information, including the sensory capabilities and constraints (e.g. angle of field view) and geometric relationships between different sensor platforms. One research challenge here is to create a joint model for multiple sensor platforms with heterogenous attributes to gather intelligence of an object of interest (e.g. a threat), where information synthesis is of particular importance.

L_WP2.2: Robust signal processing techniques under uncertainty, modelling uncertainty with stochastic dynamic processes, and characterization of uncertainty with a game theoretic framework [PDRA3/PS2]

Robust signal processing techniques based on convex optimizations will be developed to tackle uncertainty. Mathematical models and approximation techniques will be developed to model an uncertainty region as a convex hull so that low complexity algorithms can be developed. Robust techniques based on both a probabilistic approach and worst case optimizations will be developed. The application scenario will include distributed/networked beamformer design under manifold uncertainty, imperfect sensor measurements and radar clutters. Instead of treating uncertainty as caused by a static collection of events and associated relationship, the uncertainty will be investigated within the framework of dynamically evolving phenomena. In this framework, uncertainty will be considered as caused by dynamic entities having states and transitions from one state to another resulting from actions in the battlespace. Both hidden Markov model and Bayesian networks will be used to characterise uncertainty. To enhance characterization of uncertainty and to understand the underlying mechanisms further, this WP will consider uncertainty as caused by dynamically varying actions created by various players in the battlespace, e.g. coalitional forces and enemies. Hence a game theoretic framework will be developed. The work will start with a non-cooperative game theoretic framework and will be extended to Bayesian games to account for incomplete information. The framework will then be extended to stochastic games (Markov games) to model dynamically changing actions and evolution of uncertainty. The possible battlespace scenarios that will be considered within this framework will include air formation to ground attack-defence system, defence against jamming in radars (linked to L_WP 4.1) and counteracting uncertainty created by deception by enemies, for example fake RF signal injection.

2.3 Progress made in the first two years in addressing the original objectives

Staffing

L_WP2.1: In April 2013 Dr Miao Yu was appointed as a research associate to work on L_WP2.2. In October 2014, Mr Runxiao Ding joined as an affiliated UDRC PhD student.

L_WP2.2: In April 2013 Dr Anastasia Panoui was appointed as a research associate to work on L_WP2.2. In October 2013, Mr Anastasios Deligiannis was appointed as a UDRC PhD student. Two more affiliated UDRC PhD students, Ms Gaia Rossetti and Mr Abdullahi Daniyan, joined in October 2014. L_WP2.2 also benefits from Dr Alex Gong, a lecturer in communications and signal processing at LU.

Overview

The original aim of L_WP2 was “to develop a generic learning framework for handling uncertainties in the measurements acquired in the networked battlespace environment”. There has not been any significant change on this stated aim, and the focus remains on the development of signal processing algorithms for handling uncertainties by incorporating domain knowledge and game theoretic methods.

Engagement with partners

The leading industrial partner for this work package is QinetiQ. We have had a number of meetings with Professor Malcolm Macleod. Discussions have been had in terms of technical support and way of engagements. There are a few changes in terms of Dstl technical contact for this work package. The current technical contacts for L_WP2.1 and L_WP2.2 are Dr Marcel Hernandez from the Advanced Signal Processing & Fusion Team and Dr Jordi Barr from the Sensors & Countermeasures Department, respectively. Both Dr Hernandez and Dr Barr are experienced signal processing experts and have provided a number of very insightful comments and suggestions to this work package.

2.3.1 L_WP2 progress

The current focus of the work in L_WP2.1 is exploiting the domain knowledge in the world model to develop new signal processing algorithms based on the Bayesian framework. To accomplish this, we have been studying in the following sub-areas in the first two years:

- We compared different implementations of generic Bayesian frameworks, particularly particle filtering and Gaussian mixture algorithms. Although Bayesian theory provides a rigorous framework in developing algorithms for incorporating domain knowledge in signal processing, it is difficult to implement and, in general, not computationally tractable. Most notably, the incorporation of the knowledge significantly distorts the statistic distribution

even if the distribution for the dynamic systems without constraints is Gaussian. Particle filtering and Gaussian mixture algorithms are two popular numerical implementations of the generic Bayesian framework. A detailed study on a GMTI radar tracking benchmark consisting of Doppler blindness zone, missed detection and multiple manoeuvring modes of the moving object (i.e. constant velocity, acceleration, and stop) has been performed. Our research [Pub. 2.1.6] has shown that the IMMPPF (Interactive Multiple Model Particle Filtering) yields much better tracking performance (in particular when the vehicle is in stationary) than the latest multiple model Gaussian mixture methods with acceptable computational burden.

- We incorporated different types of domain knowledge into the current state-of-the-art algorithms. Firstly, for a tracking example, we investigated how to incorporate knowledge, not only where a moving object shall be or more likely to be, but also where the moving object is unlikely or impossible to be. Geographic Information Systems (GISs) are used to extract available domain knowledge, and advanced multiple model particle algorithms are developed where measurements and particle swarm optimisation algorithms are exploited to improve particle samplings and the algorithm efficiency. The corresponding work has been submitted for publication as in [Pub.2.1.5]. Secondly, we proposed a multiple target tracking algorithm in [Pub.2.1.3] which exploits constraint information. The new developed algorithm is a combination of multiple hypothesis tracking (MHT) for data association and moving horizon estimation (MHE) which effectively incorporates the constraint information for a more accurate state estimation.
- We developed a new dynamic modelling approach for utilizing domain knowledge in signal processing [Pub.2.1.4]. It needs to be noticed that various dynamic models that could be used as the state models for developing target tracking or more broadly signal processing algorithms have been proposed (e.g. the survey paper [Ref.2.1.1]); however, most of the current dynamic models either do not take environmental information into account or consider the influence of the environment in a limited way by directly adding environmental constraints on the targets states. That is, it is assumed that the state model evolves itself (e.g. without taking into account domain knowledge) and then constraints imposed by the environment are added to that. This approach cannot capture the true nature of an object(s) of interest since the environment actually affects and/or reshapes the distribution of the target movement (i.e. interaction between an object and its operational environment). To this end, we refine the current dynamic modelling approach by incorporating environmental information into the *control input* of a dynamic model so as to modify the distribution of the evolvement of underlying system dynamics. The incorporation of the environmental information is achieved by both introducing "forces" terms to reflect the interactions between the moving

object and its environment, and imposing feasible regions of its control parameters introduced by the environmental constraints.

- Based on the developed dynamic models, new signal processing algorithms are being developed to fully exploit the domain knowledge. Specifically, two related algorithms are under development:
 - I. The new developed dynamic model is directly incorporated into the Moving Horizon Estimation (MHE) framework for target tracking. More comprehensive domain knowledge, including both the environmental interaction information and environmental constraint information, is exploited by the new MHE framework for better tracking performance.
 - II. Secondly, it is considered in a realistic scenario, a target may move in different regions and is then affected by different types of environmental conditions. A new hybrid modelling system is proposed to better reflect the target movement. Based on the new modelling system, Bayesian inference framework is developed for target state estimation and the implement of the Bayesian framework is achieved by both the generic sequential Monte Carlo (SMC) method and a more advanced SMC algorithm which exploits the measurement information for constructing a better importance sampling function.

The current focus of the work in L_WP2.2 is the development of mathematical optimization techniques and game theoretic framework for distributed resource allocation and detection in radar networks. To accomplish this, we have been studying in the following sub-areas in the first two years.

- The focus has been on distributed game theoretic algorithms for power control and waveform design for radar networks. The game theoretic framework allowed various radars in a multi-static network to adjust their transmission parameters such as power and waveforms without a need for explicit communication among themselves. We have established existence and uniqueness of the Nash equilibrium. The distributed power allocation technique has been published in [1], [2] and the distributed autonomous waveform selection method has been published in [3] and the Nash equilibrium analysis will be submitted for publication [4].
- The focus of Anastasios Deligiannis is on the development and analysis of signal processing algorithms for a MIMO radar network. A two dimensional fully overlapped subarray technique that makes use of the advantage of both coherent beamforming and MIMO waveform diversity has been developed

and published in [5] and [6]. The focus of the current work is on distributed beam steering technique for a multi-static MIMO radar network using game theoretic methods.

- The recently joined affiliated UDRC PhD students, Ms Gaia Rossetti and Mr Abdullahi Daniyan have their focus on cognitive radar networks and target tracking. The aim is to develop convex optimization based waveform design that exploits available prior knowledge such as clutter map obtained through domain knowledge and/or through previous scanning of the environment. A convex optimization and sequential Bayesian estimation framework are considered. For tracking, approaches based on probability hypothesis density (PHD) recursions and cardinalized PHD (CPHD) recursions are considered. The aim is to incorporate prior knowledge provided by tracking algorithms to determine optimal waveforms for subsequent illuminations using sequential Bayesian approaches. Both the affiliated PhD students have completed necessary background study and literature survey.

2.4 Technical Details

2.4.1 Technical Details of WP2.1

The Bayesian inference framework is a generic method which could be applied in different types of signal processing applications in a realistic environment, such as targets localization, targets tracking, and information fusion. Different types of algorithms have been developed based on the Bayesian framework for signal processing. Besides, due to the abundance of previously collected information of a battlespace and increasing availability of mobile communication and storage, rich information may be available for sensor platforms when performing signal processing as they operate in a networked battlespace. The related information could be incorporated to reduce the reliance on real-time measurements in the battlespace.

The aim of this work package is to incorporate different types of information (domain knowledge) into the Bayesian inference framework for new algorithms development. New generic Bayesian learning frameworks will be designed for handling uncertainties in the measurements acquired in the networked battlespace environment by the aid of the domain knowledge for different signal processing applications and corresponding new algorithms will be developed. Many works have been done to achieve this aim during the last two years, especially for the target tracking application.

Firstly, we have compared different implementation methods (mixture of Gaussians and interactive multiple model particle filter (IMMPF)) of implementation the Bayesian inference framework for manoeuvring target tracking. Besides, we have incorporated complicated domain knowledge (such as the GIS information) into the multiple model particle filtering algorithm and applied an advanced particle swarm optimization (PSO) technique to improve the particle filtering performance by

optimizing the measurement likelihood function. The details of these two works were presented in the first year report.

In order to fully incorporate different domain knowledge (environmental constraint information and the interaction between object and surrounding environment) for improving the performance of signal processing algorithms, a new dynamic model was developed whose control input is environment dependent. Based on single/hybrid environment dependent dynamic model(s), different new target tracking algorithms have been developed. The details of the developed new dynamic model and the new algorithms are reported in Section 2.4.1.1 and Section 2.4.1.2 respectively.

2.4.1.1 Developing a new dynamic modelling approach for utilizing domain knowledge in signal processing

Normally, the target dynamic model follows a general form as

$$\mathbf{x}_{k+1} = F_k(\mathbf{x}_k) + G\mathbf{w}_k \quad (2.1)$$

where \mathbf{x}_k represents the state vector, G is a constant matrix, the dynamic function F_k describes a state dynamic type for a vehicle to follow and \mathbf{w}_k represents the control parameter with a certain distribution $p(\mathbf{w}_k)$ to reflect the uncertainty of the target dynamics.

The traditional dynamic models (e.g. in [Ref.2.1.1]) either do not take the environmental information into account or model the moving target freely as in Equation (2.1) and then add the constraints to the state \mathbf{x}_{k+1} to incorporate the environmental constraints. However, they consider a fixed distribution of the control input \mathbf{w}_k , which conflicts with the real scenario where the control of a target is actually affected by its environment (if a vehicle is quite close to the edge of a road, the driver is more likely to control the vehicle to move away from the edge).

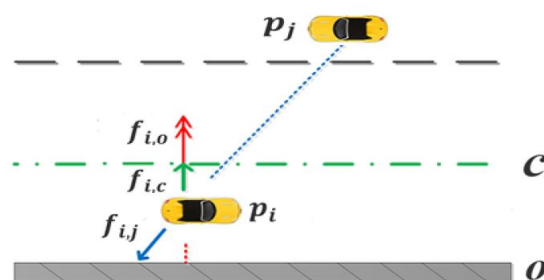


Fig. 2.1 A vehicle p_i receives interaction force $f_{i,j}$ from another vehicle, attractive force $f_{i,c}$ from the centreline & repulsive force $f_{i,o}$ from the border.

In this work, we propose a novel dynamic modelling approach to incorporate the environmental information into the control parameters of a dynamic model. Firstly, the *interactions* between a target and the surrounding environment are considered

and the interactions are modelled by the ‘forces’ as in Fig. 2.1. It shall be highlighted that although the concept of the force has been used in a number of applications to model the interactions between different objects, or between an object and its environment such as crowd modelling [Ref.2.1.2] and planning (path planning or collision avoidance), so far little work has been done in using it for the purpose of improving signal processing with domain knowledge. Another feature in our model is that, the force does not only depend on the disturbance as in other models (e.g. [Ref.2.1.2] and [Ref.2.1.3]) but also on velocity and other state variables. The latter is particularly important for an object having significant changes of its velocity such as vehicles or aircraft. As an example, forces could be represented as exponential forms as in (Eqn 2.2) and (Eqn 2.3).

$$\mathbf{f}_{i,j}^{repulsive} = A \cdot \exp\left(\frac{-d_{ij}^{prediction}}{B}\right) \mathbf{n}_{ij} \quad (2.2)$$

$$\mathbf{f}_{i,j}^{attractive} = A \cdot \left(1 - \exp\left(\frac{-d_{ij}^{prediction}}{B}\right)\right) \mathbf{n}_{ji} \quad (2.3)$$

where $\mathbf{f}_{i,j}^{repulsive}$ and $\mathbf{f}_{i,j}^{attractive}$ represent the repulsive and attractive forces between object i and j , $d_{ij}^{prediction}$ is the predicted distance according to the desired dynamics F_k as in (2.1) and it is related to both the target position and velocity. A and B are two constants, \mathbf{n}_{ij} is the unit vector pointing from j to i . Forces introduced from surrounding objects are summed to be a total one denoted as $\mathbf{f}_i^{environment}$ and applied on the control parameter \mathbf{w}_k as in (2.4) to shift its distribution, particularly the mean of the distribution.

$$\mathbf{w}'_k = \frac{\mathbf{f}_i^{environment}}{m} + \mathbf{w}_k \quad (2.4)$$

where m represents the object mass and \mathbf{w}'_k is used to replace the original \mathbf{w}_k in (2.1).

Secondly, we also consider the effect of the surrounding environment and *constraint*, which may change other statistic property of the control such as the variances and determines the feasible region of the control parameters \mathbf{w}'_k (for example truncated distribution). The distribution of the control parameter is truncated by the feasible region and its uncertainty is then reduced. Considering the feasible region, the distribution of \mathbf{w}'_k becomes a truncated one as in (2.5) and the uncertainty of \mathbf{w}'_k is then reduced.

$$p_T(\mathbf{w}'_k) = \begin{cases} \frac{p(\mathbf{w}'_k)}{\int_{C_{\mathbf{w}'_k}} p(\mathbf{w}'_k) d\mathbf{w}'_k} & \text{for } \mathbf{w}'_k \in C_{\mathbf{w}'_k} \\ 0 & \text{otherwise} \end{cases} \quad (2.5)$$

The term $\int_{C_{w'_k}} p(w'_k) dw'_k$ could be analytically estimated for some special cases (i.e. if $C_{w'_k}$ is a linear inequality region and $p(w'_k)$ is a Gaussian distribution) or be estimated by Monte-Carlo integration.

With the aid of the environmental information (including the environmental interaction and constraints), the distribution of the control input of a dynamic model is modified to better reflect the target dynamics affected by the environment.

2.4.1.1.1 Simulations

As shown in [Ref.2.1.4], the statistics related to vehicles' road lateral positions in a real scenario (A2, Greenland, near Belfast High School) are surveyed (Note, the lateral position here is measured as a distance between the road edge and the vehicle's right wheel along the lateral direction of the road). The positions distribution is well fitted by a Gaussian model with the mean being 235 (cm) and standard variation being 24 (cm) as in Fig. 2.2.

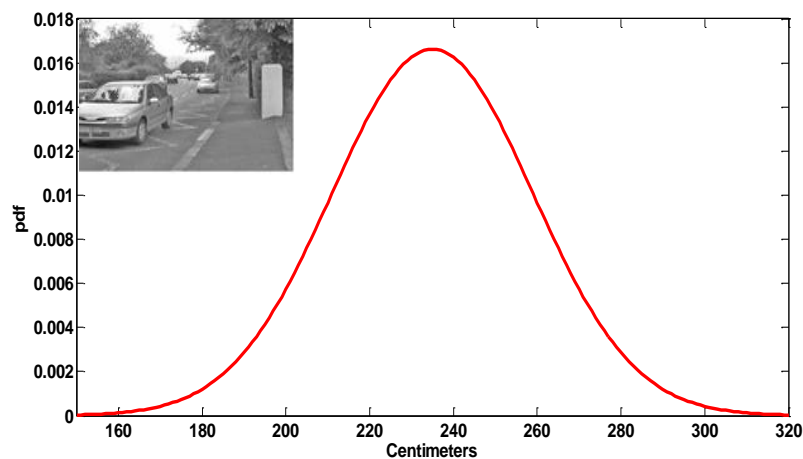


Fig. 2.2 The fitted Gaussian distribution of the lateral positions of vehicles.

Different modelling approaches are applied to simulate vehicle lateral positions, which include the original one as in (1), original one with imposing road constraints on the positions (both accept/reject and projection based methods as in [Ref.2.1.5] and [Ref.2.1.6] are tried to guarantee the generated vehicle positions lie within the constraint region) and our method with the environment related control input (including different force definition schemes). In this study, the constraint region for the lateral position is [150--320] (cm) as in [Ref.2.1.4] and both repulsive/attractive forces from the constraint region borders/centre are considered in our new modelling method. The original model in (1) is set to follow a widely applied constant velocity (CV) dynamic form as in [Ref.2.1.1].

For each modelling approach, different model parameter settings are chosen by grid search method [Ref.2.1.7] (the parameter settings for different models are listed in Table 2.1). Under each parameter setting, a particular modelling approach performs 100 Monte-Carlo simulations for vehicle lateral positions generation while

each simulation generates 100 position samples. The histogram of the generated lateral positions is compared with the one corresponding to the ground truth fitted Gaussian distribution with respect to the Bhattacharyya distance (denoted as B-distance) [Ref.2.1.7].

Table 2.1 Parameters settings for different modelling approaches

	Parameters	Setting values	Explanations
Original model	σ	$5 \cdot 10^{\text{linspace}(-1,1,10)}$	The standard deviation of the control parameter in the model
Original model with accept/reject			
Original model with projection			
Proposed modelling approach	A	$5 \cdot 10^{\text{linspace}(0,2,10)}$	The force parameter as in (2) and (3)
	B	$10^{\text{linspace}(-3,-1,10)}$	The force parameter as in (2) and (3)
	σ	$5 \cdot 10^{\text{linspace}(-1,1,10)}$	The standard deviation of the control parameter in the model

Note, $\text{linspace}(a,b,c)$ represents obtaining c samples from $[a,b]$ with equal intervals

The minimum B-distance obtained among all the modelling parameter settings for each model approach is chosen for comparison as shown in Table 2.2, and the corresponding histograms which achieve these minimum B-distances are plotted in Fig. 2.3. Results show that the proposed modelling approach with the new force definition achieves smaller minimum B-distance than the others and the related histogram has the most similar shape to the ground truth Gaussian distribution, which mean that the vehicle's realistic lateral movement could be most accurately reflected by the proposed dynamic model.

	Original model in (1)	Original model with Projection [Ref.2.1.4]	Original model with accept/reject [Ref.2.1.5]	Proposed method	
				Force definitions ([Ref.2.1.2],[Ref.2.1.3])	New force definition scheme
B-distance	0.4105	0.3702	0.3274	0.2198	0.1038

Table 2.2 The minimum B-distances for different modelling approaches

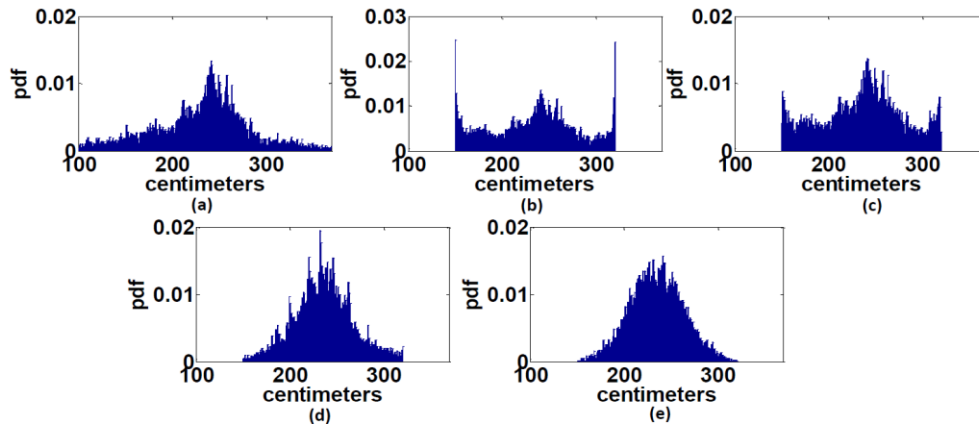


Fig. 2.3 The estimated histograms of generated lateral positions, which obtain the minimum Bhattacharyya distances to the ground truth one for different modelling approaches: (a) Original model (b) Original model with projection (c) Original model with accept/reject (d) Proposed modelling approach with the traditional force forms (e) Proposed modelling approach with new force forms.

A more accurate dynamic model which could better reflect the vehicle movement which be applied in different signal processing applications, such as vehicle tracking. The new dynamic model could improve the tracking performance, especially when the obtained measurements are limited.

2.4.1.2 Novel signal processing algorithms for target tracking aided by the new dynamic modelling approach

Based on the proposed new dynamic model approach, new target tracking algorithms which could effectively incorporate domain knowledge have been developed.

2.4.1.2.1 New moving horizon estimation framework for single target tracking

Moving horizon estimation (MHE) technique is a window-based state estimation technique. It could efficiently incorporate different types of constraints for an accurate state estimation. As mentioned in [Ref.2.1.8], MHE achieves the best performance in incorporating the non-linear and inequality constraints for state estimation compared with other methods.

In this work, we extend the MHE technique to incorporate more comprehensive domain knowledge. Both the environmental constraints and interactions are incorporated into the MHE framework for target tracking. Firstly, information related to environmental constraints could be directly incorporated for the target state estimation via the nature of the MHE algorithm; then, the new dynamic model whose control input is environment dependent is applied to build a new MHE framework to incorporate the environmental interaction information.

2.4.1.2.1.1 Moving horizon estimation framework

Considering a horizon length of N past time steps, the joint conditional density could be given by:

$$p(X_{k-N-1:k}|Y_{0:k}) = c \prod_{j=k-N}^k p(\mathbf{y}_j|\mathbf{x}_j) \prod_{j=k-N}^k p(\mathbf{x}_j|\mathbf{x}_{j-1}) p(\mathbf{x}_{k-N-1}|Y_{0:k-N-1}) \quad (2.6)$$

where $X_{k-N:k} = \{\mathbf{x}_{k-N}, \dots, \mathbf{x}_k\}$ represents the ensemble of state vectors and $Y_{0:k} = \{\mathbf{y}_0, \dots, \mathbf{y}_k\}$ is the ensemble of measurements. c is a normalization factor.

For target state estimation, our aim is to find the optimal $X_{k-N:k} = \{\mathbf{x}_{k-N}, \dots, \mathbf{x}_k\}$ which maximizes (2.6). In order to achieve this, we try to minimize the MHE cost function, which is a negative logarithm of the joint density in (2.6):

$$\phi_k^* = \arg \min_{X_{k-N:k}} \|\mathbf{x}_{k-N-1} - \hat{\mathbf{x}}_{k-N-1}\|_{I^{-1}}^2 + \sum_{j=k-N}^k \|\mathbf{x}_j - f(\mathbf{x}_{j-1})\|_{Q^{-1}}^2 + \sum_{j=k-N}^k \|\mathbf{y}_j - h(\mathbf{x}_j)\|_{R^{-1}}^2, \quad \text{where } \mathbf{x}_{k-N}, \dots, \mathbf{x}_k \in C_x \quad (2.7)$$

where $f(\mathbf{x}_j)$ is determined according to the state model and $h(\mathbf{x}_j)$ is determined by different types of measurement models (radar and camera). Q and R represent the covariance matrices of the process and measurement noises. C_x represents the environmental constraint on the state vector. $\hat{\mathbf{x}}_{k-N-1}$ and I represent the estimated mean and covariance of the distribution-- $p(\mathbf{x}_{k-N-1}|Y_{0:k-N-1})$ as in (2.6).

2.4.1.2.1.2 MHE for incorporating the interaction with environment

Traditionally, $f(\mathbf{x}_j)$ takes the form of (2.1) without considering the effect of the environmental information on the model control input. By applying a force term $f^{environment}$ to represent the interaction between a target and its surrounding environment, the state model could be represented as:

$$f(\mathbf{x}_j) = F\mathbf{x}_{j-1} + G\left(\frac{f^{environment}}{m} + \mathbf{w}_k\right) \quad (2.8)$$

from equations (2.1) and (2.4).

The new state model with the form (2.8) leads to the new form of state representation as:

$$\mathbf{x}_k = F^{N+1}\mathbf{x}_{k-N-1} + \sum_{i=0}^N F^{N-i} G \left(\frac{f^{environment}}{m} + \mathbf{w}_k \right) \quad (2.9)$$

By substituting (2.8) and (2.9) into (2.7), a new MHE function is then derived. The new MHE function considers both the environmental constraints (by C_x) and the interaction information (by applying new state model with additional force terms).

Due to the non-quadratic property of (2.7) caused by the non-linear state or measurement models, global optimization methods such as the generic algorithm could be applied to solve the optimization problem in (2.7).

2.4.1.2.1.3 Simulation results

For the simulation study, we follow the previous study of [Ref.2.1.9] to set up the test scenario. A moving vehicle on a circular road section is considered as shown in Figure 2.4. The road is defined by two boundaries with two arcs of $r_1 = 96\text{m}$ and $r_2 = 100\text{m}$, respectively, centered at the origin of a Cartesian coordinate system. The vehicle dynamics is described by a constant velocity (CV) model and it is assumed that the range and bearing angle of the vehicle are measured.

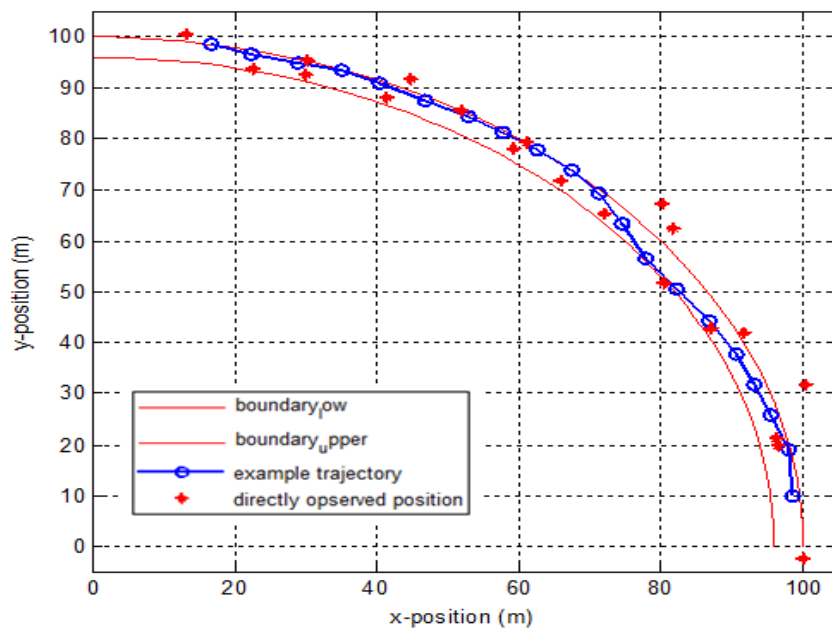


Fig. 2.4 The example trajectory and observed positions of a vehicle moving on a bend road segment.

Figs. 2.5 and 2.6 show the comparison results between the traditional MHE approach which considers the road constraint (denoted as C-MHE for short), and the proposed new MHE approach (denoted as IC-MHE) which considers both the constraint and the interaction between the road boundary and target (represented by force as in (2)). It is shown that the C-MHE method always estimates the vehicle position to be at the road boundary (as the green line in Fig. 2.6), which is not accurate. The proposed IC-MHE method achieves a more accurate estimated trajectory with smaller root mean square error (RMSE).

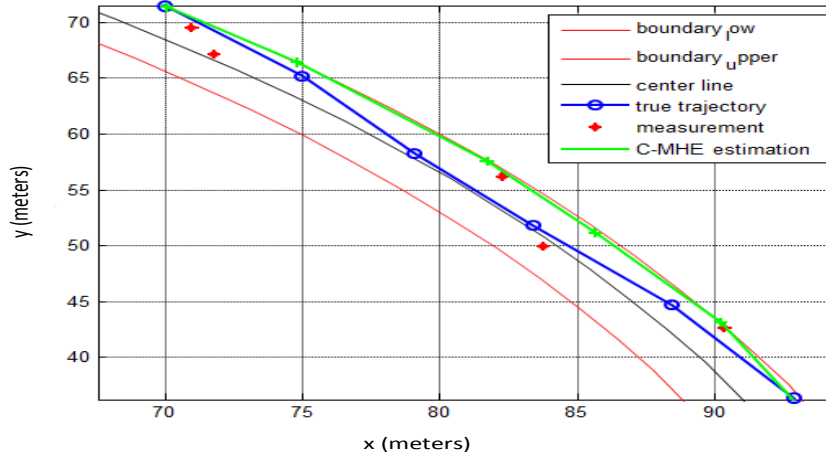


Fig. 2.5 Estimation results by the traditional MHE, with the root mean square error (RMSE) being 5.82 meters. The estimated positions are always on the road boundary, which are not accurate.

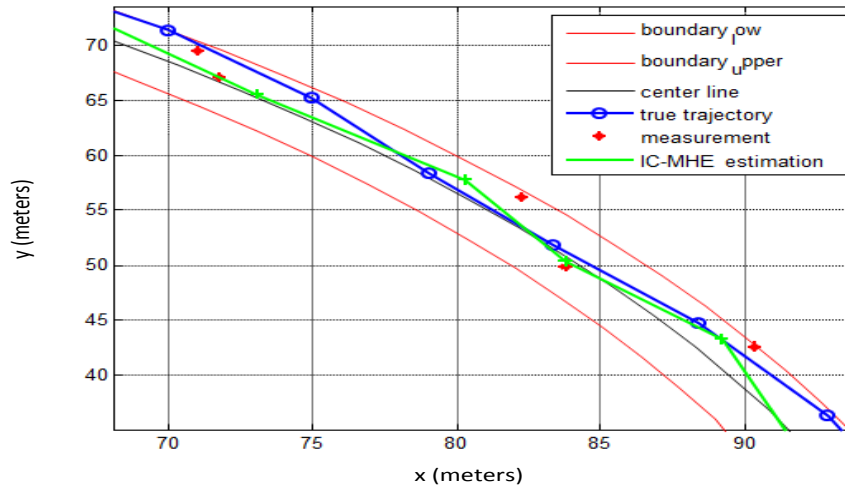


Fig. 2.6 Estimation results by the new MHE approach, with the root mean square error (RMSE) being 2.99 meters.

2.4.1.2.2 A novel Bayesian inference algorithm for target tracking aided by a new hybrid modelling system

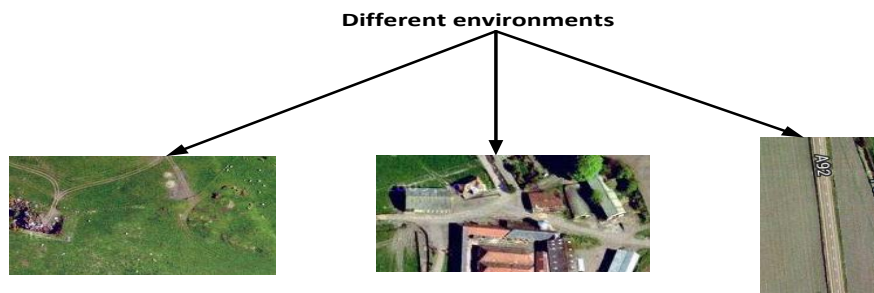
Driven by the fact that in a realistic scenario, a vehicle moves in different regions and is then affected by different environmental conditions, it is unlikely that one dynamic model can reflect the realistic movement of a target in different operational environments well. To reflect this realistic movement of a vehicle, a new hybrid modelling system is proposed. This hybrid modelling system contains multiple dynamic models with the control parameters being related to the corresponding environmental information for a particular model m_k . In this way, the vehicle's movements in different regions affected by different environmental conditions could

be reflected by multiple dynamic models. Besides, the transition between different dynamic models could be set to a non-Markov jump form. The transition probabilities between different dynamic models are thereby not assumed to be constant, but in a more realistic *state-dependent* way.

Based on the new hybrid modelling system, the corresponding Bayesian inference framework is then developed for target state estimation. Considering the incorporation of the environmental information (both the environmental interaction and environmental constraints) into dynamic models makes them neither linear nor Gaussian, different types of Sequential Monte Carlo (SMC) methods are therefore applied to implement the Bayesian inference framework.

2.4.1.2.2.1 A new hybrid modelling system

The dynamics of a vehicle moving in a realistic environment are affected by surrounding environmental conditions; besides, a vehicle may move in a different environment (such as on road or off road) in realistic. In order to accurately reflect the realistic movement of a vehicle affected by different environmental conditions, multiple state models are applied as in Fig. 2.7. Each model is used for describing the vehicle movement in a particular environment condition and the control input of the dynamic model is environment dependent.



Multiple dynamic models: $s_{t+1} = F_t(s_t, m_1) + Gw_t(m_1)$ $s_{t+1} = F_t(s_t, m_2) + Gw_t(m_2)$ $s_{t+1} = F_t(s_t, m_3) + Gw_t(m_3)$

Fig. 2.7 Different dynamic models whose control parameters are environment dependent are applied to describe movements in different environment.

The environment condition of the moving target depends on the target's state (such as the position and velocity). The transitions between different environment conditions are then state-dependent. Considering the fact that different environment conditions associate with different dynamic models, so the transition probabilities between different dynamic models are also represented in a realistic state-dependent way as in [Ref.2.1.10].

The structure of the proposed hybrid modelling system is presented in Fig. 2.8. Multiple models are involved and the particular model m_k associated with particular environmental conditions at a particular time instance depends on the target state

X_{k-1} . And the control input w_k , which determines the target dynamic, is environmental dependent. Y_k in the Fig. 2.8 represents the measurements.

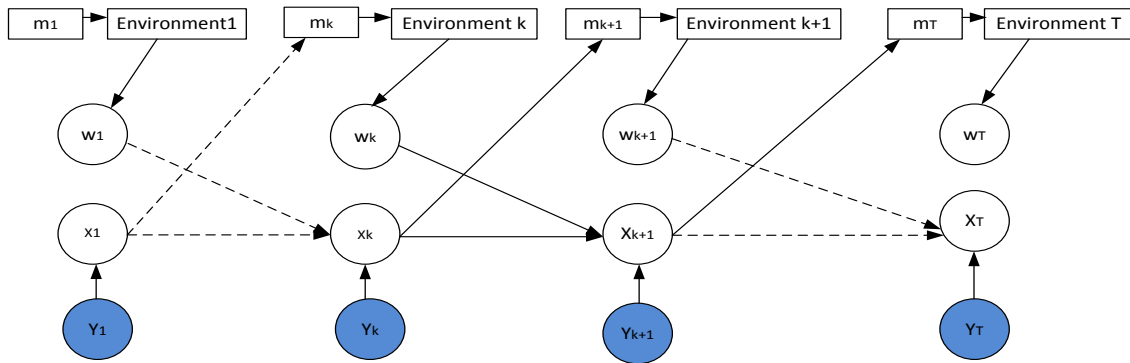


Fig. 2.8 The graph representation of the proposed new hybrid modelling system.

2.4.1.2.2.2 Bayesian inference framework of the new hybrid model system for state estimation

Based on the proposed new hybrid modelling system, a Bayesian inference framework can be derived for the state estimation which is divided into the following four steps (x_t represents the state vector, Y_t represents the measurements and m_t represents the model index):

- Mixing:

$$p(x_{t-1}, m_{t-1} | Y_{t-1}) \xrightarrow{\text{Mixing}} p(m_t | Y_{t-1})$$

$$p(m_t | Y_{t-1}) = \int \sum_{m_{t-1} \in M} p(m_t, x_{t-1}, m_{t-1} | Y_{t-1}) d x_{t-1}$$

$$= \int \sum_{m_{t-1} \in M} p(m_t | x_{t-1}, m_{t-1}) p(m_{t-1}, x_{t-1} | Y_{t-1}) d x_{t-1}$$

(2.10)

- Interacting:

$$p(x_{t-1} | m_{t-1}, Y_{t-1}) \xrightarrow{\text{Interacting}} p(x_{t-1} | m_t, Y_{t-1})$$

$$p(x_{t-1} | m_t, Y_{t-1}) = \frac{p(x_{t-1}, m_t | Y_{t-1})}{p(m_t | Y_{t-1})}$$

$$= \frac{\sum_{m_{t-1} \in M} p(m_t | x_{t-1}, m_{t-1}) p(x_{t-1}, m_{t-1} | Y_{t-1})}{p(m_t | Y_{t-1})}$$

(2.11)

- Evolving:

$$p(\mathbf{x}_{t-1}|m_t, \mathbf{Y}_{t-1}) \xrightarrow{\text{Evolving}} p(\mathbf{x}_t|m_t, \mathbf{Y}_{t-1})$$

$$p(\mathbf{x}_t|m_t, \mathbf{Y}_{t-1}) = \int p(\mathbf{s}_{t-1}|m_t, \mathbf{Y}_{t-1}) p(\mathbf{x}_t|\mathbf{x}_{t-1}, m_t, \mathbf{Y}_{t-1}) d\mathbf{x}_{t-1}$$
(2.12)

where the state evolution probability $p(\mathbf{x}_t|\mathbf{x}_{t-1}, m_t, \mathbf{Y}_{t-1})$ is derived from the distribution of the environment dependent control parameter ($p(\mathbf{w}_t)$ in (2.5)) as:

$$p(\mathbf{x}_t|\mathbf{x}_{t-1}, m_t, \mathbf{Y}_{t-1}) = \int \delta(\mathbf{x}_t - F_k(\mathbf{x}_t, m_t) - G\mathbf{w}_t) p(\mathbf{w}_t) d\mathbf{w}_t$$
(2.13)

- Correcting:

$$p(\mathbf{x}_t|m_t, \mathbf{Y}_{t-1}) \xrightarrow{\text{Correction}} p(\mathbf{x}_t|m_t, \mathbf{Y}_{t-1})$$

$$p(\mathbf{x}_t, m_t|\mathbf{Y}_t) \propto p(\mathbf{y}_t|\mathbf{x}_t, m_t) p(\mathbf{x}_t|m_t, \mathbf{Y}_{t-1}) p(m_t|\mathbf{Y}_{t-1})$$
(2.14)

2.4.1.2.2.3 Sequential Monte-Carlo implementation

Considering the non-linearity and non-Gaussianity of the dynamic model due to incorporation of the environmental information, the SMC technique is applied to implement the Bayesian inference framework. If we assume initially, $\{u_{t-1}^{r,i}, \mathbf{x}_{t-1}^{r,i}\}_{i=1,\dots,N}$ are applied to represent $p(\mathbf{x}_{t-1}, m_{t-1} = r|\mathbf{Y}_{t-1})$, the Bayesian inference could be implemented as:

- Mixing:

$$p(m_t = m|\mathbf{Y}_{t-1}) \approx \sum_{r \in M} \sum_{i=1}^N p(m_t = m|\mathbf{x}_{t-1}^{r,i}, m_{t-1} = r) u_t^{r,i} \equiv \Lambda_{t-1}^u$$
(2.15)

- Interacting:

$$p(\mathbf{x}_{t-1}|m_t = m, \mathbf{Y}_{t-1}) \approx \frac{\sum_{r \in M} \sum_{i=1}^N p(m_t = m|m_{t-1} = r, \mathbf{x}_{t-1}^{r,i}) u_t^{r,i} \delta(\mathbf{x}_{t-1} - \mathbf{x}_{t-1}^{r,i})}{\Lambda_{t-1}^u}$$
(2.16)

N particles $\{\bar{\mathbf{x}}_{t-1}^{m,i}\}_{i=1,\dots,N}$ are resampled from (2.16) to represent $p(\mathbf{x}_{t-1}|m_t = m, \mathbf{Y}_{t-1})$.

- Evolving:

$$p(\mathbf{x}_t|m_t = m, \mathbf{Y}_{t-1}) \approx \sum_{i=1}^{N'} u_{t-1}^{m,i} \delta(\mathbf{x}_t - \mathbf{x}_t^{m,i})$$

where $\mathbf{x}_t^{m,i} = F_k(\bar{\mathbf{x}}_{t-1}^{m,i}, m_t = m) + G\mathbf{w}_t^i$ & $\mathbf{x}_t^{m,i} \in \mathcal{C}_x$

(2.17)

C_x is the constraint region of the state vector and \mathbf{w}_t^i is the control input sample. In our work, two sampling approaches are applied to obtain \mathbf{w}_t^i :

- I. Directly sampling from the control input distribution $p(\mathbf{w}_t')$ (generic SMC method)
- II. Sampling from an importance function $p(\mathbf{w}_t'|\mathbf{Y}_t)$ which incorporates the measurement information. In this work, this importance function is designed by an unscented Kalman filtering method.

Both of these two control parameter sampling methods are implemented and compared in our simulation study.

- Correcting:

$$\begin{aligned}
 p(\mathbf{x}_t, m_t = m | \mathbf{Y}_{t-1}) &\propto p(\mathbf{y}_t | \mathbf{x}_t, m_t = m) \sum_{i=1}^N u_{t-1}^{m,i} \delta(\mathbf{x}_t - \mathbf{x}_t^{m,i}) \Lambda_{t-1}^s \\
 &= \sum_{i=1}^N u_t^{m,i} \delta(\mathbf{x}_t - \mathbf{x}_t^{m,i})
 \end{aligned}
 \tag{2.18}$$

New particle set $\{u_t^{m,i}, \mathbf{x}_t^{m,i}\}_{i=1, \dots, N}$ for every model m at time t is obtained, which could be applied for the state estimation.

The proposed algorithm based on the Bayesian inference framework for a new modelling system is generic. Firstly, it could be applied for single/multiple tracking problems with different types of sensors (radar, camera). Besides, assisted by data association or the random finite set (RFS) technique, the proposed algorithm could be directly extended to deal with more complicated scenarios such as the miss detection/ false alarms.

2.4.1.2.2.3 Simulation results

The proposed algorithm is tested on two scenarios:

Scenario I: For the first scenario, a vehicle moves along road segments $A \rightarrow B \rightarrow C \rightarrow D \rightarrow E$ as in Fig. 2.9 in a simulated road network. An observer is placed at the position (-100m, 150m), which measures the range and bearing angle of the moving vehicle. It is assumed the speed limitation of the road network is 30 miles/hour.

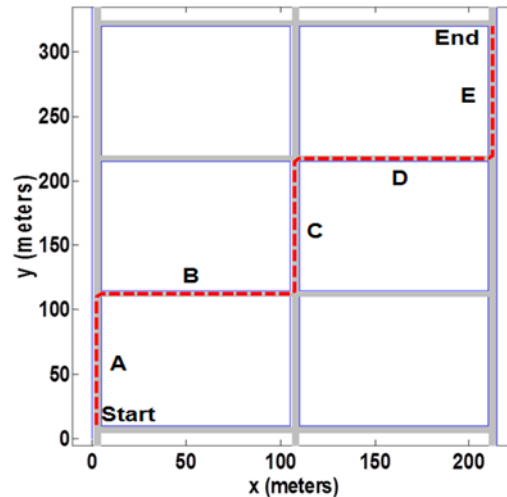


Fig. 2.9 The trajectory of a vehicle moving in a road network.

A constant velocity (CV) based model is applied as the state model for target tracking. Our proposed algorithm incorporates both the environmental constraints and the interaction between vehicle and environment into the control input of the related state model. The environmental constraints are imposed by the road network and interactions between the vehicle and environment including:

- i. the interaction between the vehicle and road border (the vehicle will keep a distance from the road border) , which is modelled as a repulsive force between the road boundary and vehicle with the form of (22.)
- ii. the interaction between the vehicle's velocity and the speed limitation (the vehicle will decrease its speed when it approaches or exceeds the speed limitation), which is represented by a force which is related to the vehicle velocity.

In different road segments, the environment constraint and forces from the boundary will be different, thus different dynamic models are applied. The transitions between different dynamic models are set in a state-dependent way as in Fig. 2.10. When the vehicle is in the interaction area of different road segments, the transition probabilities to the dynamic model C_i corresponding to connected road segments are equal. Otherwise, it is assumed that the vehicle stays on the same road segment and the transition probabilities to other dynamic models are zeros.

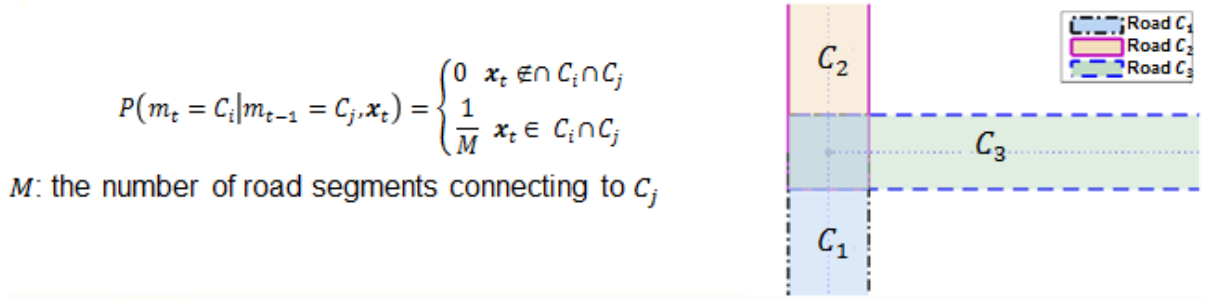


Fig. 2.10 The transition between different dynamic models corresponding to different road segments.

Fig. 2.11 (c) shows the tracking result of our proposed algorithm. For comparison, the results of the algorithm without applying the domain knowledge (SMC technique is applied for a fair comparison) and with the road constraint information as in [Ref.2.11] are presented in Fig. 2.11 (a) and Fig. 2.11(b). We can see that the proposed algorithm, which applies a new hybrid modelling approach to fully exploit the environmental information, achieves the most accurate tracking result.

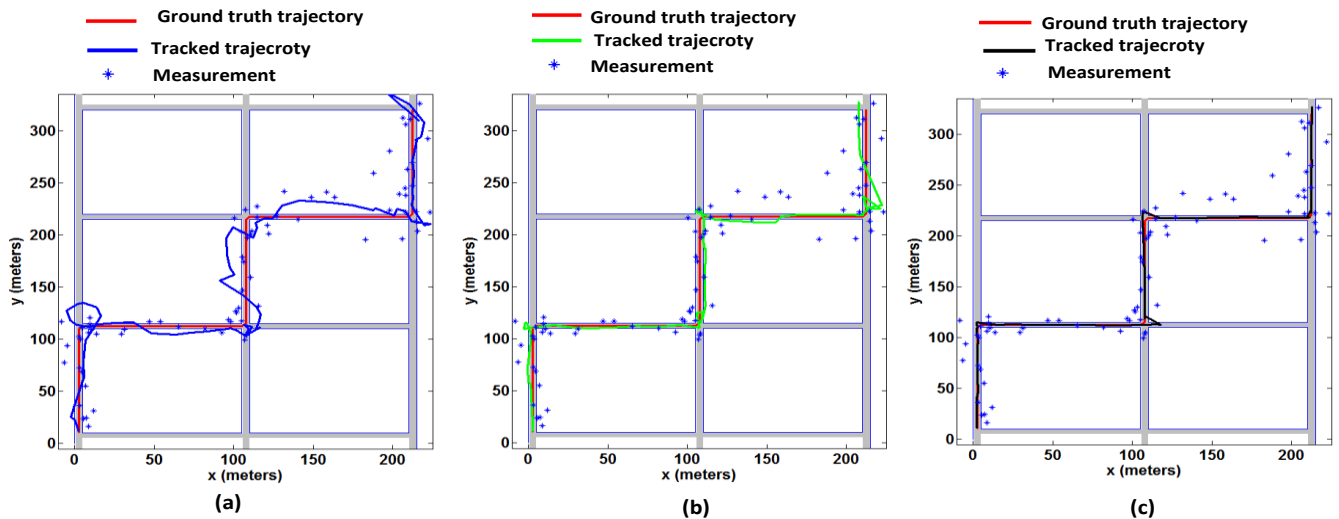


Fig. 2.11 The comparison of the tracking results between different algorithms, (a) tracking result by the particle filtering algorithm without considering the environmental information, with RMSE=26.85 (meters) (b) tracking result with the particle filtering algorithm with road network constraint, with RMSE=13.31 (meters) (c) tracking result by our proposed algorithm, with RMSE=7.47 (meters).

For a comprehensive evaluation, 50 trials of Monte-Carlo simulations are performed for RMSEs estimation. The averaged RMSE at each time instance for 50 Monte-Carlo simulations corresponding to different algorithms are plotted in Fig. 2.12 (a), from which it is shown that the proposed algorithm achieves the smallest RMSEs during all the time instances. Besides, we also compare the implementation of the Bayesian inference framework by different SMC implementations:

- (i) a generic SMC implementation method

(ii) a new SMC implementation method which applies the unscented Kalman filtering scheme for incorporating measurement information, to construct an importance function for sampling the control input used for evolution as in (17).

The comparison results are shown in Fig. 2.12 (b). It is shown that better performance could be achieved by applying the new SMC implementation method

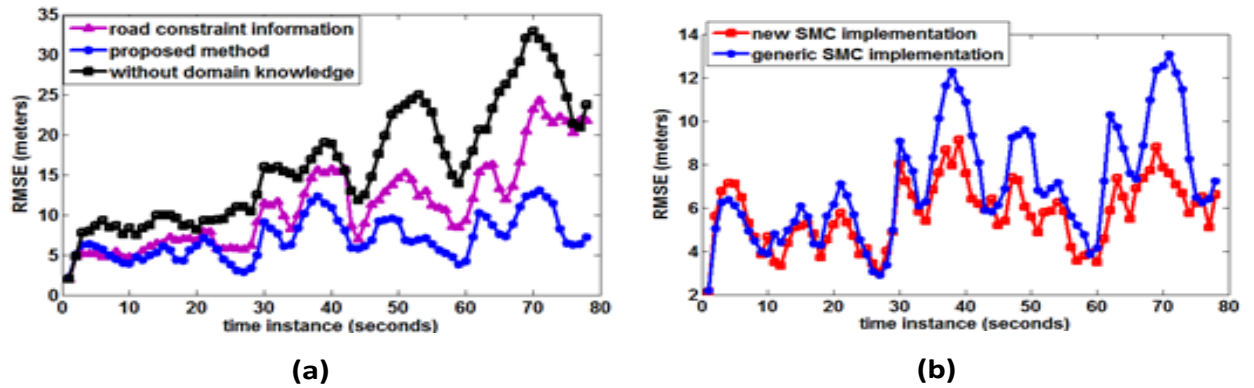


Fig. 2.12 The comparison of the averaged RMSEs for (a) different algorithms (b) different implementation methods for the Bayesian inference framework based on proposed new hybrid modelling scheme.

Scenario II: For the second scenario, we consider a more realistic environment. Three vehicles are simulated to move in a realistic region (near Loughborough, and the region’s geographic information is obtained from the GIS) as in Fig. 2.13. The ranges and bearing angles of three vehicles are measured. For a more realistic scenario, both the miss detection (with a detection probability $P_d=0.9$) and false alarms (with clutter rate $\gamma = 6.4 \times 10^{-5}$ (false alarms/area/scan)) are considered. The speed limitations of the main road (the road segment along the east-west direction) and side road (the road segment along the north-south direction) are 30 miles/hour and 20 miles/ hour respectively.

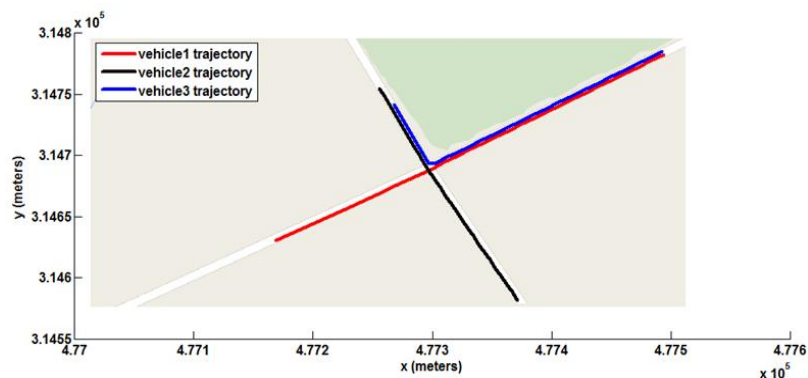
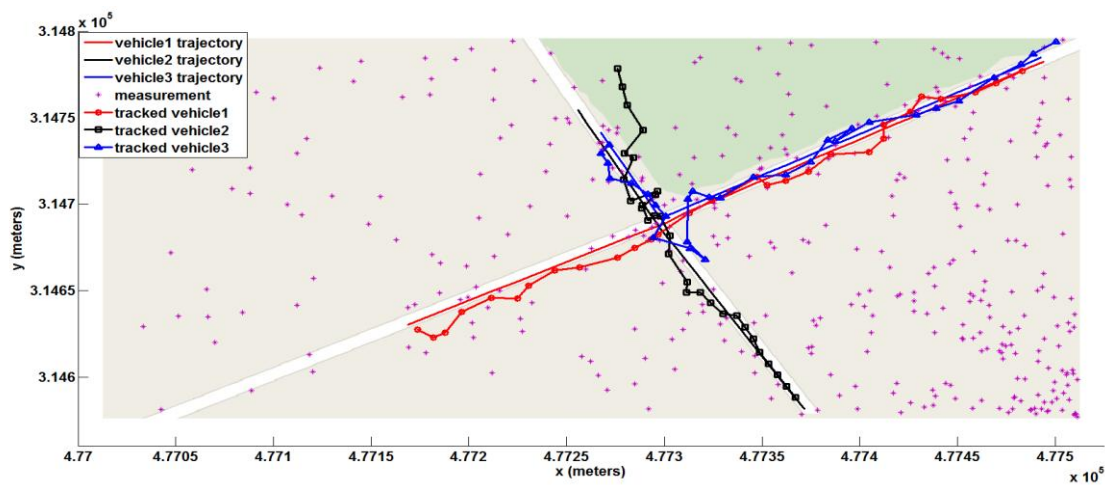


Fig. 2.13 The simulated trajectories of three vehicles moving in a realistic environment.

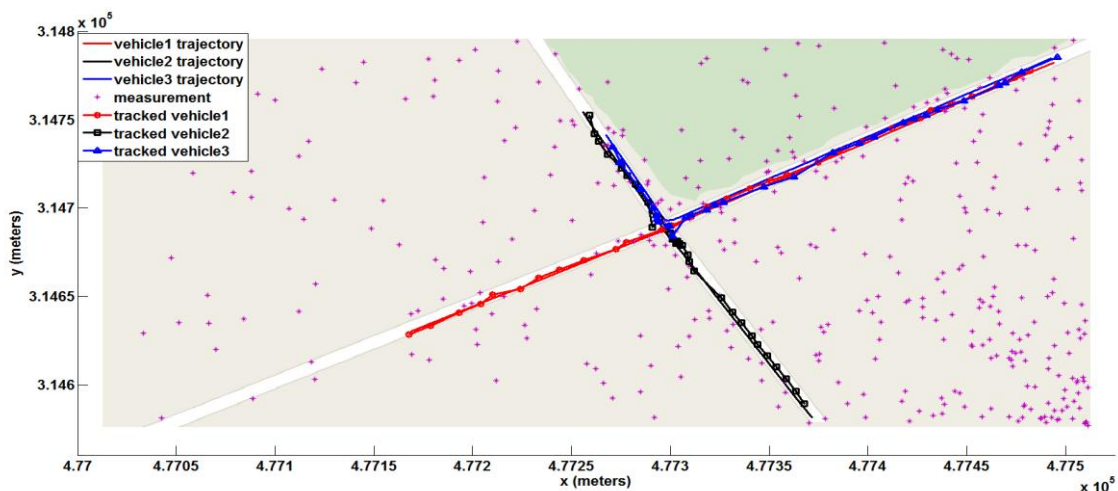
Similar to the scenario I, both the environmental constraints and interactions (including the interaction between the vehicle and road boundary and the interaction between the vehicle speed and speed limitation) are considered by incorporating them to model the dynamic model control input in an environment dependent way.

Besides, two more interactions are considered in this scenario which include: i. the interaction between different vehicles ii. the interaction between vehicles in the minor road and the junction (the vehicle in the minor road will slow down when it approaches the junction). These two interactions are represented by forces which have similar forms to (2) and (3).

Different dynamic models are applied in different road segments and the transition between different dynamic models is defined in the same way as scenario I.



(a)



(b)

Fig. 2.14 The tracking results with (a) SMC-JPDAF algorithm [Ref.2.1.12] without considering the environmental information (b) proposed algorithm.

The comparison between the tracking results with/without considering the environment information is illustrated in Fig. 2.14. The SMC technique is applied in different algorithms for a fair comparison and in order to deal with miss detection/false alarms, the joint probability data association (JPDA) technique [Ref.2.1.12] is applied for data association (other different data association techniques or the algorithm based on Random Finite Set (RFS) could also be applied). We can see that more accurate tracking results for the three vehicles are obtained by the proposed algorithm which fully exploits the environment information.

For a comprehensive numerical analysis, 50 trials of Monte-Carlo simulations are made. For each trial, the RMSE between the tracked positions and the ground truth ones are calculated. The mean and standard deviation of 50 RMSEs for three vehicles are calculated as in Table 2.3. It is shown that our proposed algorithm can achieve better performance with both the smallest mean and standard deviation of 50 RMSEs than the SMC-JPDAF algorithm in [Ref.2.1.2] without considering the domain knowledge and the extension of the work of [Ref.2.1.11] by incorporating the road constraint in a more complicated JPDAF framework.

Table 2.3 Mean and standard deviation of the 50 tracking trials' RMSEs for three vehicles by different approaches

	SMC-JPDAF in [Ref.2.1.12]	Extension of [Ref.2.1.11]	Proposed method
Mean of RMSEs for vehicle 1 (meters)	12.36	9.53	7.10
Standard deviation of RMSEs for vehicle 1(meters)	8.54	8.26	2.74
Mean of RMSEs for vehicle 2 (meters)	26.54	17.85	10.80
Standard deviation of RMSEs for vehicle 2 (meters)	16.88	11.77	4.28
Mean of RMSEs for vehicle 3 (meters)	21.66	17.07	10.16
Standard deviation of RMSEs for vehicle 3 (meters)	6.63	7.05	3.16

2.4.2 Technical Details of WP2.2

Many problems associated with sensors in networked battlefield require optimization of certain criteria such as detection probability of targets or signal to noise plus interference ratio (SINR) under various constraints such as transmission power, available bandwidth, false alarm rate and delay. Convex optimization techniques naturally fit to handle various practical constraints and provide mathematically tractable solutions. On the other hand, game theory is a mathematical process for analysing strategic interactions between various rational players or entities. There are emerging applications of game theory in networked battlefield such as distributed resource allocations in radar and sensor networks, tracking intelligent targets and electronic counter measures. The aim of this work package is to handle uncertainty using convex optimization and game theoretic frameworks. This includes distributed optimization of various sensor or radar parameters for enhancing detection performance under uncertainty, for example created deliberately by jamming or naturally due to lack of knowledge of the environment and various battlefield activities. We tackle these using a variety of signal processing approaches, however, with application of interests in radars, though the proposed methods can be readily extended to other applications including sonars, and other sensors. Our immediate contributions have been on distributed power allocations and waveform design for radar networks using game theory, which will be extended to handle uncertainties created by jamming. The distributed game theoretic power allocation techniques have been presented in year 1 report, hence we present only the distributed waveform selection method using game theory in Section 2.4.2.1. The second contribution in Section 2.4.2.2 is on convex optimization based signal processing algorithm for fully overlapping subarrays based waveform diversity and beamforming in radars. This work will be extended to include uncertainty on array manifold, target location etc. The work presented in.

2.4.2.1 Distributed waveform allocation for statistical MIMO radar network using game theory

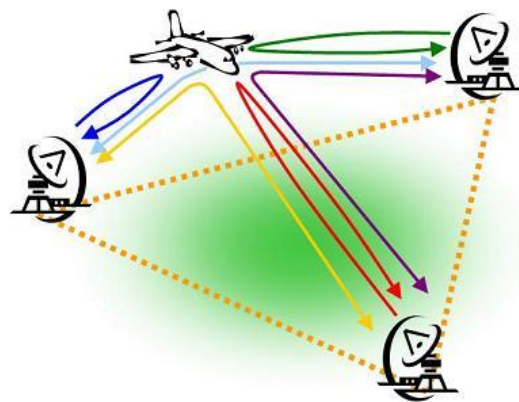


Figure 2.15: An example radar network.

We considered a surveillance scenario where multiple low power radars are placed in a geographical area without requiring any significant coordination among them. The whole radar network aims to achieve a common goal in terms of maximising SINR by choosing most appropriate waveforms for illumination of signals. As these multiple radars operate within the same frequency band, in order to mitigate interference, proper coordination among radars is required for the allocation of waveforms. However, in many situations, coordination among radars is neither feasible nor attractive. Hence, we proposed a non-cooperative waveform allocation technique for a radar network. We considered a set of clusters of radars as depicted in Figure 2.15, and assumed no communication between radars in various clusters; however, radars within each cluster have the ability to coordinate. The radars in each cluster are expected to determine appropriate set of waveforms for illumination so that signal to disturbance (noise plus clutter return) ratio (SDR, also known as SINR) is maximised at any radar receiver. Accordingly, radars in each cluster communicate to determine a set of orthogonal waveforms, while assuming no communication between radars in various clusters. We solved this problem using a non-cooperative potential game theoretic framework which offers the freedom to every MIMO radar group to act independently and select waveforms. The waveform allocation algorithm converges to a unique equilibrium known as Nash equilibrium.

2.4.2.1.1: Problem formulation and signal model

We consider a radar network C where the radars are partitioned into K clusters C_1, \dots, C_K , each containing M radars, $C_k = \{R_{1k}, \dots, R_{Mk}\}$. We assume that radars within the same cluster can exchange information, while communication between radars that belong to different clusters is infeasible. As a result, inter-cluster interference is unavoidable. However, clusters do not compete with each other; hence the interfering signals are unintentional.

The return signal at the n^{th} radar of cluster k is given by

$$x_{kn} = \sum_{r=1}^M \alpha_{krn} s_{kr} + \sum_{\substack{\ell=1 \\ \ell \neq k}}^K \sum_{t=1}^M \sum_{m=-N+1}^{N-1} J_m s_{\ell t} + \sum_{r=1}^M \sum_{\substack{m=-N+1 \\ m \neq 0}}^{N-1} \gamma_{krn,m} J_m s_{kr} + n_{kn},$$

where the first term is the return signal coming from the target, and the second term is the sum of interfering signals coming from radars in all clusters except from cluster k . Clutter returns and the system noise are described in the two last terms, respectively. The SDR for radar R_{kn} can be written as

SDR =

$$\frac{G_{knkn} \sum_{r=1}^M |\alpha_{krn}|^2 |s_{kr}^H s_{kr}|^2}{G_{knkn} \sum_{t=1}^M \sum_{r=1}^M \sum_{\substack{m=-N+1 \\ m \neq 0}}^{N-1} |Y_{ktn,m}|^2 |s_{kr}^H J_m s_{kt}|^2 + \sum_{\ell \neq k}^K \sum_{t=1}^M G_{\ell tkn} \sum_{r=1}^M \sum_{m=-N+1}^{N-1} |s_{kr}^H J_m s_{\ell t}|^2 + \sigma_n^2 \sum_{r=1}^M |s_{kr}^H s_{kr}|^2}$$

where $G_{\ell tkn}$ denotes the antenna gain for radar R_{kn} in the direction of the radar $R_{\ell t}$, for $k, \ell, n, t \in \{1, \dots, K\}$. The antenna gains are known to all radars in the network. The aim of each cluster is to determine an appropriate set of orthogonal waveforms for its radars to maximise SDR, using game theoretic decentralised methods.

2.4.2.1.2: Potential Game

We model the interaction of the clusters in the network as a potential game $\Gamma = \langle C, \{S_k\}_{k \in \{1, \dots, K\}}, \{u_k\}_{k \in \{1, \dots, K\}} \rangle$, where the clusters are the players. The action set S_k of the players $k = 1, \dots, K$ is a predefined set of waveforms that is assumed the same for all players and it is publicly known. The utility function for cluster k is defined as

$$u_k(s_1, \dots, s_K) = - \sum_{n=1}^M \left(\sum_{r=1}^M s_{kr}^H s_{kr} + G_{knkn} \sum_{t=1}^M \sum_{r=1}^M \sum_{\substack{m=-N+1 \\ m \neq 0}}^{N-1} |s_{kr}^H J_m s_{kt}|^2 \right. \\ \left. + \sum_{\substack{\ell=1 \\ \ell \neq k}}^K \sum_{t=1}^M G_{\ell tkn} \sum_{r=1}^M \sum_{m=-N+1}^{N-1} |s_{kr}^H J_m s_{\ell t}|^2 + \sum_{\substack{\ell=1 \\ \ell \neq k}}^K \sum_{t=1}^M G_{kn\ell t} \sum_{r=1}^M \sum_{m=-N+1}^{N-1} |s_{\ell r}^H J_m s_{kt}|^2 \right).$$

The clusters engage in an iterative process, where at time t player k updates the waveform according to the following maximisation

$$s_k^t = \arg \max_{s_k \in S_k} P(s_1^t, \dots, s_{k-1}^t, s_k, s_{k+1}^{t-1}, \dots, s_K^{t-1}),$$

where $P(s_1, \dots, s_K)$ is the potential function of the game and is defined as

$$P(s_1, \dots, s_K) = - \sum_{k=1}^K \sum_{n=1}^M \left(\sum_{r=1}^M s_{kr}^H s_{kr} + G_{knkn} \sum_{t=1}^M \sum_{r=1}^M \sum_{\substack{m=-N+1 \\ m \neq 0}}^{N-1} |s_{kr}^H J_m s_{kt}|^2 \right. \\ \left. + \sum_{\substack{\ell=1 \\ \ell \neq k}}^K \sum_{t=1}^M G_{\ell tkn} \sum_{r=1}^M \sum_{m=-N+1}^{N-1} |s_{kr}^H J_m s_{\ell t}|^2 \right).$$

The clusters update their waveforms in a sequential manner, until the game theoretic algorithm converges to equilibrium. At each time step, only one cluster updates the waveform.

2.4.2.1.3: Uniqueness of the Equilibrium

The existence of the equilibrium is guaranteed due to the finite nature of our game, with respect to the number of players and their action sets. The equilibrium, as the (optimum) action set, strongly depends on the waveform library that is chosen for a particular application. Hence, we examine its uniqueness only for the specific waveform library.

In general, the set of equilibria does not coincide with the set of points that maximise the potential function, but it includes it. According to a result in [Ref 2.2.1] if the potential function satisfies the larger midpoint property (LMP), then these two sets are identical. Hence, the problem of proving uniqueness of the equilibrium for potential games reduces to showing that the potential function has a unique maximiser, which is a less complex task. Using results on discrete convexity [Ref 2.2.1]), we have mathematically proven that the potential function of our model satisfies the LMP. Due to the discrete nature of the waveform library and its reasonable size, it was possible to evaluate the potential function on all waveforms, and show that the equilibrium is unique for the specific library.

2.4.2.1.3 Simulation Results

For the simulation, we considered two network topologies. For the first case, the MIMO radar network consists of two clusters with two radars each ($K = 2, M = 2$), while for the second case, we have three clusters with two radars each $K = 3, M = 2$. The initial waveforms for all clusters are chosen randomly from a set of possible waveforms. The waveforms that are used by radars from different clusters might be correlated.

Fig. 2.16a and Fig. 2.16b show the convergence of the game theoretic algorithm to equilibrium (solid line) for the two network configurations. In Fig. 2.16a, the network consists of two clusters with two radars in each cluster, while in Fig. 2.16b we have three clusters with two radars per cluster. The sequential update of the waveform for each player is clearly depicted. In order to demonstrate the advantages of our game theoretic model, both Fig. 2.17 and Fig 2.18 show also the SDR for the players when they choose the waveforms randomly (random choice model). For each player in the random choice model, the SDR is the average over 100 realisations. The game theoretic waveform selection provides substantially better SDR as compared to selection of waveforms randomly.

Fig. 2.17 shows effect of network size on the SDR of the first player. As seen, good performance of the game theoretic model is preserved, independently of the size of the network. Additionally, we tested our game theoretic algorithm on a waveform library developed by Strathclyde University [Ref 2.2.2]. The results depicted in Fig. 2.18 confirm superior performance of the game theoretic method as compared to random waveform allocation.

Simulation results for all different network configurations illustrated the convergence of the game theoretic algorithm to Nash equilibrium, where significant performance improvement as compared to random waveform allocation is obtained. The convergence of the algorithm to unique Nash equilibrium has been proven mathematically using larger midpoint property and discrete concavity [4]. This enabled various players to select transmission waveforms optimally regardless of the initialization of other players.

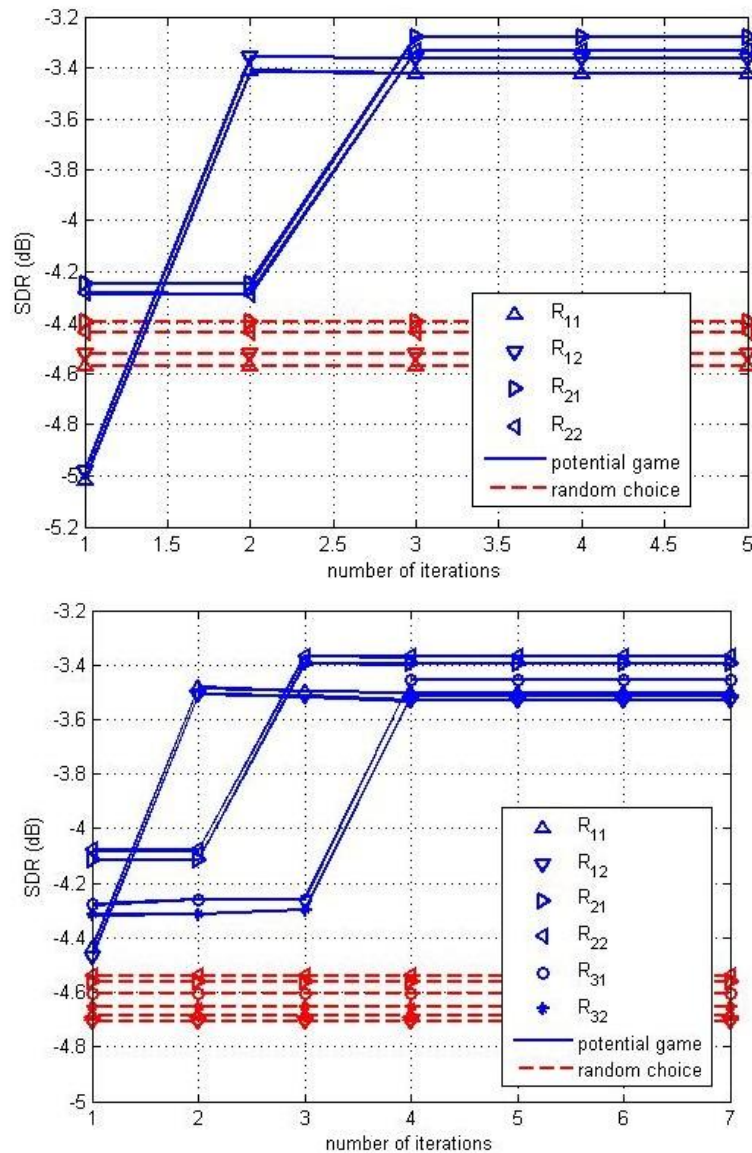


Figure 2.16 SDR values for all radars using the game theoretic model and the random choice. (a) (top) Network of two clusters with two radars per cluster (b) Network of three clusters with two radars per cluster.

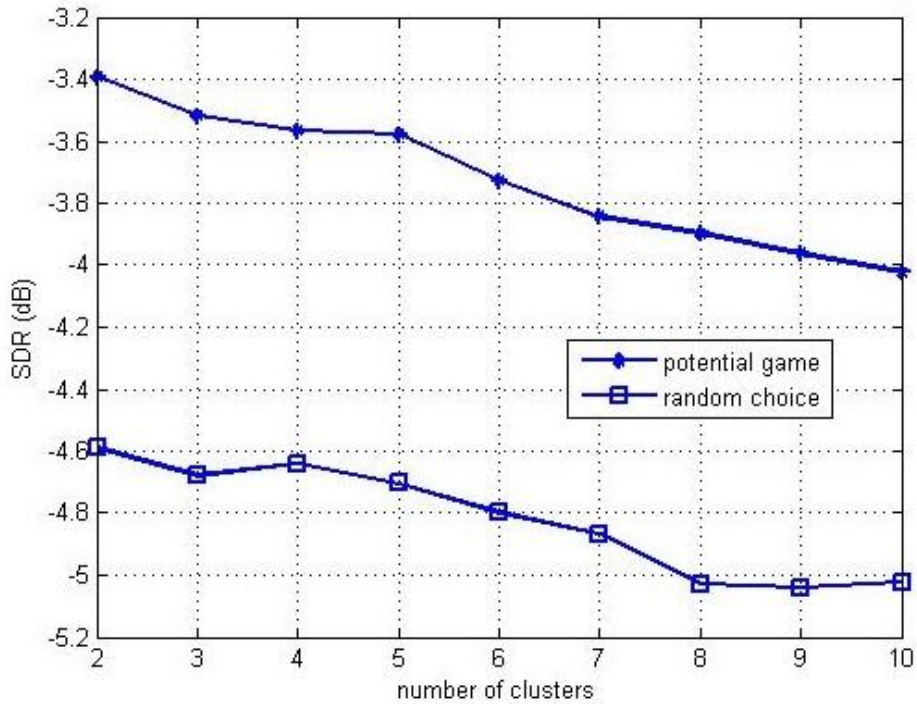


Figure 2.17 Average of the two SDR values of the radars R_{11} and R_{12} in the game theoretic model and the random choice for a network with increasing number of clusters. All clusters in the network consist of two radars.

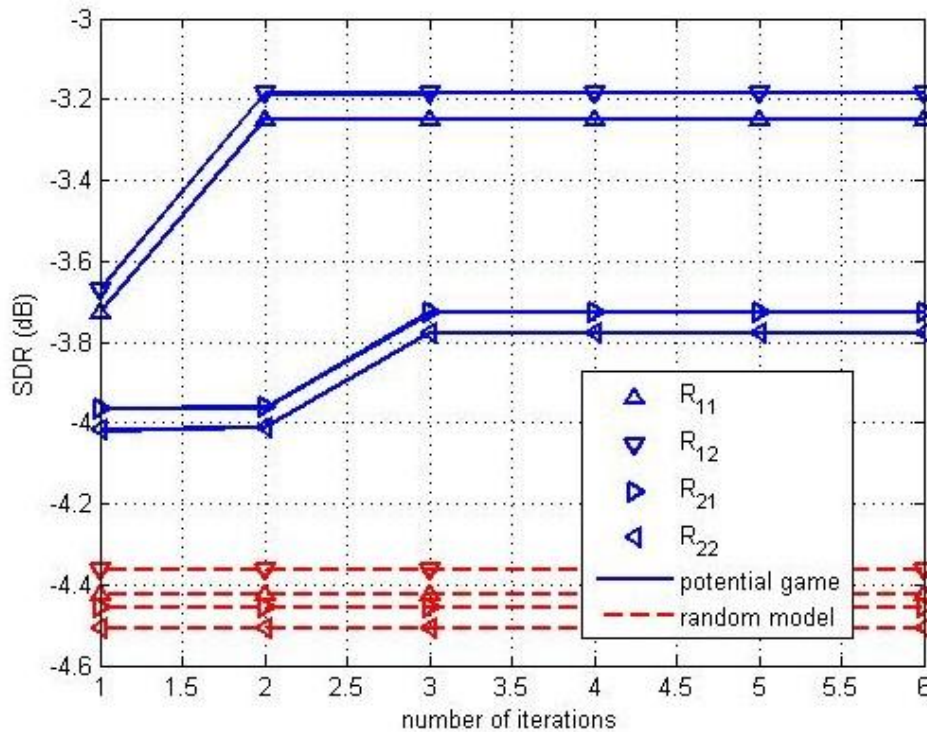


Figure 2.18 SDR values for all radars using the game theoretic model and the random model. Network of two clusters with two radars in each cluster.

[The action set of the clusters is a waveform library provided by Strathclyde University.]

2.4.2.2 Beamformer Design for Two-Dimensional Phased-MIMO Radar with Fully-Overlapped Sub-arrays

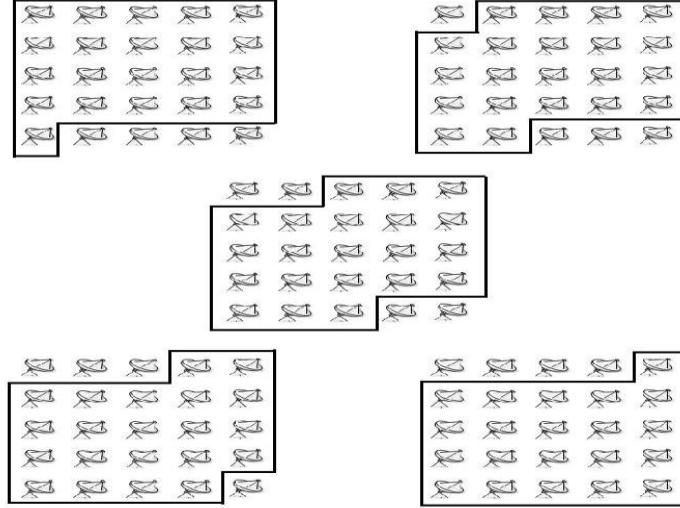


Figure 2.19: Overlapped sub-arrays.

MIMO radars provide spatial diversity through illumination of multiple orthogonal waveforms. However, the advantages of MIMO radars come at the loss of transmit coherent processing gain offered by the phased-array radar. To overcome this, recent work considered design of overlapping phased array of antennas [Ref 2.2.3]. We extended this work for two dimensional array of antennas, Figure 2.19. Accordingly, we split the whole two dimensional array into a number of overlapping two dimensional sub-arrays so that various orthogonal waveforms can be transmitted from each sub-array, however, beamformer coefficient vector needs to be determined for each sub-array in order to steer the waveform in the desired two dimensional sector. We have used convex optimization techniques to solve this problem.

The main idea is the partition of the 2D transmit array into K subarrays, which are fully overlapped. The objective is to focus the energy of the transmit array into a 2D spatial sector determined by the direction of the target. We form K transmit beams, each of them is steered by the corresponding subarray. The power of the emitted signal from the k^{th} subarray focused at a generic focal point with coordinates (θ, φ) can be modeled as:

$$P_k(\theta, \varphi) = \mathbf{a}_k^H(\theta, \varphi) \mathbf{E}\{s_k(t)s_k^H(t)\} \mathbf{a}_k(\theta, \varphi) = \frac{M_t N_t}{K} \mathbf{a}_k^H(\theta, \varphi) \mathbf{w}_k \mathbf{w}_k^H \mathbf{a}_k(\theta, \varphi)$$

where $\mathbf{a}_k(\theta, \varphi)$ is the steering vector associated with the k^{th} subarray, $s_k(t)$ is the complex envelope of the signals at the output of the k^{th} subarray and can be

designed by $s_k(t) = w_k \psi_k(t)$, $w_k \in \mathbb{C}^{M_t N_t \times 1}$ is the transmit weight vector, used to form the k^{th} transmit beam, $\psi_k(t)$ is the independent waveform vector of size $K \times 1$ and t refers to the time index within the radar pulse. The total transmission power defines the array transmit beampattern:

$$P_k(\theta, \varphi) = \sum_{k=1}^K \frac{M_t N_t}{K} a_k^H(\theta, \varphi) w_k w_k^H a_k(\theta, \varphi)$$

2.4.2.2.1 Conventional Beampattern Design

Non-adaptive beamforming is the simplest technique to design the transmit and overall beampatterns. It offers the highest possible output SNR gain only when a single target is observed in the background of white Gaussian noise. The transmit and receive weight vectors are given by the normalized transmit and virtual receive steering vectors respectively.

2.4.2.2.2 Adaptive Beampattern Design

The derivation of the transmit weight vector for each subarray is achieved by solving a convex optimization problem that minimizes the difference between the desired transmit beampattern and the beampattern produced by the 2D array of antennas, under a constraint in terms of uniform power allocation across the transmit antennas [5,6]. This work considers strong clutter imposed by an obstacle within a certain 2D spatial sector, estimated as $\Theta_c = [\theta_{c1} \ \theta_{c2}]$ and $\Phi_c = [\varphi_{c1} \ \varphi_{c2}]$ from training signals. Hence, the second constraint is to restrain the sidelobe level in the prescribed region under a certain value.

$$\begin{aligned} \min_{w_1, \dots, w_K} \quad & \max_{\theta, \varphi} |P_d(\theta, \varphi) - \sum_{k=1}^K \text{Tr}\{a_k(\theta, \varphi) a_k^H(\theta, \varphi) X_k\}| \\ \text{s. t.} \quad & \sum_{k=1}^K \text{diag}\{X_k\} = \frac{E}{M_t N_t - (K - 1)} \mathbf{1}_{M_t N_t \times 1} \\ & \left| \sum_{k=1}^K \text{Tr}\{a_k(\theta_c, \varphi_c) a_k^H(\theta_c, \varphi_c) X_k\} \right| - \delta \leq 0, \quad \theta_c \in \Theta_c, \varphi_c \in \Phi_c \\ & X_k \geq 0, \quad k = 1, \dots, K \end{aligned}$$

where $X_k = w_k w_k^H \in \mathbb{C}^{M_t N_t \times M_t N_t}$, $k = 1, \dots, K$, $P_d(\theta, \varphi)$ is the desired beampattern, E is the total available power. The problem is derived as a convex optimization

problem and solved using semidefinite programming (SDP). After obtaining the optimal solution, denoted as X_k^* , we derive the optimal transmit weight vectors w_k . If X_k^* is of rank one, which is the ideal scenario, the optimal weight vector w_k is obtained straightforwardly as the principal eigenvector of X_k^* multiplied by the square root of the principal eigenvalue of X_k^* . However, if the rank of X_k^* is greater than one, we resort to randomization techniques to obtain the optimal transmit weight vectors.

Adaptive techniques are also used at the 2D receive array in order to maximize the output SINR. An adaptive beamformer that satisfies both the steering capabilities whereby the signal is always protected and the cancellation of interference so that the output SINR is maximized, is the Minimum Variance Distortionless Response (MVDR) beamformer.

$$\min_{w_r} w_r^H \hat{R}_{yy} w_r \quad \text{subject to} \quad w_r^H u(\theta_t, \varphi_t) = 1$$

where $\hat{R}_{yy} = \frac{1}{N} yy^H$ is the sample covariance matrix of the observed data samples that can be collected from N different radar pulses, $u(\theta, \varphi) = (c(\theta, \varphi) \odot d(\theta, \varphi)) \otimes b(\theta, \varphi)$ is the $KM_r N_r \times 1$ virtual steering vector of the system, $b(\theta, \varphi)$ is the $M_r N_r \times 1$ steering vector of the receive array $c(\theta, \varphi) = [w_1^H a_1(\theta, \varphi), \dots, w_K^H a_K(\theta, \varphi)]^T$ is the $K \times 1$ transmit coherent processing vector, $d(\theta, \varphi) = [e^{-j\tau_1(\theta, \varphi)}, \dots, e^{-j\tau_K(\theta, \varphi)}]^T$ is the $K \times 1$ waveform diversity vector and $\tau_k(\theta, \varphi)$ is the time required for the signal to cover the distance between the first element of the transmit array and the first element of the k^{th} subarray. The solution to the MVDR beamformer optimization is

$$w_r = \frac{\hat{R}_{yy}^{-1} u(\theta_t, \varphi_t)}{u^H(\theta_t, \varphi_t) \hat{R}_{yy}^{-1} u(\theta_t, \varphi_t)}$$

The receiver weight vectors derived are employed to design the overall transmit-receive beampattern in our simulations.

2.4.2.2.3 Simulation Results- Conventional

We assume a 5×5 uniform rectangular array (URA) with half-wavelength spacing between adjoining antennas. The desired target is located at directions $\theta_t = -30^\circ$ and $\varphi_t = 60^\circ$. We also assume one interfering source at directions $\theta_i = 30^\circ$ and $\varphi_i = 90^\circ$. For the 2D Phased-MIMO model the transmit array is divided into 5 subarrays that are fully overlapped. The noise is considered as complex Gaussian with zero mean and variance 0.1. In order to derive the sample covariance matrix we use $N = 100$ data samples.

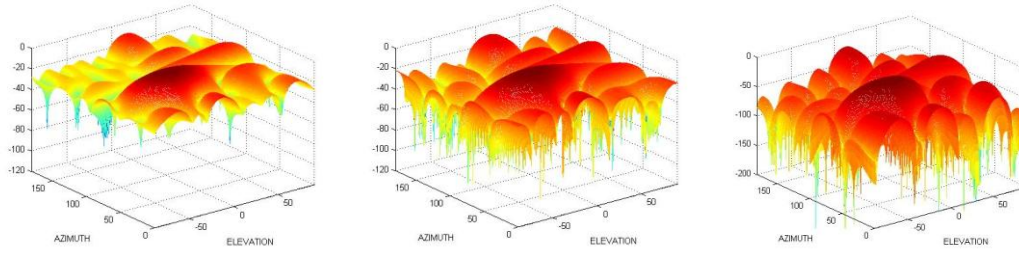


Fig. 2.20: The transmit, waveform diversity and overall beampatterns for the non-adaptive 2D Phased-MIMO radar.

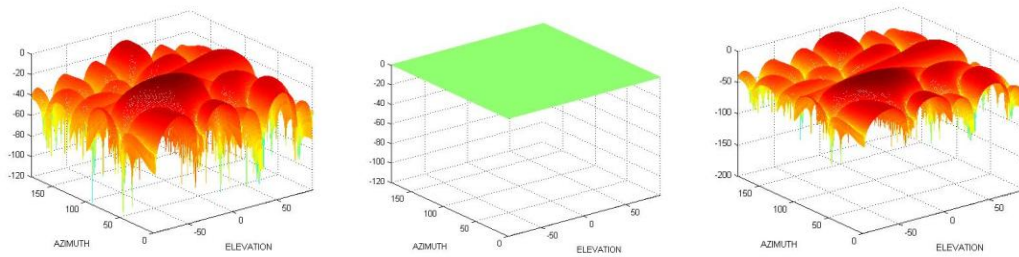


Fig. 2.21: The transmit, waveform diversity and overall beampatterns for the non-adaptive 2D phased-array radar.

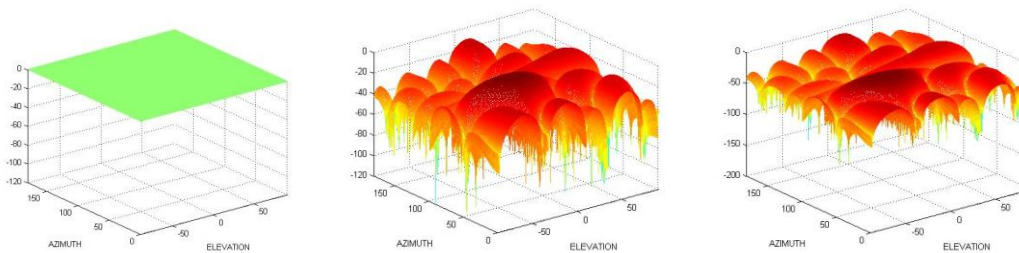


Fig. 2.22: The transmit, waveform diversity and overall beampatterns for the non-adaptive 2D MIMO radar.

To facilitate the comparison between the three models, Fig. 2.23 shows the cross section plotted against the elevation angle by keeping the azimuth angle constant at 60° . As reported for the case of the one-dimensional (1D) linear array in [Ref 2.2.3], for the 2D array also it is evident from Fig. 2.23. that although the phased-array radar has the most efficient transmit conventional beampattern due to its high transmit coherent processing gain, it has zero waveform diversity gain. On the other hand, the MIMO radar has flat (0dB) transmit beampattern, but it has the most accurate waveform diversity beampattern, because of the simultaneous emission of $MtNt$ orthogonal waveforms. However, it is clear from that the 2D Phased-MIMO radar remarkably outperforms the phased array and MIMO radars in terms of the overall transmit-receive beampattern, as it has lower sidelobes and approximates better the desired target direction. Moreover, it is important to highlight that in the case of

conventional beamforming the overall beampatterns of the phased-array and the MIMO radar are exactly the same.

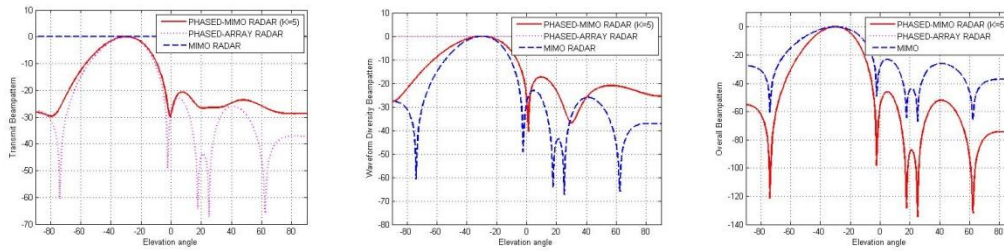


Fig.2.23: Cross sections at $\varphi = 60^\circ$ of the transmit, the waveform diversity and the overall beampatterns, respectively.

2.4.2.2.4 Simulation Results- Adaptive

We employ adaptive beamforming techniques to derive the transmit and receiver beampatterns. In particular, we use convex optimization techniques to determine the transmit beamformer weight vectors and the MVDR (CAPON) based receiver beamformer for the receive weight vectors. In our simulations we assume strong clutter at the 2D spatial sector defined by $\Theta_c = [-90^\circ, -60^\circ]$ and $\Phi_c = [140^\circ, 180^\circ]$. We consider $\delta = 0.01$ (-20dB) to restrain the sidelobe level in the clutter region. The total available power for our system is equal to one ($E = 1$) and the interference to noise ratio (INR) is fixed to 30dB . The 2D transmit beampattern for the Phased-MIMO radar is shown in Fig. 2.24a. Similarly, by solving the same optimization problem considering the whole URA as one subarray ($K = 1$), we generated the 2D transmit beampattern for the phased-array scheme as shown in Fig. 2.24b. It is clear that the power allocation of both beampatterns is concentrated in the desired space and the sidelobe level is very low, especially over the predefined clutter regions, where it has values lower than 20dB .

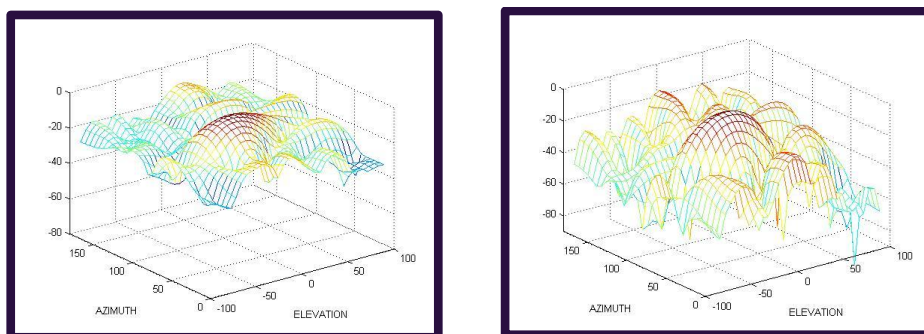


Fig.2.24 (a,b): Transmit beampatterns for the 2D Phased-MIMO and the phased-array radar respectively, using convex optimization.

At the receiver array, the MVDR beamformer is employed to derive the overall transmit-receive beampatterns for all radar schemes investigated, as shown in Fig. 2.25. Similar to the first example, Fig. 2.26 shows the cross sections of the overall beampatterns to compare the three types of radar configurations. It is clear that the 2D Phased-MIMO radar exploits the transmit superiority of the phased-array model and the waveform diversity of the MIMO scheme to produce in a substantially improved overall beampattern.

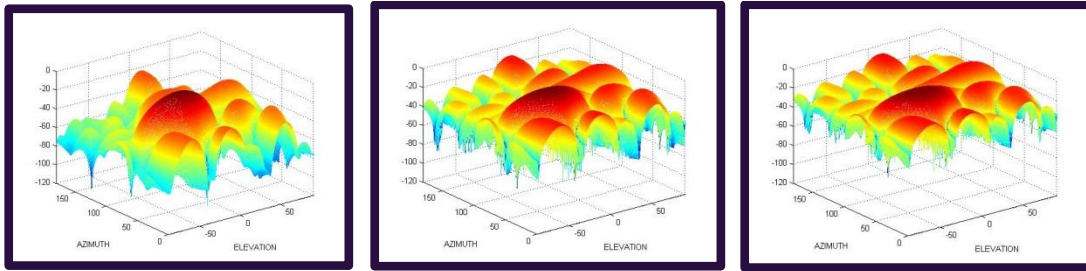


Fig.2.25: Adaptive overall beampatterns using MVDR beamformer for the 2D Phased-MIMO, the phased-array and the conventional MIMO radar, respectively.

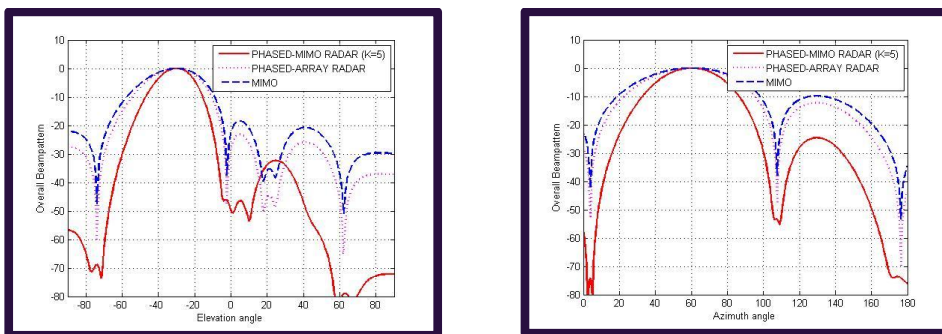


Fig. 2.26: Cross sections of the overall beampattern at $\varphi = 60^\circ$ and $\theta = -30^\circ$.

The simulation results confirmed that there are substantial improvements of the overall transmit/receive beampattern of the 2D Phased-MIMO radar as compared to the phased-array and the conventional MIMO model. In particular, it was demonstrated that the Phased-MIMO scheme combines the transmit coherent processing gain of the phased-array radar and the waveform diversity of the MIMO model to produce a more efficient and accurate overall beampattern with very low sidelobe levels. This superiority is highlighted using both non-adaptive (conventional) and adaptive (convex optimization and MVDR) beamforming techniques.

2.5. Future Work

Plans for WP 2.1:

Developing new signal processing algorithms with the new modelling approach of the interaction between objects and environment

The next task is to apply the new modelling approach to develop new signal processing algorithms. Specially, a *unified* Bayesian inference framework will be developed for target state estimation, which could both incorporate environmental information and deal with more complicated scenarios, such as miss detection/false alarms/target missing/appearing. To achieve this, the Bayesian inference based on the new hybrid modelling system will be extended to a random finite set (RFS) framework. And new methods will be investigated for the implementation of the Bayesian inference.

Chemical and Biological dispersion tracking with the aid of local domain knowledge

Chemical and biological agent dispersion models which exploit the local environmental information will be reviewed and implemented. Based on the new models, corresponding new chemical and biological agent tracking algorithm will be developed.

Integrating these two parts by exploiting the influence of the local environment on the dispersion of chemical and biological agents as the force terms

As our currently developed dynamic model for vehicle tracking, force terms will be introduced to represent the interaction between the local environment and chemical/biological agents. The current dispersion modelling approaches will then be modified by the aid of the force terms to model the interaction. New Bayesian inference framework for chemical/biological agents localization/tracking will be developed based on the modified models which incorporate the interaction information.

Plans for WP 2.2:

Game Theoretic Algorithms for Radar-Jammer interaction

The next task is to develop a game theoretic scheme for a MIMO radar application that includes jamming. The jamming can either be studied from the target's point of view (jamming for target protection), or from the point of view of a radar that aims to detect an intelligent target that is equipped with a jammer. Game theoretic framework will also be extended to sensor topology control.

Distributed Beamforming for radars networks using Game Theory

The distributed power allocation and waveform selection method will be extended to distributed beamforming design using game theoretic framework. The problem will consider no direct communication among radars, however, the algorithm should have intelligence to enable each radar to steer beams towards targets and suppress interference without requiring explicit coordination. As the receiver beamformer is a function of transmitter beamformer, the overall problem will turn out to quartic optimization which needs specific optimization approaches.

Waveform Design and Power Allocation for Cognitive Radar network

Unlike traditional fixed transmission waveforms, cognitive radar exploits a prior knowledge of the environment and the target to adaptively update the transmission parameters including waveforms, beamforming and illumination power. Convex optimization based waveform design and Bayesian optimization framework will be developed for cognitive radar design.

Multiple-Targets Tracking in Cognitive Radar

The cognitive radar framework will be incorporated within the target tracking loop. Using Bayesian framework, radar transmission parameters will be adaptively changed to assist multiple-target trackers that will be operating using probability hypothesis density (PHD) recursions and cardinalized PHD (CPHD) recursions.

2.6. Outputs during the last two years:

Outputs for L_WP 2.1:

Three conference articles have been accepted for publication:

Pub.2.1.1. M. Yu, WH. Chen and J. Chambers, "*Truncated unscented particle filter for dealing with non-linear and inequality constraints*", Sensor Signal Processing for Defence, Edinburgh, 2014

Pub.2.1.2. M. Yu, C. Liu, WH. Chen and J. A. Chambers. *An improved ground vehicle tracking algorithm by integrating Bayesian tracking framework with an auxiliary particle filter*, "Signal Processing, Sensor/Information Fusion, and Target Recognition XXIII" conference, in SPIE Defense + Security, 5-9 May 2014, Baltimore, Maryland USA.

Pub.2.1.3. R. Ding, M. Yu and WH Chen, "*A Multiple Target Tracking Strategy Using Moving Horizon Estimation Approach*", accepted by the 24th International Technical Conference on the Enhanced Safety of Vehicles (ESV), Gothenburg, Sweden, 2015.

Two journal papers under reviews:

Pub.2.1.4 M. Yu, R. Ding and WH. Chen, “*Dynamic Modelling of a Vehicle’s Movement Affected by Environment*”, submitted to *Electronic Letters*

Pub.2.1.5 M. Yu, H. Oh and WH. Chen, “*A GMTI Manoeuvring Ground Vehicle Tracking Method Aided by Geographic Information*”, submitted to *IET Radar, Sonar and Navigation*.

One journal paper is under major revision:

Pub.2.1.6 M. Yu, C. Liu, B. Li and WH Chen, “A novel GMM-based particle filter for GMTI radar tracking”, major revision, submitted to *IEEE Transactions on Aerospace and Electronic Systems*.

Output for L_WP 2.2:

1. A. Panoui, S. Lambotharan and J.A. Chambers, “Game Theoretic Power Allocation Techniques for a MIMO Radar,”, *IEEE International Symposium on Communications, Control and Signal Processing (ISCCSP)*, Athens, May 2014.

2. A. Panoui, S. Lambotharan and J.A. Chambers, “Game theoretic power allocation for multistatic radar network in the presence of estimation error,” *Sensor Signal Processing for Defence (SSPD)*, Edinburgh, UK, 2014

3. A. Panoui, S. Lambotharan and J.A. Chambers, “Waveform Allocation for a MIMO Radar Network Using Potential Games,” *IEEE International Radar Conference*, Arlington, VA, 2015

4. A. Panoui, S. Lambotharan and J.A. Chambers, “Game theoretic distributed waveform design for multistatic radar network” to be submitted to an *IEEE Transactions on Aerospace and Electronic Systems*, April 2015.

5. A. Deligiannis and S. Lambotharan, “Transmit Beamforming Design for Two-Dimensional Phased-MIMO Radar with Fully-Overlapped Subarrays,” *Sensor Signal Processing for Defence*, Edinburgh, September 2014.

6. A. Deligiannis and S. Lambotharan, “Beamforming for Fully-Overlapped Two-Dimensional Phased-MIMO Radar,” *IEEE International Radar Conference*, Arlington, USA, May 2015.

2.7 List of affiliated PhD students:

L_WP2.1:

Affiliated PhD students:

Mr. Runxiao Ding

PhD title: Multiple object tracking for autonomous ground vehicle operation.

L_WP2.2:

Affiliated PhD students:

Mr A Deligiannis

PhD title: Game theory in radar

Ms Gaia Rossetti

PhD title: MIMO-radar

Mr Abdullahi Daniyan

PhD title: Tracking in radar

References

Ref.2.1.1. X. Li and P. Jilkov, "Survey of maneuvering target tracking. Part I: Dynamic models", *IEEE Trans. on Aerospace and Electronic Systems*, vol. 39, no. 4, pp. 1333–1364, 2003.

Ref.2.1.2. D. Helbing, I. Farkas and T. Viscek, "Simulating dynamic features of escape panic", *Nature*, vol. 407, pp. 487–490, 2000.

Ref.2.1.3. G. Bang, I. Kweon, "Multi-target tracking using social force model in discrete-continuous optimisation scheme", *Electronic letters*, vol. 49, no. 21, pp. 1331–1333, 2013.

Ref.2.1.4. B. Gunay and D. Woodward, "Lateral position of traffic negotiating horizontal bends", *Proc. of the ICE-Transport*, Vol. 160, no. 1, pp.1–11, 2007.

Ref.2.1.5. L. Lang, W. Chen and B. Bakshi, P. Goel, S. Ungarala, "Bayesian estimation via sequential Monte Carlo sampling constrained dynamic systems", *Automatica*, 2007, vol. 43,no. 9, pp. 1615–1622, 2007

Ref.2.1.6. X. Shao, B. Huang and J. Lee, “Constrained Bayesian state estimation: A comparative study and a new particle filter based approach”, *Journal of Process Control*, vol. 20, no. 2, pp. 143–157, 2010.

Ref.2.1.7. B. Cyganek, “Object Detection and Recognition in Digital Images: Theory and Practice”, Wiley-Blackwell, Hoboken, NJ, USA, 2013.

Ref.2.1.8. D. Simon “Kalman filtering with state constraints: a survey of linear and nonlinear algorithms”, *IET Control Theory&Application*, vol. 4, no. 8, pp. 1303 –1318, 2010.

Ref.2.1.9. O. Straka, J. Dunik and M. Simandl, “Truncation nonlinear filters for state estimation with nonlinear inequality constraints”, *Automatica*, vol. 48, no. 2, pp. 273 – 286, 2012.

Ref.2.1.10 H. Blom and E. Bloom, “Exact Bayesian and particle filtering of stochastic hybrid systems”, *IEEE Transactions on Aerospace and Electronic Systems*, vol. 43, no. 1, pp. 55 –70, 2007.

Ref.2.1.11. M. Ulmke and W. Koch, “Road-map assisted ground moving target tracking,” *IEEE Transactions on Aerospace and Electronic Systems*, vol. 42, no. 4, pp. 1264 –1274, 2006.

Ref.2.1.12. J. Vermaak, S. Godsill and P. Perez, “Monte Carlo Filtering for Multi-Target Tracking and Data Association”, *IEEE Transactions on Aerospace and Electronic Systems*, vol. 41, no. 1, pp. 309 –332, 2005.

Ref 2.2.1. T. Ui, “Discrete concavity for potential games,” *International Game Theory Review*, vol. 10(1), pp.137-143, 2008

Ref 2.2.2. C. Clemente, C. Ilioudis, D. Gaglione, K. Thompson, S. Weiss, I. Proudler and J. Soraghan, “Reuse of Fractional Waveform Libraries for MIMO Radar and Electronic Countermeasures,” 6th International Symposium on Communications, Control, and Signal Processing (ISCCSP 2014), Athens, Greece, May 2014

Ref 2.2.3. A. Hassanien, and S. A. Vorobyov, ”Phased-MIMO Radar: A Tradeoff Between Phased-Array and MIMO Radars”. *IEEE Trans. Signal Processing*, 58(6):3137-3151, Jun. 2010.

L_WP3: (SS) Signal Separation and Broadband Distributed Beamforming

3.1 Staffing

Work Package Leaders: Dr Wenwu Wang (SU) and Prof John McWhirter (CU)
Other Academics Involved: Prof. Ian Proudler, Prof. Jonathon Chambers, Dr. Philip Jackson, Prof. Josef Kittler, Dr. Stephan Weiss, Dr. Yulia Hicks, and Dr Syed Mohsen Naqvi
Research Associates: Dr Swati Chandna (SU) (May 2013 – Nov 2014), Dr Mark Barnard (Nov 2014 –)
Research students: Mr Luca Remaggi (SU), Miss Jing Dong (SU), Mr Zeliang Wang (CU), Waqas Rafique (SU)
Lead & New Project Partners: Richard Brind (Atlas Elektronik) and Alastair Cowley (Atlas Elektronik)
Dstl contact: Julian Deeks (Naval Systems Dept), Alan Johnson (Sensors & Countermeasures Dept), Nick Goddard (Naval Systems Dept)

3.2 Aims and Introduction

This work package concerns the development of low-complexity robust algorithms for underdetermined and convolutive signal separation, broadband distributed beamforming, facilitated by low-rank and sparse representations, and their fast implementations, and the application of these techniques to the defence related problems, especially for processing underwater acoustic and sonar data, such as for signal denoising, source localisation, separation and extraction.

We aim at proposing novel methods to address the challenges in source separation in dense signal environments. This include extracting signals of interest and suppression of interference from corrupted sensor measurements, e.g. for the problems of convolutive mixing (i.e. multipath signal propagation) underdetermined mixing (i.e. more sources than sensors), and unknown number of target signals. This work package links to L_WP1 in weak signal detection; L_WP2 in unknown number of targets and order selection; L_WP4 in MIMO signal detection; and L_WP5 in data reduction.

L_WP3.1 is devoted to the problem of multichannel convolutive source separation and broadband distributed beamforming, with a focus on polynomial matrix decomposition techniques and their variants. L_WP3.2 focuses on reverberant, underdetermined and noisy source separation, with a focus on the techniques such as robust statistics and bootstrapping, time-frequency masking, sparse representation, and Bayesian estimation. Both L_WP3.1 and L_WP3.2 have focussed on the underwater acoustic data e.g. the Portland 3 sonar dataset.

3.3 Available Datasets

Currently we have access to the following datasets:

- Portland 3 dataset
- An underwater acoustic channel simulator

- Surrey's BRIR datasets
- Surrey's RIR datasets

3.4 Overview of Technical Progress

We have made progressed a number of areas in the past year, which are summarized as follows.

- A novel multichannel spectral factorization algorithm has been proposed, where the multichannel spectral factorization problem is reduced to a number of independent single channel problems by using polynomial matrix decomposition techniques. It has been shown to achieve a high degree of accuracy in terms of recovering the input parahermitian polynomial matrix from its outer and inner spectral factors.
- The ideas of MSME-SMD (Corr *et al.*, 2014) are harnessed to create a faster converging version of SBR2 that however still enjoys the SBR2 family's low complexity. This algorithm is developed based on the original SBR2 algorithm. It can achieve faster convergence than its predecessor by means of transferring more off-diagonal energy onto the diagonal at each iteration akin to the MSME-SMD algorithm.
- The technique of bootstrap averaging has been used to improve the parameter estimates of a Gaussian mixture model. This is further employed to derive time-frequency masks in highly convolutive mixing environments. The proposed bootstrap averaging technique has been shown to provide more accurate estimates in particular for reverberant mixtures.
- A sparse sequential Bayesian method has been implemented. Specifically, we have been implementing a sparse reconstruction method for sequential data. This is done by extending the classical Bayesian approach for sequential Maximum a Posterior (MAP) estimation of the signal over time. A sparsity constraint is enforced through the use of a Laplacian like prior at each time step. An adaptively weighted LASSO cost function is sequentially minimised using the new measurement received at each time step.
- We proposed a new analysis dictionary learning algorithm named Analysis SimCO (Dong *et al.*, 2014) and also an extended version Incoherent Analysis SimCO by incorporating incoherent constraint. In these algorithms, the idea of simultaneous codeword optimisation used in the synthesis model dictionary learning has been adapted and applied to the analysis model. The algorithm iterates between the two steps: analysis sparse coding and dictionary updates, until it converges based on an error performance cost function. The Analysis SimCO algorithm has also been used for image denoising, SAR image despeckling and audio super-resolution.
- A new independent vector analysis method based on multivariate Student's t distribution has been introduced, where the Student's t distribution is used to model the dependencies between the frequency bins of frequency domain blind source separation. The advantage of the Student's t distribution has been exploited in both the IVA and the FastIVA algorithms by changing the source prior from a multivariate Gaussian distribution to a multivariate Student's t distribution.

- A novel system has been developed for room boundary estimation. Both 2D and 3D reflector localization model have been developed given where room impulse responses (RIRs) are given as input to the system. The method is evaluated in room acoustics, and has the potential to be used in underwater acoustics for harbour boundary estimation.

3.5 Technical Details

3.5.1 Multichannel Spectral Factorization and MS-SBR2 for Polynomial Matrix EVD

1) Multichannel Spectral Factorization

Spectral factorization plays a crucial role in constructing a casual system which corresponds to a given spectral density function. Most existing spectral factorization algorithms, with the exception of those due to Wilson (1972) and Janashia (2011), do not extend to the multichannel situation. Wilson's algorithm seems to provide a viable approach to the multichannel spectral factorization problem in terms of stability and reliability but is reputed to run into problems when the number of channels grows too large.

The proposed multichannel spectral factorization starts by diagonalising the input parahermitian polynomial matrix using the SBR2 algorithm. This process breaks the multichannel problem down into a set of distinct single channel problems. Each polynomial element in the diagonal matrix defines a one dimensional spectral factorization problem which can be accurately solved using, for example, Wilson's algorithm (Wilson, 1972). In essence, the SBR2 algorithm builds a bridge between multichannel and single channel spectral factorization. The resulting outer (inner) spectral factors of the diagonal matrix are then used to construct the spectral factor of the input parahermitian polynomial matrix. As the polynomial orders of the paraunitary matrix $\underline{H}(z)$ and diagonalized matrix $\underline{D}(z)$ may potentially increase with each iterative paraunitary transformation in the SBR2 algorithm, the computed spectral factors can accumulate time delays which are unnecessarily large. However, when the outer and inner spectral factors are multiplied together, such delays cancel and the resulting parahermitian polynomial matrix is none the less accurate. This reflects a fundamental indeterminacy in spectral factorization whereby if $\underline{R}^+(z)$ is a valid outer spectral factor of $\underline{R}(z)$ so also is $\underline{R}^+(z)\underline{P}(z)$ where $\underline{P}(z)$ represents any paraunitary polynomial matrix which preserves the essential properties associated with an outer spectral factor.

In conclusion, the proposed multichannel spectral factorization algorithm has been shown to achieve a high degree of accuracy in terms of recovering the input parahermitian polynomial matrix from its outer and inner spectral factors. The algorithm is seen to offer a significant advantage in that the multichannel spectral factorization problem is reduced to a number of independent single channel

problems for which suitable algorithms already exist. However, it must be noted that the spectral factors generated by this algorithm can accumulate numerous very small or zero coefficients which may be a nuisance but can be truncated by virtue of the fundamental indeterminacy associated with spectral factorization. Further details about this algorithm can be found in our published conference paper (Wang and McWhirter, 2014), presented at the *10th IMA International Conference on Mathematics in Signal Processing*.

2) Multiple Shift Second Order Sequential Best Rotation Algorithm (MS-SBR2) for Polynomial Matrix EVD

The aim of developing this algorithm is to see whether some of the ideas of MSME-SMD (Corr *et al.*, 2014) can be harnessed to create a faster converging version of SBR2 that however still enjoys the SBR2 family's low complexity.

This algorithm is developed based on the original SBR2 algorithm. It can achieve faster convergence than its predecessor by means of transferring more off-diagonal energy onto the diagonal at each iteration akin to the MSME-SMD algorithm. With MS-SBR2, there are two main steps involved at each iteration. The first step involves multiple shifts operations, and the second step is to perform a sequence of Jacobi rotations corresponding to the multiple shifts.

Based on what we found about this improved SBR2 algorithm, a paper (Wang *et al.*, 2015) has been submitted to the *EUSIPCO 2015* conference. Some key results are shown below in Figure 3.1 to compare its convergence characteristics and computational complexity with the original SBR2, SMD and MSME-SMD algorithms.

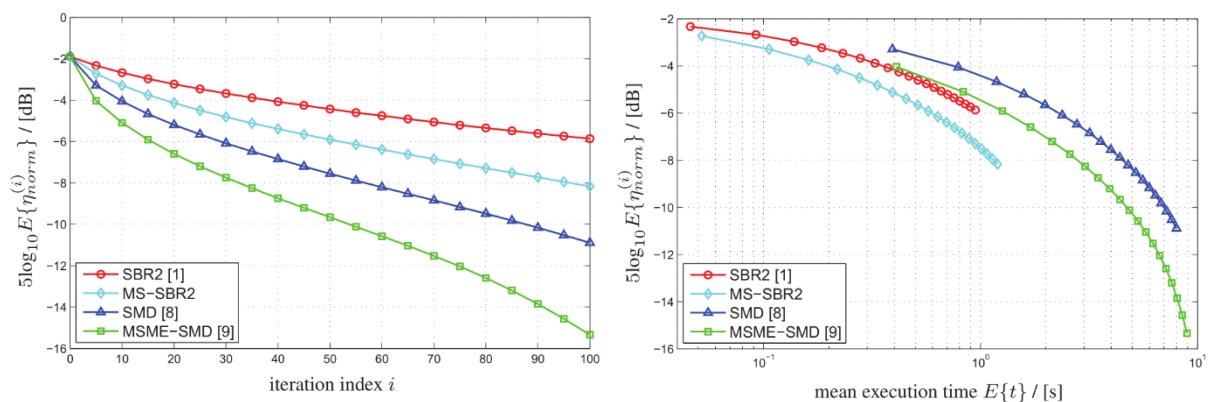


Figure 3.1 Comparison of the convergence characteristics and computational complexity among SBR2, MS-SBR2, SMD and MSME-SMD.

3.5.2 Bootstrap Technique for Underdetermined Convolutional Source Separation

Underdetermined convolutional blind source separation (BSS) concerns with the problem of simultaneously separating I sound sources from M mixtures acquired in a reverberant environment, where the number of sources is greater than the number of sensors, i.e. $I > M$. Traditional matrix inversion based de-mixing as in the exact or over-determined case ($I \leq M$) do not apply. In the underdetermined case, BSS is often achieved by assuming a statistical model for a chosen set of cues. For example, in stereo (two-channel) source separation, interaural cues such as the interaural level and phase difference as well as the mixing vector cue have been used in the literature to perform source separation for speech mixtures which are known to satisfy a sparsity condition in the time-frequency domain. Such techniques proceed by assuming an appropriate statistical model for such cues with their parameters depending on unobserved source signals. The expectation-maximization (EM) algorithm is used to obtain maximum likelihood estimates of these unknown parameters. A useful by-product of the EM algorithm is that it allows a probabilistic classification of each time-frequency point as being dominated by each of the source signals. For each source index $i = 1, \dots, I$, we have a $W \times T$ matrix of weights which give the probability that source i is dominant at the $W \times T$ time-frequency points, where T and W denote the number of time and frequency bins. This matrix of weights, known as the T-F mask allows separation of the sources via a simple inverse short-time-frequency transform.

The cues of interest are estimated from the given reverberant mixture and the accuracy of the estimation tends to be affected by reverberation effects. Due to the diffuse characteristic of reverberation, data points/cues with high reverberation may not fit a source model particularly well and as a result may lead to poor parameter estimates. The resulting T-F masks derived from these parameter estimates can be un-reliable, leading to potentially poor separation performance, especially when the mixtures are acquired under high reverberation. In addition, from an inference point of view, we note that the T-F mask that is used for source separation is derived from one length- N sample of the mixture signal. In a controlled environment, such as in a room with low reverberation, there may not be a large variation in the estimates over different observations of the speech mixture, however, with data recorded in other environments such as underwater acoustic data, one would expect the estimates to be very sensitive to the underlying measurements. Thus, the T-F mask estimated from just one length- N recording may not be very reliable.

To address the above limitations, we have proposed the technique of bootstrap averaging to obtain better separation results for highly reverberant mixtures (Chandna and Wang, 2014). The technique of bootstrap averaging also known as bagging was first suggested in the area of machine learning by Breiman (1996). Although, commonly used in statistical classification and regression problems, it has never been used in the area of blind source separation. Let $\mathbf{y} = [y_1, \dots, y_p]$ denote a p -variate process with a probability distribution denoted by $F_y(\cdot)$. Let $\mathbf{Y} \equiv [\mathbf{y}_1, \dots, \mathbf{y}_N] \in \mathbb{C}^{N \times p}$ denote a sample obtained from \mathbf{y} , by independently drawing N samples from the probability distribution F_y . Let $\hat{\theta}(\mathbf{Y}) \equiv \hat{\theta}$ denote the statistic of interest derived from \mathbf{Y} , then bootstrap averaging relies on the result that the aggregated estimator

$$\hat{\theta}_A(B) = \frac{(\hat{\theta}_1 + \dots + \hat{\theta}_B)}{B}$$

obtained by generating B samples Y_1, \dots, Y_B from F_y , and computing $\hat{\theta}_j$ from Y_j has a smaller mean squared error than $\hat{\theta}$. Since in practice, the underlying distribution of the given sample is unknown, the aggregated estimator can be constructed by bootstrapping the given sample \mathbf{Y} to obtain, Y_1^o, \dots, Y_B^o from which the corresponding bootstrap estimates $\hat{\theta}_1^o, \dots, \hat{\theta}_B^o$ can be derived. Then, we define the bootstrap sample version of the aggregated estimator given above as

$$\hat{\theta}_A^o(B) = \frac{(\hat{\theta}_1^o + \dots + \hat{\theta}_B^o)}{B}.$$

In our work, we bootstrap the given mixture and use the bootstrap averaged maximum likelihood parameter estimates and the corresponding T-F mask to perform source separation using one of the model-based source separation algorithms. We used a recently proposed technique (Chandna and Walden, 2013) based on circulant embedding to generate statistically similar samples of the given mixture. This simulation methodology generates samples from non-parametric spectral estimates of the given sample via circulant embedding. The spectral density estimate captures the second order statistics of the data set and the circulant embedding approach based on circulant matrices makes it a very fast re-sampling technique. One of the key assumptions for this simulation methodology to work is the stationarity of samples. For non-stationary signals such as speech or underwater acoustic signals, this technique is not directly applicable. However, a fairly reasonable assumption for such signals as speech is that blocks of length 30 ms are stationary or quasi-stationary. Therefore, consecutive blocks of length 30ms are bootstrapped and then joined together to get a bootstrap sample of the entire signal.

During the period of the past year, we have performed systematic studies to verify the technique for a Gaussian mixture model and the parameter estimates obtained using EM algorithms. We also then performed extensive experimental evaluations to investigate its performance for time-frequency mask estimation and source separation. A comparison of the bootstrap averaged mean interaural level difference estimate with the ground-truth direct path interaural level difference shows that our estimates are very smooth as compared to the estimate obtained from the original source-separation algorithm. We performed source separation using the corresponding bootstrapped average T-F mask; we see a significant increase in the average Signal-to-Distortion Ratio (SDR) for different experimental set-up configurations. The results confirm that our method can be used to improve the performance of model-based source separation algorithms. The details of the study and the results obtained are reported in a paper (Chandna and Wang, 2014) which we submitted to IEEE Transactions on Signal Processing, and is currently under peer review.

3.5.3 Sparse Bayesian algorithm for Underwater Acoustic Data Denoising

Underwater acoustic data acquired by the hydrophone arrays are often noisy. During this period, part of our research has focussed on the localisation and de-noising of

underwater acoustic signals. To this end, this work has been primarily implementing sparse sequential Bayesian methods. Specifically, we have been implementing a sparse reconstruction method for sequential data. This is done by extending the classical Bayesian approach for sequential *Maximum A posterior* (MAP) estimation of the signal over time. A sparsity constraint is enforced through the use of a Laplacian like prior at each time step. An adaptively weighted LASSO cost function is sequentially minimised using the new measurement received at each time step. A function φ is derived to give a source estimate at each time step k ,

$$(\hat{x}_{k+1}, \lambda_{k+1}) = \varphi(y_k, \lambda_k)$$

where \hat{x}_{k+1} is a MAP source at time step k estimated under a sparsity constraint and $\lambda_k = (\lambda_{k1} \dots \lambda_{kM})^T$ is the Laplacian prior where M is the number of hypothetical source locations and y_k is the sensor array output.

First the LASSO cost function is generalised by weighting the regularisation parameters. Hence the Laplacian prior can be updated based on the past history of observations. The weighted LASSO cost function, which minimises the negative log likelihood of the current source vector at time k given all the array outputs up to time step k , is given by

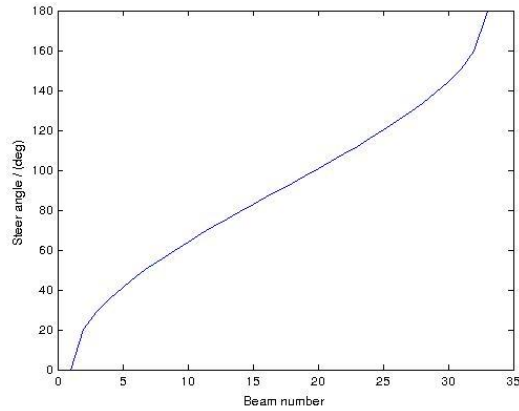
$$-\ln p(x_k | Y_k) = \frac{\|y_k - Ax_k\|_2^2}{\sigma^2} + \|\lambda_k \odot x_k\|_1 + c_k$$

where A is an $N \times M$ matrix, where N is the number of sensors and $N \ll M$ and σ^2 is the noise variance. The final term in the equation c_k is given by

$$c_k = -2 \sum_{m=1}^M \ln \lambda_{km} + N \ln \pi \sigma^2 + M \ln 2\pi + \ln p(y_k)$$

This cost function promotes sparse solutions and is a convex optimisation problem.

This algorithm is currently being tested on the Portland 03 dataset. For our initial tests each element of the vector, $\lambda_1 = (\lambda_{11} \dots \lambda_{1M})^T$ is set to $1/M$ and location hypotheses in the matrix A is chosen at random from the dataset. Initially it is planned to test values of M between 500 and 1000. The Portland dataset consists of data recorded with two parallel hydrophone arrays of a small boat following different tracks around Portland harbour.



Figures 3.2 Steering angle associated with each beam in Portland 03 dataset.

Figures 3.2 and 3.3 show the beamforming results for a sequence of the Portland 03 dataset. Figure 3.2 shows the steering angle associated with each beam. Figure 3.3 shows the broadband response for a single hydrophone array for each of the beams over the entire sequence and also the spectra for each beam in the final frame of the data. In the upper plot of Figure 3.3 the track of the vessel moving across the harbour can be seen. The responses show the non-directional nature of the data, particularly at low frequencies, causing high levels of noise. Therefore an effective method of de-noising and localisation is expected to improve the results on this dataset. The next stage of work will focus on further studying the sparse Bayesian algorithm for denoising the data.

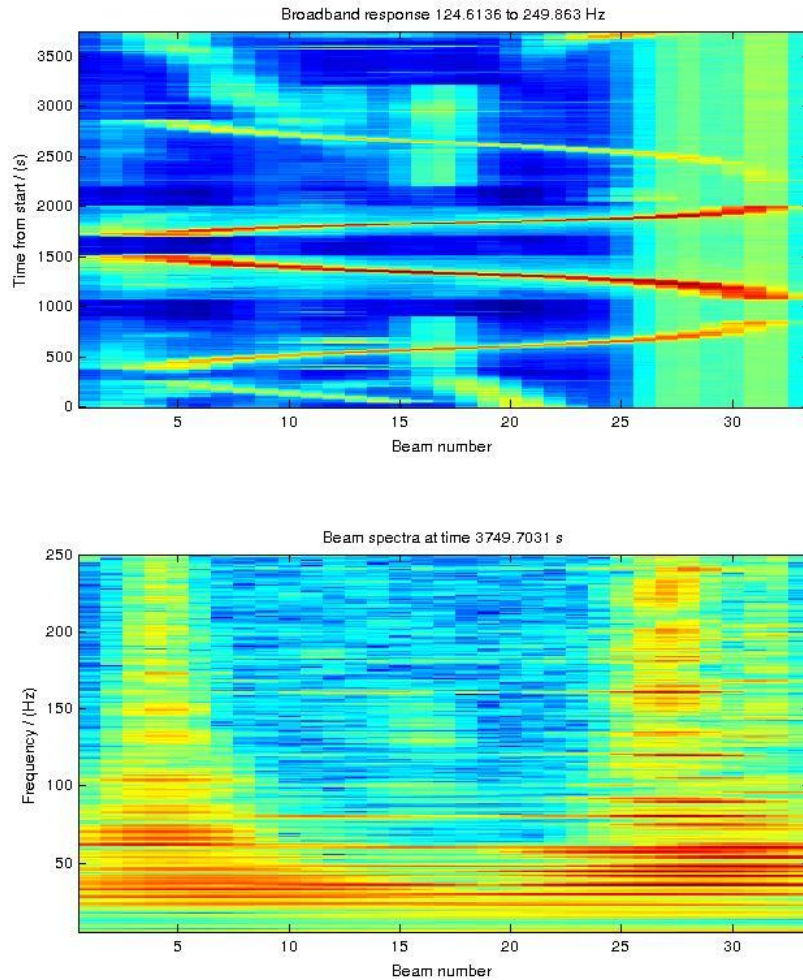


Figure 3.3 The broadband response for a single hydrophone array for each of the beams over the entire sequence (upper plot) and also the spectra for each beam in the final frame of the data (bottom plot).

3.5.4 Analysis Model Based Dictionary Learning for Sparse Representations

Sparse representation has proven to be very useful for many problems in signal processing. There are two models that have been used, namely, synthesis model and analysis model. For each model, the choice of dictionary plays a key role for signal representation. It has been shown that dictionaries learned from a set of training signals have the potential to fit these signals better than pre-defined dictionaries. Thus, learning a dictionary has become one of the most popular topics in sparse representation. In the last decade, dictionary learning based on the synthesis model has drawn much attention, but there are just a few works based on the analysis model. We focus on the analysis model based dictionary learning problem and its applications to signal recovery from noisy and incomplete data, including image denoising (Dong *et al.*, 2015), SAR image despeckling (Dong and Wang, 2014), and audio super-resolution (Dong *et al.* 2015).

2 1) Analysis SimCO Algorithms

We have proposed a new analysis dictionary learning algorithm named Analysis SimCO (Dong *et al.*, 2014). In this algorithm, the idea of simultaneous codeword optimisation used in the synthesis model dictionary learning has been adapted and applied to the analysis model. The algorithm iterates between the two steps: analysis sparse coding and dictionary updates, until it converges based on an error performance cost function. This algorithm offers good performance for signal reconstruction from noisy data. However, from our experiments, we found that there may be some similar atoms in the dictionaries learned by Analysis SimCO, which is undesirable for signal recovery. Thus, Incoherent Analysis SimCO was developed, as an extended version of Analysis SimCO, to avoid the similar atoms. Based on the formulation for the analysis dictionary learning problem in Analysis SimCO, a coherence constraint restricting the correlations of two distinct atoms of the dictionary is applied to the formulation in the Incoherent Analysis SimCO. An atom decorrelation step is inserted after the dictionary update stage of Analysis SimCO in order to apply the coherence constraint. This decorrelation step seeks for the atom-pairs that are highly-correlated and then rotates them symmetrically until the coherence constraint is satisfied.

Experiments with synthetic data and image data have been performed to compare our proposed Analysis SimCO algorithms and several baseline algorithms. For synthetic data, different parameters are tested to provide relatively comprehensive results. Experiments with image data apply the analysis dictionary learning algorithms to removing additive noise of face images and natural images. For recovering the images using the learned dictionaries, an optimization problem with l_1 -norm regularization is addressed. Some results for synthetic data and image denoising are shown below in Fig. 3.4 and Fig. 3.5 respectively.

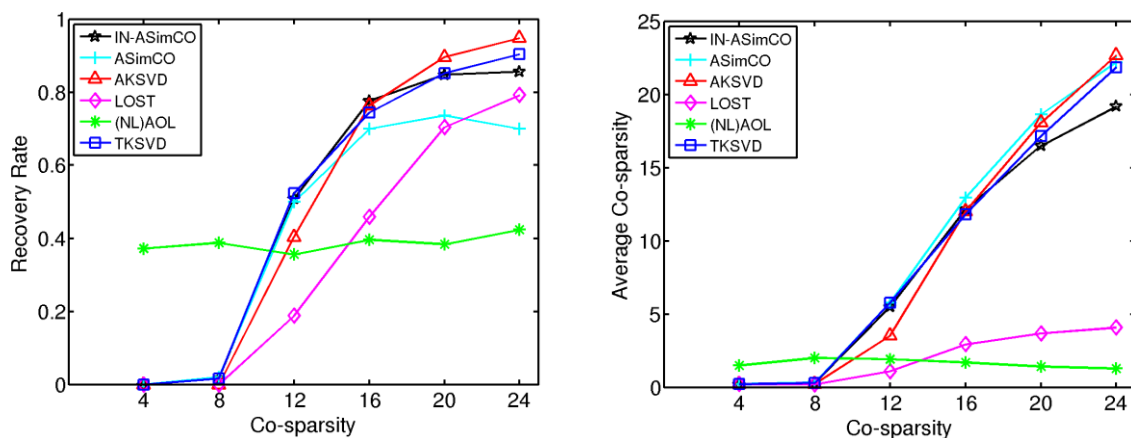


Fig. 3.4. Recovery Rate (left) and Average Co-sparsity (right) with different co-sparsities in the noiseless case.

Abbreviations are used in the legends because of space limitation (IN-ASimCO, ASimCO, AKSVD, LOST, AOL, and TKSVD are short for Incoherent Analysis SimCO, Analysis SimCO, Analysis K-SVD, Learning Sparsifying Transform, Analysis Operator Learning, and Transform K-SVD respectively). The details of these experiments and the analysis of the results are reported in (Dong *et al.*, 2015), a paper that we submitted to IEEE Transactions on Signal Processing.

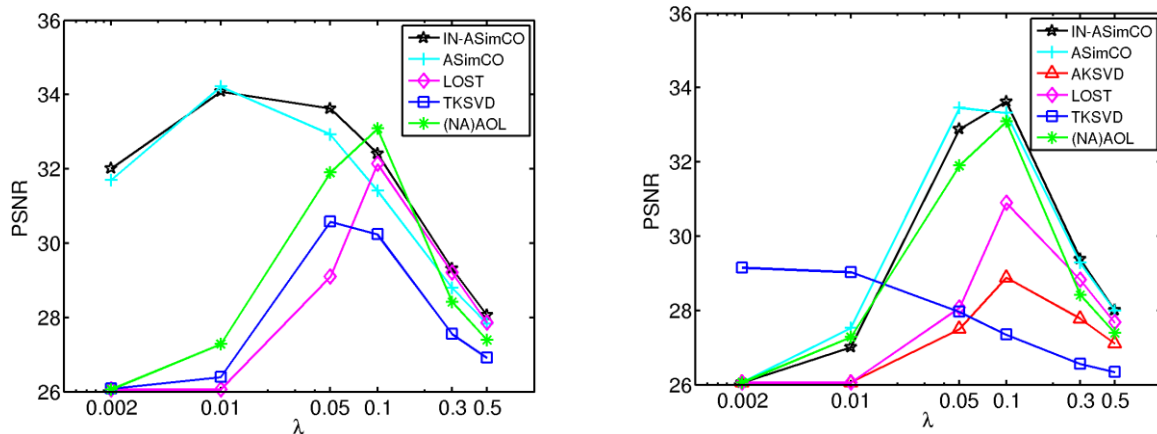


Fig. 3.5. Face image denoising ($\sigma = 12.8$). Training data are extracted from 13 other clean face images, with co-sparsity $l = 40$ (left) and $l = 80$ (right).

2) Audio Super-resolution Using Analysis Dictionary Learning

Super-resolution aims to reconstruct a high-resolution (HR) signal from a low-resolution (LR) input. Super-resolution for images is one of the most active research areas in image processing. However, little work has been done for super-resolution for audio signals. In the field of audio signal processing, the super-resolution problem can be cast to the problem of reconstructing high-frequency portions of audio signals, leading to higher quality audio signals for an improved listening experience.

We consider the super-resolution problem for audio signals in the time-frequency domain and proposed a method using analysis dictionary learning. The input to our proposed method is the LR spectrogram matrix of an audio signal, where some rows corresponding to high-frequency information are lost. First, an analysis dictionary is learned from the spectrogram of some related audio signals. The learned dictionary is then applied in an l_1 -norm regularization term for the reconstruction of the HR spectrogram. Experimental results with piano signals demonstrate the advantage of the learned analysis dictionaries in reconstructing HR spectrograms. This work has been submitted to 2015 IEEE International Conference on Digital Signal Processing (Dong *et al.*, 2015).

3.5.5 Fast Independent Vector Analysis for Source Separation

The cocktail party problem, which was first introduced by Colin Cherry in 1953, relates to the ability of a human being to recognise a sound of interest, often a speech signal in a complex auditory setting. In a room environment, humans can

generally focus on the conversation in which they are involved and can suppress the background noise of other people talking, laughing and music playing. Numerous efforts in the past decades have been dedicated to understand the capabilities of humans and map these qualities to machines. However, it remains a difficult task to accomplish as full understanding of the phenomena of human auditory perceptual capabilities remains a mystery. The solution for the cocktail party problem is to design a method for machines to extract the desired speech signals and suppress any background noise or interference.

From a signal processing perspective, attempts to solve the machine cocktail party problem are termed as Blind Source Separation (BSS), where both the sources and the mixing filters are unknown. A-priori information, such as the position or the mixing process is not available, and only the recordings of the mixtures are available.

Part of this research has considered the Independent Vector Analysis (IVA) algorithm to solve the BSS problem. IVA is an extension of well-known independent component analysis (ICA). In the conventional ICA algorithm, independence for each frequency component is measured separately at each frequency bin. The IVA method uses higher order dependencies across frequencies and it defines each source prior as a multivariate super-Gaussian distribution. Thus it measures the independence across the whole multivariate source and it can be used to preserve the higher order inter-frequency dependencies and structure of frequency components. Moreover, the permutation problem can be avoided and leads to an improved separation performance.

We have worked on both IVA algorithm and the fast version of IVA algorithm that is known as FastIVA. To improve the performance of the IVA algorithm, a new statistical model that can better preserve the dependency within the source vector is still needed. In this section a new IVA method based on multivariate Student's t distribution will be introduced. Recently, the Student's t distribution has been used to model speech signals. The Student's t distribution is a super Gaussian distribution, which has heavier tails than the Gaussian distribution and thus it is more suitable to model certain types of speech signals. Due to the random nature of certain speech signals, many useful samples can be in the tails. Thus the tail dependency can be an advantage when modelling the dependency between different frequency bins of a speech signal. This advantage of the Student's t distribution has been exploited in the IVA and the FastIVA algorithm by changing the source prior from a multivariate Gaussian distribution to a multivariate Student's t distribution.

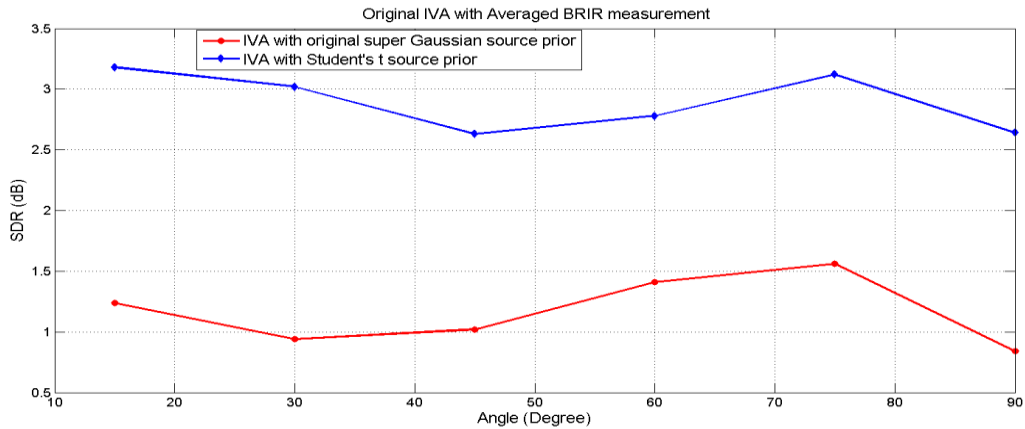


Fig. 3.6. The graph indicates results at different separation angles. The position of the listener was varied in steps of 15° between 15° to 90° . Real BRIRs were used. Results were averaged over three mixtures. Student's t source prior yields a considerable improvement at all separation angles.

Performance of the IVA and the FastIVA algorithm has been tested on the binaural room impulse responses (BRIR), which consists of the real room recordings, to give an estimate of the performance of the algorithm in the real world scenarios. Six different source location azimuths ($15^\circ - 90^\circ$) relative to the second source were used. Three measurements at six different angles are obtained to show the average separation performance. The signal-to-distortion ratio (SDR) in decibels (dB) calculated with the SiSec toolbox is used to evaluate the separation performance. In all the experiments, we used the TIMIT dataset. In each experiment we chose two different speech signals randomly from the TIMIT dataset and convolved them into two mixtures. The results are shown in Figures 3.6 and 3.7 respectively. This work has been partly presented on IMA 2014 conference (Rafique *et al.*, 2014) and also accepted to be presented on IEEE ICASSP 2015 conference (Rafique *et al.*, 2015).

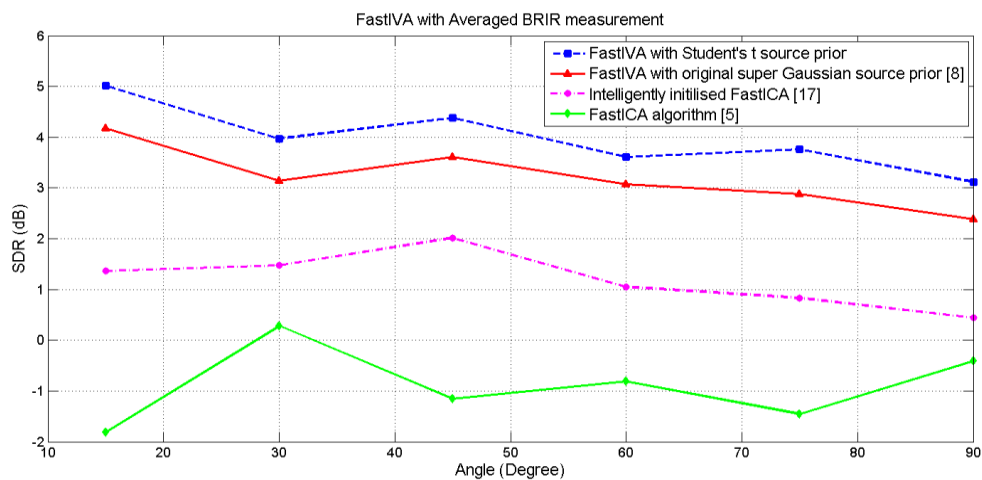


Fig. 3.7. The graph provides results for FastIVA and FastICA at different separation angles. Results are averaged over eighteen random speech mixtures. The position of the source was varied in steps of 15° between 15° to

90°. Real BRIRs were used. Our proposed Student's t source prior yields a considerable improvement at all separation angles.

3.5.6 Room Boundary Estimation

Part of our work focused on the development of a 2D and then a 3D reflector localization model given room impulse responses (RIRs). The overview of the algorithm composing the 3D method is shown in Figure 3.8.

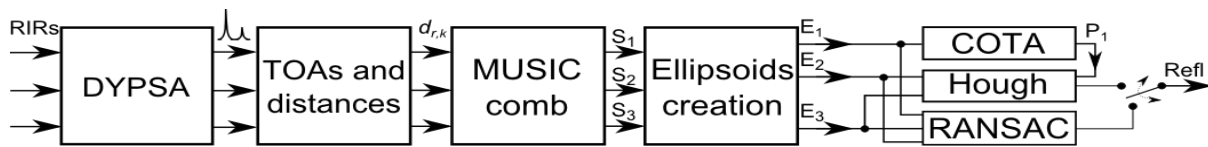


Fig. 3.8. Reflector estimation model overview.

Initially, a 2D algorithm based on Antonacci's ellipses method, which will be useful to estimate the geometry of a room giving some impulse responses, has been implemented. After this, a full 3D model for the reflector estimation has been developed. This is an extension of the 2D model previously developed. The MUSIC algorithm has been modified to be able to estimate DOAs in a 3D space. The ellipses are now substituted by ellipsoids. The cost function has been modified in order to find a plane instead of a line. The 3D Hough transform is created. Several simulations were made on the single components, to understand the origin of the errors. From this, some modifications have been made. For example, the DYPESA algorithm has been modified. The reflector estimation has been modified to reduce the computational cost. The 3D Hough transform has been modified to better estimate the points of contact between the plane and the ellipsoid. Improvements of the 3D reflector localization model have also been made. The RANSAC algorithm has been used to find the reflectors; it can now be used instead of the COTA-Hough combination. Simulations have been performed comparing the new algorithm with the previous one.

To evaluate the 3D model, a dataset of ideal RIRs has been generated using the image source method and two datasets of RIRs measured in two different rooms in University of Surrey have been used. Simulations based on these datasets were performed, and the estimation error is measured using the RMSE considering points in the space (i.e. 5 for each ellipsoid). The errors are obtained as the distance between the estimated plane and the ground truth for each of these points. The results are reported in Figure 3.9. From the results, it is clear that the 3D model improved the already presented 2D one. In addition, the COTA algorithm performs generally better than the RANSAC, but due to its high run time, for some dataset it is not possible to have a high accuracy and for such scenario, the RANSAC based algorithm is recommended. The 3D model has been accepted to present on the ICASSP 2015 conference (Remaggi *et al.*, 2015).

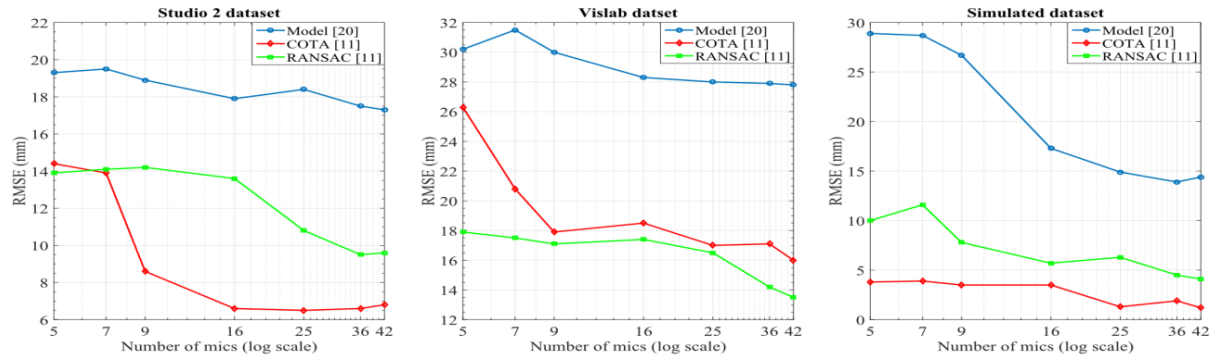


Figure 3.9. RMSE (mm) calculated for the reflector position estimation algorithm.

Based on these works, two algorithms have also been recently implemented. The first algorithm implemented is a technique to estimate the microphones position. A new way of visualizing multi-channel room impulse responses (MC-RIRs) has been developed. The MC-RIRs has been studied using a delay and sum beamformer. The algorithm to understand the exact position of the microphones identifying micro-displacement has been developed, based on the cross-correlation between the signals and the beamformed ones. Simulations have been performed showing an improvement on the cross-correlation coefficients of more than 5%. The results are reported in a paper, to be presented in ICSV conference (Remaggi *et al.*, 2015). It presents a source, sensor and reflector position estimation from acoustical room impulse responses. The second algorithm is on developing a room acoustic parametric model, to be presented on next AES convention (Remaggi *et al.*, 2015). A parametric model has been created for the generation of synthetic RIRs. The Delay and Sum beamformer used in the previous works has been potentiated in its 3D version. It will be applied to extract the direction of arrival of the direct sound and first order reflections. The model has been implemented in Matlab and informal listening tests have been performed.

3.6 Future Plans

For work package L_WP3.1, the focus is to:

- To apply the multichannel spectral factorization algorithm in minimum phase FIR precoder design. One of the applications of spectral factorization has been found in minimum phase FIR precoder design over MIMO frequency selective channel (Du *et al.*, 2013). We will investigate whether our spectral factorization method can be applied to the similar applications, and start to establish a collaboration link with the authors of this paper if it is necessary. We will also study the multichannel spectral factorization in the application of system identification of channel matrix.
- To implement multichannel spectral factorization by using other PEVD algorithms (MS-SBR2, SMD and MSME-SMD). We will study the problem of

shortening the paraunitary matrix order in the MS-SBR2 algorithm. We will also study the other two polynomial matrix decomposition algorithms (PQRD and PSVD).

- To explore the polynomial matrix decomposition algorithms in applications of MIMO communications and broadband sensor array. We will investigate how the polynomial matrix decomposition algorithms can be used in MIMO communications to achieve optimal bandwidth utilization, and the underwater acoustic sensor array to achieve better broadband beamforming.
- To apply our algorithms to defence related data. In particular, we will study the potential of these algorithms for broadband beamforming of the underwater sonar data, as well as multichannel source separation of underwater acoustic mixtures.
- To exploit sparsity constraints in polynomial matrix decompositions. In particular, we will extend conventional sparse representation algorithm for convolutive signals and impulse response modelling. To this end, we will use the polynomial matrix decomposition, such as polynomial SVD as a tool to perform polynomial dictionary learning in the way similar to the conventional K-SVD algorithm.
- To study the potential of applying the SBR2 algorithm to the modelling of room impulse responses and wideband beamforming for room boundary/reflector estimation. We will also explore the potential of such reflector boundary estimation methods for harbour boundary estimation, which is a defence-relevant application scenario.

For work package L_WP3.2, the focus is:

- To further study the Bootstrap averaging method for convolutive source separation. In particular, we will perform theoretical and numerical studies on the behaviour of the bootstrap average technique, and its impact on the estimation of the parameters of the GMM model. We will also further evaluate its performance on source separation for underwater acoustic sonar data such as Portland 03 dataset.
- To develop novel methods for underwater acoustic source denoising, separation and localisation, focussing on sparse sequential Bayesian approaches. The goal of this work will be to produce improved denoising and localisation results on the Portland 03 dataset. We also intend to extend the sparse sequential Bayesian method from its current narrowband implementation to a broadband implementation.
- To develop novel multiplicative noise removal method based on analysis dictionary learning. Multiplicative noise appears in coherent image systems, such as synthetic aperture radar, ultrasound imaging and laser imaging. In the multiplicative noise model, noise is multiplied by (rather than added to) the original image, which makes it more difficult to remove, as compared with additive noise. We consider applying the analysis dictionary learning algorithms to removing multiplicative noise. An idea is to use analysis pursuit algorithm to recover image with an analysis dictionary learned from the noisy image. Some preliminary work has been presented in (Jing and Wang, 2014)

on ISCCSP 2014. We will also look into a more sophisticated method of formulating the multiplicative noise removal problem by considering the statistic model of the noise and applying the learned analysis dictionary to a regularization term.

- To develop fast and online analysis dictionary learning algorithms. Prior work on analysis dictionary learning, including our proposed Analysis SimCO algorithms, focuses on batch learning, where the processing of the entire training set is involved. However, for large training data sets, batch learning techniques can be computationally expensive in both time and memory. Moreover, in real-time applications, data arrives sequentially, which makes batch learning infeasible. Online algorithms where data samples are allowed to be processed sequentially is worth considering, since they are usually more suitable for large data sets and the real-time case. For the analysis dictionary learning, little work for online algorithms has been done. Our future work is therefore to develop an algorithm for the online analysis dictionary learning problem.
- To further improve IVA algorithms with mixture models based source priors. A multivariate Student's t source prior is used with the IVA and the FastIVA algorithm. The source prior for the IVA algorithm is important because the non-linear score function used to retain the inter-frequency dependency is derived based on the PDF of the source. Better results have been achieved with the new source prior. We plan to work on the mixture models. Student's t and Gaussian mixture models will be used to further improve the performance of the IVA algorithm and the FastIVA algorithm. Online implementation of the algorithm will also be considered, so that it can be used in the real life context. The use of the IVA algorithm for the underwater acoustics will also be explored.

3.7 Selected Activities and Engagements

Engagement with industry partners and Dstl:

- Atlas Elektronik has joined the LSSC consortium and will be acted as the lead partner for the work package L_WP3.
- A joint project (of seven months) under the MoD MarCE scheme between Atlas and Surrey has been agreed and signed. The project is titled "Array processing exploiting sparsity for submarine hull mounted arrays". The project has started and we are now recruiting the RA to work on the project.
- Attended a sonar processing workshop organised by Nick Goddard at Dstl in October 2015.

Engagement between partners:

- Jamie Corr at Strathclyde University (associated with WP4) visited CVSSP @ Surrey in July 2014, working with Swati Chandna and Wenwu Wang on the Portland 03 dataset.
- Waqas Rafique initially with Loughborough University, worked in University of Surrey with Wenwu Wang on source separation and time-frequency masking.

3.8 Outputs

During the past year, we have generated the following publications.

Published/accepted:

- Z. Wang and J. G. McWhirter, "A New Multichannel Spectral Factorization Algorithm for Parahermitian Polynomial Matrices," in Proc. of the 10th IMA International Conference on Mathematics in Signal Processing, Birmingham, December 2014.
- S. Chandna and W. Wang, "Improving Model-Based Convolutional Blind Source Separation Techniques via Bootstrap," IEEE Statistical Signal Processing Workshop, 2014.
- J. Dong, W. Wang, and W. Dai, "Analysis SimCO: A new algorithm for analysis dictionary learning," in Proc. IEEE Int. Conf. Acoust., Speech, and Signal Process., 2014, pp. 7193-7197.
- J. Dong, and W. Wang, "Analysis dictionary learning based on Nesterov's gradient with application to SAR image despeckling," in Proc. of the 6th International Symposium on Communications, Control and Signal Processing, 2014, pp. 501-504.
- W. Rafique, S. M. Naqvi, P.B. Jackson and J. A. Chambers, "IVA algorithms using a multivariate Student's t source prior for speech source separation in real room environments", in Proc. of the International Conference of Acoustics, Speech and Signal Processing (ICASSP) , Brisbane, Australia, 2015. (Accepted)
- W. Rafique, S. Erateb, S. M. Naqvi and J. A. Chambers, "Evaluation of source separation algorithms, including the IVA algorithm with various source priors, using binaural room impulse responses", in Proc. of the 10th International Conference on Mathematics in Signal Processing, Birmingham, UK, 2014.
- L. Remaggi, P. J. B. Jackson, P. Coleman, and W. Wang, "Room boundary estimation from acoustic room impulse responses," in Proc. of the Sensor Signal Processing for Defence conference SSPD, Edinburgh, UK, 2014.
- L. Remaggi, P. J. B. Jackson, W. Wang, and J. A. Chambers, "A 3D model for room boundary estimation," in Proc. of the IEEE International Conference on Acoustics, Speech and Signal Processing (ICASSP), Brisbane, Australia, 2015. (Accepted)
- L. Remaggi, P. J. B. Jackson, and P. Coleman, "Estimation of room reflection parameters for a reverberant spatial audio object," in Proc. of the 138th Audio Engineering Society Convention (AES), 2015. (Accepted)
- L. Remaggi, P. J. B. Jackson, and P. Coleman, "Source, sensor, reflector position estimation from acoustical room impulse responses" in Proc. of the 22nd International Congress on Sound and Vibration (ICSV), Florence, Italy, 2015. (Accepted)

Submitted/under review:

- Z. Wang, J. G. McWhirter, J. Corr, and S. Weiss, "Multiple shift second order sequential best rotation algorithm for polynomial matrix EVD," submitted to EUSIPCO 2015, Nice, France, 2015.
- S. Chandna and W. Wang, "A bootstrap-based improvement for model-based convolutive blind source separation," IEEE Transactions on Signal Processing, submitted in November, 2014.
- J. Dong, W. Wang, W. Dai, M. D. Plumbley, Z. Han, and J. Chambers, "Analysis SimCO algorithms for sparse analysis model based dictionary learning", submitted to IEEE Trans. Signal Process, February, 2015.
- J. Dong, W. Wang, and J. Chambers, "Audio super-resolution using analysis dictionary learning", submitted to 2015 IEEE International Conference on Digital Signal Processing.

3.9 References:

G. T. Wilson, "The Factorization of Matricial Spectral Densities," SIAM Journal on Applied Mathematics, vol. 23, pp. 420-426, 1972.

G. Janashia, E. Lagvilava, and L. Ephremidze, "A New Method of Matrix Spectral Factorization," Information Theory, IEEE Transactions on, vol. 57, pp. 2318-2326, 2011.

J. Corr, K. Thompson, S. Weiss, J. G. McWhirter, S. Redif, and I. K. Proudler, "Multiple shift maximum element sequential matrix diagonalisation for parahermitian matrices," in Statistical Signal Processing (SSP), 2014 IEEE Workshop on, 2014, pp. 312-315.

B. Du, X. Xu, and X. Dai, "Minimum-phase FIR precoder design for multicasting over MIMO frequency-selective channels," Journal of Electronics (China), vol. 30, pp. 319-327, 2013/08/01 2013.

S. Chandna and A. Walden, "Simulation methodology for inference on physical parameters of complex vector-valued signals," IEEE Transactions on Signal Processing, vol. 61, pp. 5260–5269, 2013.

L_WP4: MIMO and Distributed Sensing

Section 4.1 Staffing and Objectives of L_WP4

4.1.1 L_WP4 Staffing

Work Package Leaders: Prof. John J. Soraghan (ST) and Prof. Ian K. Proudler (LU)
Other Academics Involved: Dr. Stephan Weiss, Prof. Sangarapillai Lambotharan
Research Associates: Dr Carmine Clemente (PDRA6- ST)
UDRC Research students: Mr Domenico Gaglione (PS6- ST), Mr Christos Ilioudis (PS5- ST)
Affiliated Research Students: Mr Jianlin Cao (ST), MrYixin Chen (ST), Mr Adriano Rosario Persico.
Lead Project Partner: Selex ES, Edinburgh
Dstl contact: Stephen Moore (Sensors & Countermeasures Dept), Brian Barber (Sensors & Countermeasures Dept)

4.1.2 Aims and the lists of the original L_WP4 in the case for support:

To develop novel paradigms for Distributed MIMO Radar Systems (DMRS). Links to L_WP1 & L_WP2 through anomalies; L_WP3 through exploiting sparsity and L_WP5 for decentralised processing. Advanced signal processing methods for active/passive DMRS will be investigated. The approaches aim to improve performance, reduce system requirements with the result of producing a set of algorithms suitable for robust applications in a cluttered networked battlespace. (T1,T3,T5,T8)

Section 4.2 Progress Update April 2014-March 2015

4.2.1 L_WP4.1 Progress

The work developed at ST on WP4.1 focuses on the development of novel signal processing techniques, paradigms and systems for high performance distributed sensing. To this end, we have been conducting fundamental and applied signal processing research in the following sub-areas in the second year.

- In L_WP4.1 Dr Clemente (PDRA6) has investigated advanced *SAR Data compression* using the Anamorphic Stretch transform to provide a powerful tool for lossless SAR data compression. This work, developed in collaboration with the University of California Los Angeles, has been presented at GlobalSIP 2015 conference [1].
- Dr Clemente worked on a proof of concept for the *GPS based passive radar* for Helicopter Classification presented in [2]. With the support of a group of 5th year MEng students, a receiver was developed and real data was acquired that demonstrated the capability to measure helicopter induced micro-Doppler using this sensor. This work has been accepted for publication at the IEEE International Radar Conference 2015 and to the 10th Electronic Warfare Symposium.

- Dr Clemente led the research developed in collaboration with the University of Sannio into extended target detection from *Foliage Penetrating SAR CFAR*. Two exchange students from the University of Sannio in Italy visited Strathclyde. Working under Dr Clemente's supervision a Multi-Model CFAR algorithm for extended target detection hiding in foliage was developed. This work provided very encouraging results on real data.
- A family of novel CFAR detectors was developed by Dr Clemente in collaboration with the University of Naples to address the challenge of *Coherent Polarimetric SAR Change detection*. These detectors, were shown to be invariant to power mismatches and can exploit special data structures. This work has led to the production of 3 Journal and 3 conference papers.
- Dr Clemente has been involved in the implementation of a *Distributed MIMO experimental setup* with the specific aim of investigating the benefits of this configuration for micro-Doppler based applications. The experimental environment uses Software Defined Radio as platforms and has been developed in collaboration with the TOBB University in Ankara through an Erasmus funded visiting master student working on this task.
- The focus of UDRC PhD student Mr Ilioudis (PS5) has been on developing a Constant Envelope framework used to force constant envelope on the *novel fractional waveform libraries* previously reported [8]. The outcome of this work was published at the SSPD 2014 conference. Moreover, Mr Ilioudis focussed on the performance analysis of the novel waveform libraries in a MIMO environment analysing performance in crowded environments and demonstrating the capabilities of the waveforms using real data in a software defined radio based environment. The outcome of this work has been accepted for the special session on MIMO radar of the IEEE International Radar Conference 2015.
- The focus of UDRC affiliated PhD student Mr Jianlin Cao is on the *design of femto-satellites* to realize satellite swarms in the space. He has investigated technical challenges and constraints typical of this family of novel systems. In particular he has developed a preliminary design of a femtosatellite using commercial off-the-shelf (COTS) technology providing acceptable level of mission capability and environmental survivability. The prototype is a flat designed femtosatellite build on Kapton film instead of conventional printed circuit board (PCB) to reduce the weight and increase the area-to-mass ratio. These features enable the femtosatellites to take advantage of solar radiation pressure for propulsion without on-board propellant, extending their orbital lifetime and mission capability. A patch antenna or Vivaldi antenna could be used as payload to perform Earth remote sensing or target detection missions.

4.2.2 L_WP4.2 Progress

The work developed at ST on L_WP4.2 focuses on the development of novel signal processing techniques and algorithms for distributed systems. To this end, we have concentrated in the following sub-areas in the second year. In November 2014 Mr Adriano Rosario Persico joined the group. He is currently researching advanced signal processing technologies for space situation awareness and defence against airborne threats.

- For L_WP4.2 Dr Clemente has focussed on the investigation of novel algorithms and approaches for *micro-Doppler based Automatic Target Recognition*, with an emphasis on both traditional and non-conventional distributed/MIMO sensors. In particular an algorithm exploiting dictionary learning for sparse representation of micro-Doppler has been developed. The technique utilises the LC-KSVD algorithm [3] and does not need the computation of any time-frequency representation and thus, it is independent of the contextual nature of the received signal, since no parameters have to be adapted based on the input signal. The developed algorithm has been tested with both real and simulated data providing good results with low computational cost. The outcome of this work will be submitted to the DSP conference 2015 in Singapore.
- Dr Clemente worked on novel concepts for Ballistic Missile Defence systems. In particular a CDE funded project is ongoing entitled: *Micro-Doppler Signature Based Recognition of Ballistic Missiles and Associated Functional Assessment*. This project investigates the feasibility of micro-Doppler based recognition of warheads and decoys. The project has had a successful outcome to date. The results will be presented in a forthcoming Journal paper.
- UDRC PhD student Mr Domenico Gaglione (PS6) worked on the development of a *full polarimetric version of the ATR* algorithm [4] exploiting the Krogager decomposition. The polarimetric decomposition enhanced the performance obtained in [5] and the outcome of this work was presented the SSPD Conference 2014 [4]. Furthermore, Mr Gaglione developed a template-based algorithm for micro-Doppler classification. This algorithm does not need any training datasets and time frequency representations. The algorithm was tested on both synthetic and real data and will be presented at the IEEE International Radar Conference 2015.
- The focus of affiliated PhD student Mr Adriano Rosario Persico has been the review of the literature on the field of *ballistic missile classification* and the initial investigation of novel feature extraction techniques and how to make them robust for the purpose of discriminating warheads and decoys. Furthermore, Mr Persico has been involved in the CDE project managing the experimental apparatus for gathering the real data and producing the ballistic missiles replicas.
- The focus of affiliated PhD student Mr YixinChen has been the development of a novel modulation scheme for *under water acoustic communication*. The novel scheme introduces the Partial Fractional Fourier Transform concept to deal with double-dispersive channels. The outcome of this work has been submitted to Eusipco 2015.

Section 4.3 L_WP4 Technical Details

4.3.1 Constant Envelope Fractional Waveform Libraries in MIMO radars.

As modern radar systems are increasingly being required to operate in fast changing and electromagnetically overcrowded environments, their operational capabilities may be significantly conditioned by interference, frequency occupancy and performance constraints like high resolutions and power requirements. In the presence of these difficulties, the selection of robust waveform designs that allow good resolution, high signal energy using low peak power and high spectrum efficiency poses a major challenge.

In L_WP4.1 we investigated the application of Fractional Fourier Transform (FrFT) and Gerchberg-Saxton algorithm (GSA) on phase coded sequences to generate novel families of waveform libraries. The FrFT is a generalization of the Fourier transform in which the resulting sequence can be in time- frequency domain instead of pure frequency. The impact of FrFT on conventional radar sequences such as Barker and P4 codes has been previously investigated showing potential improvement in ambiguity function (AF) quality parameters [6] and reuse [7]. One drawback of the FrFT base waveform libraries is that they do not satisfy the constant envelope (CE) constraint, which is a common requirement for most radar systems. A modified version of GSA was proposed to enforce the constant envelope constraint on the FrFT modulated sequences while minimising any change from the original waveform. The analysis of the AF performance and orthogonality were performed in [8]. Moreover a performance analysis of CE-FrFT base waveform libraries in a MIMO radar scenario was carried out in [9]. Simulation results demonstrated that the proposed method offers similar detection performance as linear frequency modulated waveforms of the same Time-Bandwidth product, while outperforming other modulation techniques. Additionally an experimental validation of CE-FrFT waveforms generated from the same code sequence and different fractional order evidenced their good orthogonality properties. In Figure 4.1 shows the output of a matched filter when presented with a received signal that is a combination of three orthogonal CE-FrFT waveform s_1 , s_2 and s_3 .

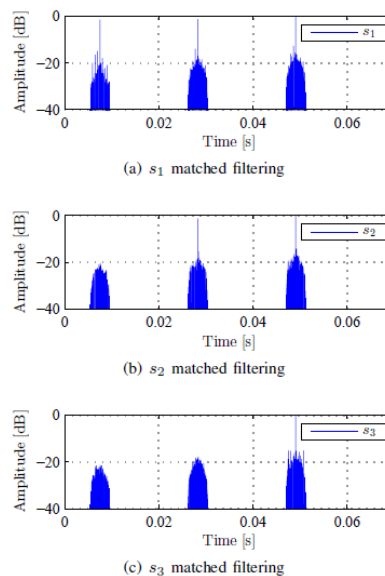


Figure 4.1 Matched filter outputs of the received sequence after applying the matched filter with (a) s_1 , (b) s_2 and (c) s_3 respectively.

Analytically the transmitted waveform is described as s_1 , $(s_1 + s_2)$ and $(s_1 + s_2 + s_3)$ for the first, the second and the third pulse respectively. It can be seen that after applying the respective matched filters all waveforms can be retrieved correctly from the three pulses. Future works include the development of a multistatic AF and evaluation of the CE-FrFT libraries in various detection scenarios.

4.3.2 Passive Bistatic Radar (PBR) For Micro-Doppler based Target Identification: Proof of concept

This research task is aimed to demonstrate the PBR concept developed in [10]. A proof of concept hardware for the analysis of the micro Doppler effect in a passive bistatic GPS radar system to determine the characteristics of a helicopter's rotor blades was developed. Such a system could be used to detect and identify helicopters that fly below altitudes that can be observed by conventional radar. Another benefit is that because the receivers are relatively cheap - as they do not have to transmit high power signals - a series of receivers can be deployed across a boundary without fear of a major loss of investment.

Real data acquisitions were performed in proximity of Cumbernauld Airport in Scotland. The satellites visible at the time of acquisition (with reference to their PRN codes) were: 5, 10, 15, 26 and 28. Measurements were obtained with two different helicopters used for pilot training purposes. For this reason the helicopters were following a set path of taking off performing a circuit of the airport and landing. The two helicopters used were a small two seat Robinson R22 and a larger four seat Robinson R44, both use two bladed main and tail rotors. The R22 has a main rotor repetition of 8.5 RPS (Rotations Per Second), the tail rotor has a repetition rate of 53.3 RPS. The motor rotor blades are 3.84 m in length and the tail rotor has a length of 0.53m. The R44 main rotor has a rotation rate of 6.8 RPS with a blade length of 5.03 m. The tail rotor has a repetition rate of 40.5 RPS with a blade length of 0.74 m. Taking into account the flight path of the helicopters, satellite number 26 was identified as the one providing the best geometry, considering the flight path of the helicopters. Notice that a receiver in an operational scenario can easily perform the selection of the best geometry, for example a specific selection can be used if the interest is to monitor a given area or all the available satellites can be used to cover most of the possible directions. The received signals are then cross-correlated with the C/A sequence of the selected satellite. In order to remove the direct signal and the other signal components (i.e. fuselage return) the Singular Value Decomposition technique proposed in [11] is used.

In Figure 4.2-a the spectrogram of the extracted micro-Doppler signature of the main rotor of the R44 is shown. The measured interval between two flashes is 0.0735 s leading to a rate of 13.6 flashes per seconds. The signature shows that an even number of blades are present in the rotor, thus the 13.6 flashes per second correspond to 6.8 RPS for a 2 bladed helicopter. This value matches the characteristics of the main rotor of the R44 helicopter. The same processing has been applied to the returns collected when the R22 was flying and whose spectrogram is shown in Figure 4.2-b.

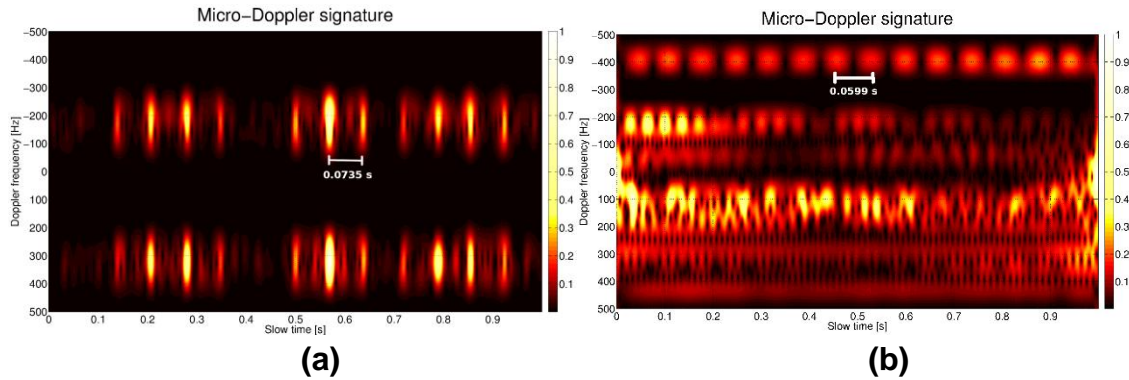


Figure 4.2 Measured micro-Doppler signature for the R44 (a) and R22 (b) helicopters.

The periodic component due to the flash of the tip of the blade is visible from the top portion of the spectrogram. The separation between two consecutive flashes is 0.0599s leading to 16.69 flashes per second. Assuming 2 blades in the rotor this leads to 8.34 RPS in agreement with the possible values of RPS around 8.5 RPS reported in the pilot manual of the R22 helicopter.

The capability of extracting micro-Doppler signatures of main rotor of helicopters exploiting GNSS signals of opportunity has been demonstrated through the acquisition of real signals from 2 helicopters flying in the Cumbernauld Airport area. The results demonstrate that in the near forward scattering regime the main rotor return scan be detected and that the micro-Doppler signature can be used for helicopters identification.

4.3.3 Krogager Decomposition and Pseudo-Zernike Based ATR

Automatic Target Recognition (ATR) is one of the main applications of modern radar systems. It is an essential requirement in battlefield scenarios, where the correct identification of a target must be guaranteed with high degree of confidence. In this context, multiple sources of information are often available (i.e. spatial, temporal, frequency, waveform and polarization diversities) and they can be potentially combined leading to an improvement of the performance.

In [4] we presented an algorithm for target classification from multi-sensor full-polarimetric SAR data, which exploits both the diversity offered by the use of different sensors, and the different scattering responses of an object in each polarimetric channel. In this task, a novel extension of the algorithm presented in [4] was proposed. It takes as input the four polarimetric components of the object under test, from which features are extracted and used to recognize the target by using a classifier. Feature extraction based on both pseudo-Zernike moments and Krogager polarimetric decomposition [5] were used. If multiple views are available, they are processed separately and then the decisions of all the classifiers are combined, leading to an estimate of the class to which the target belongs.

The algorithm was tested using the GOTCHA dataset [12], which is a collection of real full-polarimetric circular SAR images acquired by an airborne X-band sensor (carrier frequency 9.6 GHz) with a 640 MHz bandwidth at 8 different elevation angles; the set consists of 2880 full-polarimetric images, 360 for each pass, of several civilian vehicles and calibration targets. Six different analyses were carried out, involving two configurations for the training set and three configurations for the

test set. The training set was formed by images coming from the lowest altitude pass; either 10 or 30 images for each vehicle were used to train the classifiers, selected each 36 degrees or 12 degrees in azimuth. The test set was formed by all of the images. Three configurations were considered: in the first scenario, one image was used in order to classify the target; in the other two scenarios, 2 and 3 images were used, respectively, to show the benefits of the multi-sensor framework.

The performance of the proposed algorithm, which is labelled as Integrated Intensity-Krogager (IIK) approach, is shown and compared with the performance of the Intensity Approach (IA), proposed in [4], and of the Krogager Approach (KA); the latter consists of classifying the target by using only the Krogager based features. In Figures 4.3-5 the performance is shown in terms of percentage of correct classification and 'unknown' classifications when 1, 2 and 3 images were used to perform the classification, respectively.

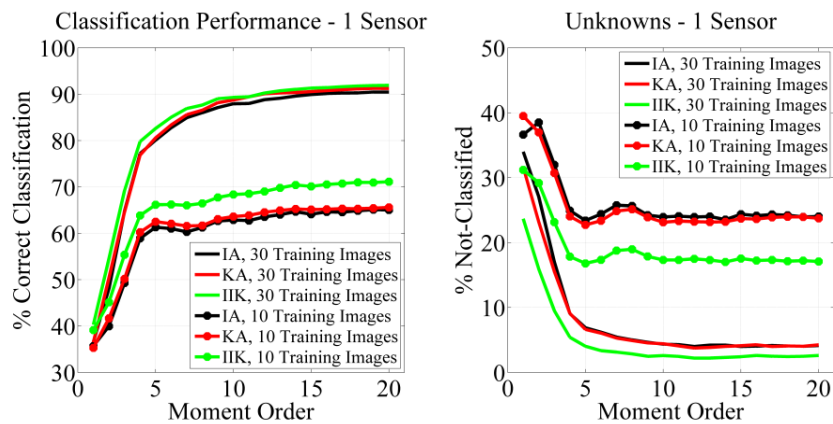


Figure 4.3 - Results with 1 sensor: (left) Percentage of correct classification and (right) percentage of unknowns.

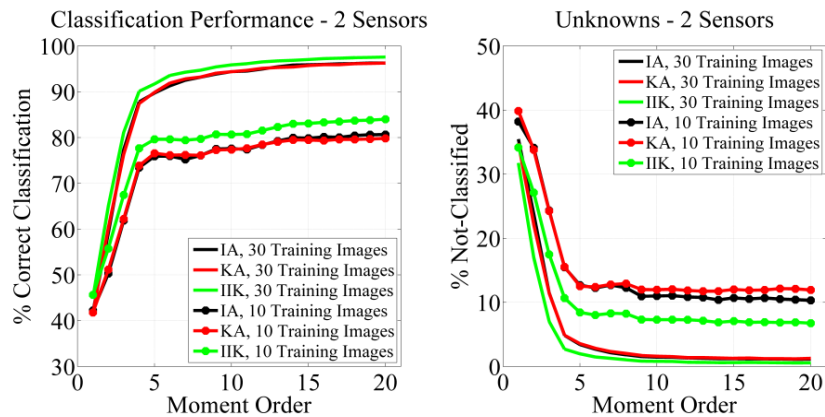


Figure 4.4 - Results with 2 sensors: (left) Percentage of correct classification and (right) percentage of unknowns.

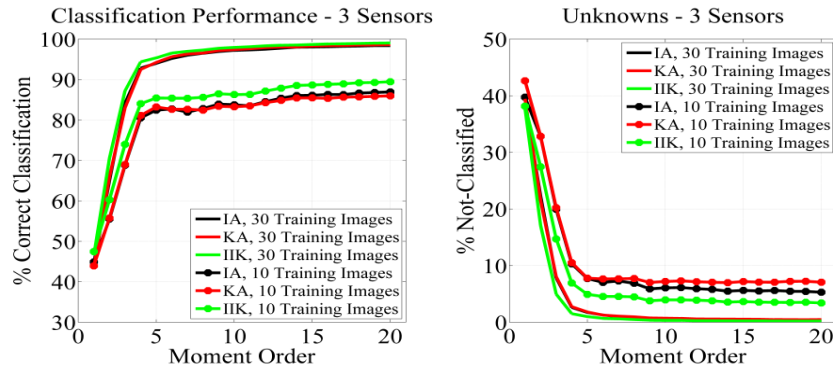


Figure 4.5 - Results with 3 sensors: (left) Percentage of correct classification and (right) percentage of unknowns.

The results show that the IIK approach achieves better performance than the approach presented in [4] in terms of percentage of correct classifications and percentage of 'unknown' classifications for all the configurations in which it has been tested, only at cost of a slight increase in computational complexity, since no additional information is required as input of the algorithm with respect to the IA. In particular, improvements up to 5.5% and 7.0% are achieved for the percentage of correct classifications and 'unknown' classifications, respectively. Moreover, the PZ moments properties of translation and rotation independence, combined with the roll invariant characteristic of the Krogager decomposition, makes the algorithm robust with respect to both the target orientation in the image plane and the acquisition elevation angle. Furthermore, it is worth highlighting that the framework can also find application in a real-time scenario, in which several sensors are involved.

4.3.4 Model-Based Method for Automatic Classification of Helicopters

The micro-Doppler (mD) effect refers to the variations of the Doppler frequency induced by micro motions of some components of a target, such as oscillations of arms and legs of a walking human or rotations of rotor blades of a helicopter. Such a variation represents a unique signature of the target, which can be exploited for military purposes as classification, identification and radar imaging. Based on the mD features of a target, the latter can be classified. The capability to classify a helicopter by analysing its mD properties was first investigated in [13], after that in [14] it was demonstrated that the theoretical return signal from propeller blades depend on the number, the length and the rotation speed of the blades themselves.

In this task, an automatic helicopter classification algorithm was developed. It consists of three stages: (1) synchronization of the first flash of the received signal with the instant $t = 0$; (2) estimation of the helicopter's mD parameters by using a modified version of the Pruned Orthogonal Matching Pursuit (POMP) presented in [15]; (3) classification of the target, based on the parameters estimated during stage (2).

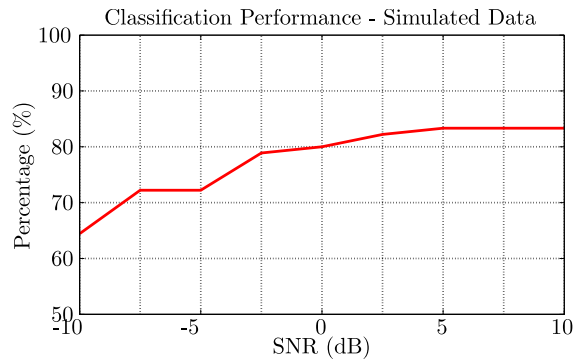


Figure 4.6 – Performance on simulated data in terms of percentage of correct classification.

The algorithm was tested with both simulated and real data. Regarding the former one, 90 trial radar return signals from different helicopters were generated with a carrier frequency of 5 GHz. The performance is shown in Figure 4.6: even at SNR = -7.5 dB, the helicopters are correctly classified in the 72.22% of the cases, while for values of the SNR above 0 dB, the percentage of correct classification is above 80%. The real dataset is a collection of radar return signals from a two-bladed helicopter scale model acquired with a 24 GHz CW radar. Application of the algorithm on such a dataset, confirms the validity of the approach, leading to an average 96% of correct classification in the cases of most interest.

The proposed method does not require the use of a training set or adaptive processing of the received signal. It does not need the computation of any time-frequency representation, which makes it independent of the dynamics of the received signal, since no parameters have to be adapted to the input signal, such as, for example, the window length for the computation of the Short Time Fourier Transform (STFT). Moreover, it is robust with respect to the initial position of the blades and the angle that the LOS forms with the perpendicular to the plane on which the blades lie.

4.3.5 Complex SAR Data Compression using Anamorphic Stretch Transform

In this research task a nearly lossless SAR image compression technique has been developed for focused SAR images.

The technique exploits the Discrete Anamorphic Stretch Transform (DAST) [16], [17] to compress SAR complex-valued images. DAST is a physics-inspired mathematical transformation that emulates diffraction of the image through a physical medium with a specific non-linear diffraction property [16], [17]. It reduces the image data size by performing space-bandwidth product compression. This is achieved through warping the image and not through modification of the sampling process as in compressive sensing (CS) [18], [19]. This technique does not need feature detection and is operated in open-loop fashion.

The DAST is related to the recently introduced technique for analog time-bandwidth compression of one-dimensional temporal signals [20]–[22] and has been employed for the first demonstration of optical analog real-time data compression [23].

The selective warping capability of the DAST is exploited in this work to deal with the problem of the compression of complex valued SAR images. Our approach is used to increase the spatial coherence of the SAR image and reduce the spatial

bandwidth. The error on both the magnitude and phase has been quantified demonstrating that the DAST based approach allows a nearly lossless compression, limited only by the quantization error that cannot be removed in the current digital framework scheme.

The real data used for testing is one of the images from the X-band Coherent Change Detection Challenge dataset acquired by the Air Force Research Laboratory (AFRL) [24]. The data contains passes acquired with three polarizations (HH, VV and HV) and resampled range and cross-range resolution of 0.3 m, with pixels with single precision (16 bits for each real and imaginary part). The data size before compression is 59.7 MB.

For comparison we consider JPEG2000 as standard compression as well as secondary compression in our algorithm (used after the application of the DAST). In both cases it was applied obtaining a compressed real and imaginary parts with 16 bit precision, achieving a final image size (for both approaches) of 4.8 MB which means a compression factor of 12.43.

In Figure 4.7 the magnitudes of the complex images are shown. In Figure 4.7-a the original image is shown while in Figure 4.7-b and Figure 4.7-c the JPEG2000 and DAST+JPEG2000 images respectively are shown. While in Figures 4.7-d,-e and -f a zoomed image of the building on the bottom right of the image is shown for the three cases. It is evident that using JPEG2000 only does not preserve the same image quality, while the use of the DAST allows a higher fidelity reproduction of the image. In order to quantify the compressed complex image quality we evaluate the Peak Signal to Noise Ratio (PSNR) and the Mean Phase Error (MPE) and the results are reported in Figure 4.8.

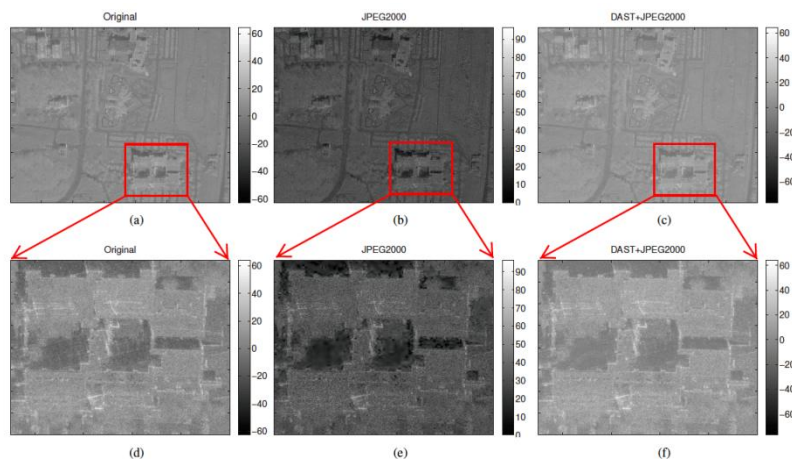


Figure 4.7 – Compression results, qualitative performance on a X-band SAR image.

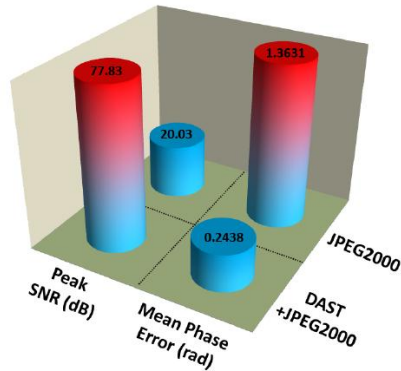


Figure 4.8 – Compression results, performance quantification on a X-band SAR image.

Further validation of the algorithm has been performed using S, and C band SAR Data, providing similar results.

4.3.6 Foliage Penetrating CFAR Detection of Extended Target

The problem of target detection in a complex clutter environment, with Constant False Alarm Ratio(CFAR), is addressed in this research task. In particular an algorithm for CFAR target detection is applied in the context of Foliage PENetrating (FOPEN) Synthetic Aperture Radar (SAR) imaging. The Extreme Value Distributions family of probability distributions is used to model the data. Exploiting the location-scale property of this family of distributions leads to a multi-model CFAR algorithm. Performance analysis on real data confirms the capability of the new algorithm to control the false alarm probability and to detect extended targets concealed in foliage.

The architecture of the new CFAR algorithm is shown in Figure 4.9, where starting from the data under test, the location and scale parameters of the data's statistical distribution are estimated in order to set a threshold ensuring the CFAR property. The algorithm has an adaptive threshold setup and is also able to deal with different forest densities thanks to a multi-model statistical approach.

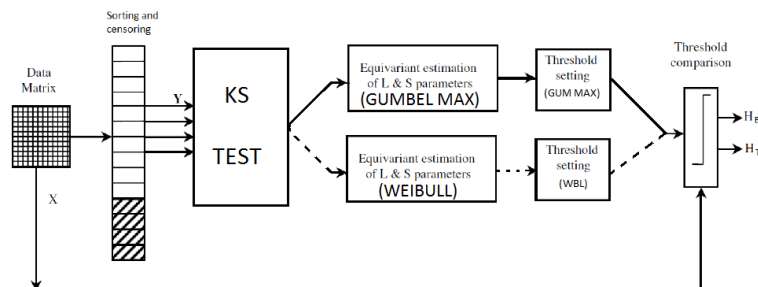


Figure 4.9 – CFAR detection algorithm.

The algorithm has been tested using the CARABAS II dataset [25], a dataset of Foliage Penetrating SAR Images of military vehicles concealed in forest. The results

on different acquisitions (1 to 6) from 2 different forest densities (high and low), with 6 censoring depths and a nominal probability of false alarm of 10^{-4} , are shown in Table 4.1.

Forest2	1	2	3	4	5	6
0	5.5498×10^{-5}	4.6248×10^{-5}	5.0873×10^{-5}	2.3124×10^{-5}	1.8499×10^{-5}	2.3124×10^{-5}
32	9.2496×10^{-5}	8.0009×10^{-4}	1.9887×10^{-4}	6.7522×10^{-4}	2.6361×10^{-4}	2.8211×10^{-4}
64	2.7749×10^{-4}	13×10^{-4}	2.9599×10^{-4}	11×10^{-4}	4.5786×10^{-4}	4.5323×10^{-4}
96	1.3874×10^{-5}	2.8674×10^{-4}	4.1623×10^{-5}	1.7574×10^{-4}	1.3874×10^{-5}	6.4747×10^{-5}
115	1.3874×10^{-5}	1.9424×10^{-4}	2.3124×10^{-5}	1.0637×10^{-4}	1.3874×10^{-5}	6.9372×10^{-5}
128	1.3874×10^{-5}	2.3587×10^{-4}	2.7749×10^{-5}	1.3874×10^{-4}	9.2496×10^{-6}	8.3247×10^{-5}
Forest 1	1	2	3	4	5	6
0	5.0873×10^{-5}	2.1737×10^{-4}	3.6998×10^{-4}	2.9136×10^{-4}	8.3247×10^{-5}	6.4747×10^{-5}
32	6.7522×10^{-4}	1.6×10^{-3}	6.8910×10^{-4}	2.0×10^{-3}	4.9023×10^{-4}	5.9660×10^{-4}
64	1.2×10^{-4}	3.1×10^{-3}	10×10^{-4}	3.6×10^{-4}	8.4634×10^{-3}	11×10^{-4}
96	2.9136×10^{-4}	9.2959×10^{-4}	2.9136×10^{-4}	1.4×10^{-3}	1.4799×10^{-4}	1.6649×10^{-4}
115	1.2949×10^{-4}	6.7522×10^{-4}	1.6649×10^{-4}	1.0×10^{-3}	8.7881×10^{-5}	9.7121×10^{-5}
128	1.7574×10^{-4}	7.9547×10^{-4}	1.8962×10^{-4}	1.2×10^{-3}	1.11×10^{-4}	1.1562×10^{-4}

Table 4.1 – Estimated False Alarm Probabilities for a nominal P_FA of 10^{-4}

The results confirm the capabilities of the proposed approach to control the false alarm probability for this particular challenge.

4.3.7 Coherent Change Detection from Polarimetric SAR

This research task considers the problem of coherent multi-polarization SAR change detection assuming the availability of image pairs possibly exhibiting power mismatches/miscalibrations. The principle of invariance is used to characterize the class of scale-invariant decision rules, which are insensitive to power mismatches and to ensure the Constant False Alarm Rate (CFAR) property. Then, the Generalized Likelihood Ratio Test (GLRT) was used both for the cases of two- and three-polarimetric channels. Some additional invariant decision rules have also been derived.

Starting from the multi-polarization data model developed in [26] and [27], in [28] and [29] a new and systematic framework for change detection based on the theory of invariance in hypothesis testing problems is proposed. This setup allows decision rules to be constructed which exhibit some natural symmetries that lead to important practical properties such as the Constant False Alarm Rate (CFAR) behaviour.

Starting from the framework proposed in [28], in this research we introduce the capability to account for a possible scale mismatch factor.

The new approach is able to produce scale-invariant decision rules, providing advantages in terms of robustness to intensity, miscalibration and false alarm rejection compared to [28]. This is an important property as images over the same scene can exhibit different intensity scales due to different observation angles and propagation properties. These effects can often lead to false alarms in a change detection algorithm that is not designed to be robust with respect to such scale variations. We also compute the GLRT detector and prove that it belongs to the class of scale-invariant decision rules.

Both simulated and real radar data are exploited to show the effectiveness of the new approach.

To validate the behaviour of the proposed tests on real SAR images, we use a high-resolution change detection dataset, available from Air Force Research Laboratory (AFRL) [24] and collected from an X-band SAR. The analysis highlights the capability of the proposed detectors to provide scale invariance in real environments and, at the same time, to ensure satisfactory detection performance.

In Figure 4.10 the Probability of false alarm versus scale factor, for three polarimetric channels and for four detectors derived with the proposed framework is shown.

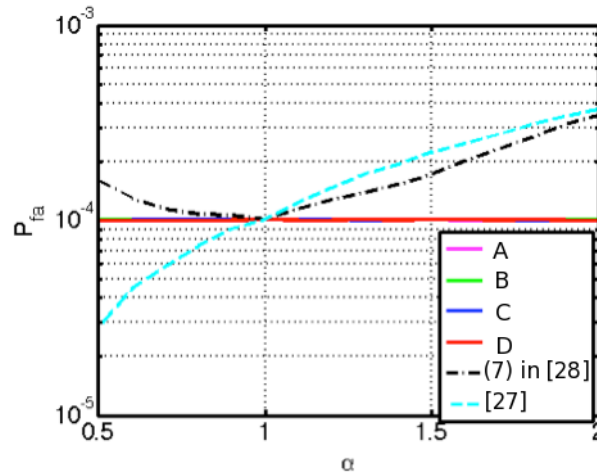


Figure 4.10 - Estimated False Alarm Probabilities for a nominal P_{FA} of 10^{-4} .

The behaviours of the detector (7) in [28] and of the detector proposed in [27] are also displayed. In all the situations, the invariant detectors provide a stable probability of false alarm. In comparison, the detector (7) in [28] and the one in [27] fail to provide a constant false alarm rate in the presence of scale variations between the reference and test images. Similar performance is obtained for the detection probability too.

4.3.8 Ballistic Missile Recognition based on Micro-Doppler

This work (funded by the contract CDE36521) aims to demonstrate the potential of exploiting radar micro-Doppler signatures in order to provide a reliable discrimination of Ballistic Missiles (BM) warheads from decoys. Furthermore the approach may have the potential of being used to provide useful information in the kill-assessment task through the detection of functional discontinuities that occur due to a non-kinetic/kinetic weapon that has been used against the threat. The project demonstrated the concept using laboratory-based experiments to analyze performance in different scenarios and conditions and the associated real time capabilities. In Figure 4.11 the experimental setup used to acquire the data is shown. In particular the figure shows two robotic arms holding the target replicas with the radar positioned in front of them.



Figure 4.11 Experimental setup for ballistic missile assessment.

A ballistic missile trajectory is usually divided into three parts:

- Boost phase, which consists in the powered flight portion;
- Midcourse phase, the free-flight portion that constitutes most of the flight time and during which the missile deploys the decoys in order to make its detection more difficult for Defence Systems;
- Re-entry phase, during which the warhead re-enters the Earth's atmosphere to approach the target.

Throughout the midcourse phase, warhead and decoys exhibit different micro-motions due to their different composition/construction that if appropriately acquired may be used to distinguish between them. In particular, the missiles make *precession* and *nutation* movements, while the decoys *wobble* after they leave the missile itself. Precession comprises two different motions: *conical movement*, which is a rotation of the axis of symmetry of the warhead that draws a cone, and *spinning*, that is the rotation of the warhead around its axis of symmetry.

The aim of the experiment is to acquire signals scattered by simulated warheads and decoys for different azimuth and elevation angles in an S-Band radar scenario. In particular, acquisitions are carried out for each target and for each possible elevation/azimuth angles, choosing among three possible values: 0° , 45° and 90° . In order to change the angle of elevation the radar is moved whereas to change the azimuth angle the radar is kept in its position while the robotic manipulator is moved.

Moreover, two possible types of warheads are considered, approximated by a simple cone and a cone with triangular fins at the base, respectively; concerning the decoys, a cylinder, a cone and a sphere are used. The precession angle chosen for both the types of warheads is 10° , while the spinning angular velocity is around 1 Hz. The nutation frequency is 10 Hz for all the signals, which are then used to test the classification algorithms.

The concept has been proved with a real time implementation of different feature extraction algorithms. Here the results of the Pseudo-Zernike moments based micro-Doppler classification algorithm presented in [30] and [31] are reported. The results

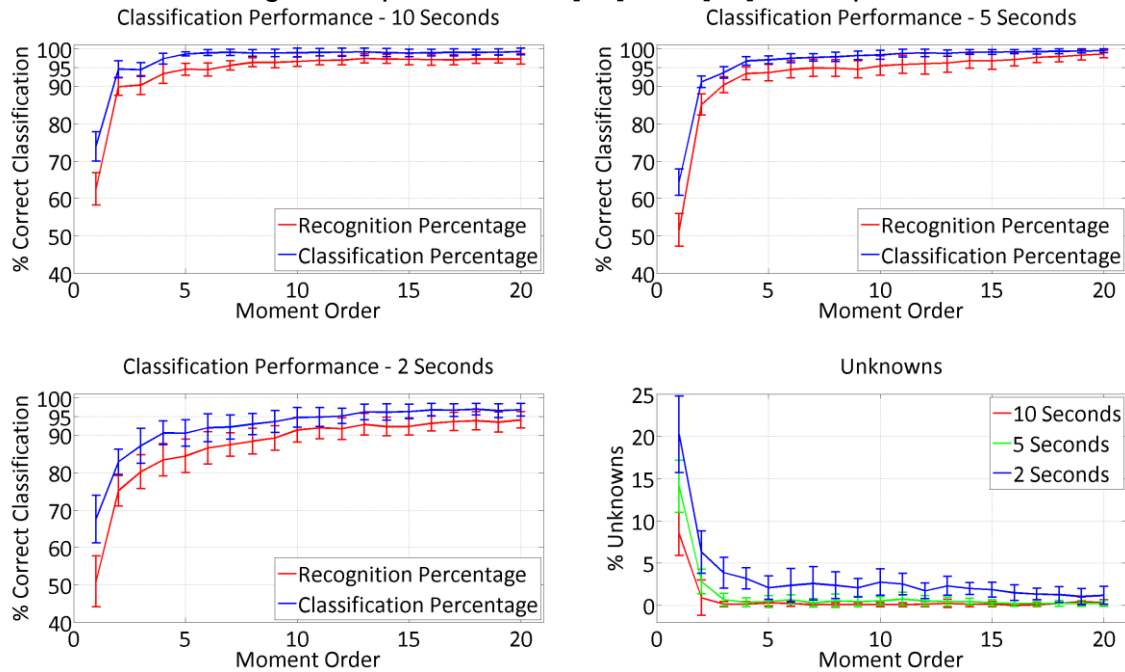


Figure 4.12: Performance of the pZ Based Feature Vector Algorithm.

are shown in Figure 12, both in terms of percentage of correct recognition and classification, and in terms of percentage of 'unknown' classification; the error bars indicate the variability from 10 different runs. The performance improves as the maximum order of the moments increases. The obtained results confirm the capability of micro-Doppler signatures to provide a powerful technique for the ballistic missile defence task.

4.3.9 Enhanced Under-water acoustic communication

Underwater acoustic communication (UWA) suffers from significant time delays reaching fractions of seconds as well as severe Doppler spread attributed to relative motion between transmitter and receiver. The problem is exacerbated due to the low speed of sound in water (1500m/s). Orthogonal Frequency Division Multiplexing (OFDM), is widely used in situations that exhibit high dispersion due to its superior resistance to Inter-Symbol Interference (ISI) and its low complexity. This aspect is improved by having a large number of subcarriers. However with an increase of subcarrier numbers, the bandwidth of each subcarrier will be smaller; therefore the system becomes more vulnerable to a loss in orthogonality caused by high Doppler spread, leading to Inter-Carrier Interference (ICI).

In this research task, a novel method called Partial Fractional Fourier Transform (PFRFT) is investigated in conjunction with banded MMSE equalization to enhance communications over UWA channels. The Partial Fast Fourier Transform (PFFT) [32] [33] [34], decomposes a received signal into several segments using non-rectangular windows, followed by FFT demodulation and a weight compensation process on each segment. The working principle of the PFFT is based on the fact that the channel coherence time increases.

A simulated doubly selective channel scenario is considered. The results show the superior performance of the PFrFT approach compared with conventional PFFT and FrFT-OFDM ones. Moreover, the performance is obtained using a low cost equalizer based on least squares (LSMR) approach [36] [37], which uses a tradeoff between performance and complexity are presented.

Figure 4.13 compares the BER performance of the partial Fractional Fourier Transform (PFrFT), Discrete Fourier Transform (DFrFT) and conventional partial Fourier Transform (PFFT) based OFDM scenarios with LSMR iterative equalization. Figure 4.13 shows that PFrFT-OFDM is superior to DFrFT-OFDM by approximately up to 8dB, attributed to the PFFT demodulation. Finally, Figure 4.14 compares the performance of PFrFT-OFDM based on different length of the segments used in the PFFT.

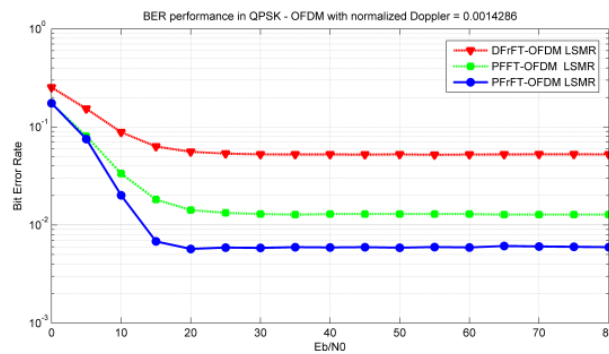


Figure 4.13: BER of PFrFT-OFDM and PFFT-OFDM, and DFrFT-OFDM based on LSMR iterative equalization.

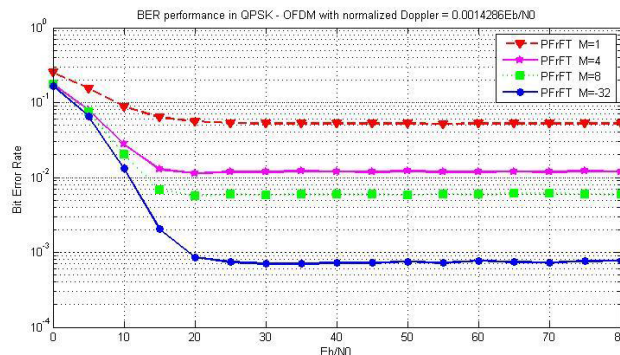


Figure 4.14: BER of PFrFT-OFDM based on M=1, 4, 8 and 32.

The results confirm that an improved BER is achievable using larger values of M. However it comes with an increase in computational cost.

4.3.10 Other activities

- The student Fraser Coutts joined the group for the a Summer Internship working on dictionary learning for sparse representation of micro-Doppler signals, the outcome of this project will be finalised and published in 2015;
- In collaboration with National Instruments a one day hands-on training course on Software Defined Radio was organised for the Sensor Signal Processing and Defence researchers, the event was attended by 14 people;
- A preliminary analysis on the MSAR data was performed and in collaboration with Brian Barber. An application for a Dstl case award to fund a PhD studentship to work on this topic was submitted;

- A CDE project responding at the call “Defence against airborne threats” has been granted and was developed between October 2014 and March 2015;
- 2 Kband radar, 2 UWB C band Radars, 2 2x2 MIMO USRP RIO and 8 Nooelec SDR have been acquired to provide enough experimental capabilities to gather data and test algorithms. Moreover a 12 TB hard disk unit has been acquired for data storage;
- Prof. Soraghan, Dr Clemente, Mr Gaglione, Mr Ilioudis, Mr Cao and Mr Chen attended the SSPD 2014 Conference. Moreover 3 papers were presented at the conference;
- The IEEE Radar Conference 2014 in Cincinnati was attended by Dr Clemente and Prof. Soraghan where 3 papers were presented;
- The International Radar Conference 2014 in Lille was attended by Dr Clemente and 2 papers were presented;
- Prof. Soraghan and Dr Clemente attended and gave a demonstration at the soft opening of the Technology Innovation Centre of the University of Strathclyde. Over 100 guests including the First Minister of Scotland, funding partners, local government and industry partners, attended the event;
- Prof. Soraghan and Dr Clemente organised as Conference Chair and Publicity Chair the European Embedded Design in Education Conference (EDERC) 2014 in Milan (Italy);
- Knowledge exchange meetings with National Instruments, Plextek LTD, Bath Labs, Juice DSP and Tannoy took place to investigate possible collaborative opportunities;
- The students Marco Liguori and Alessio Izzo from the University of Sannio visited the Sensor Signal Processing & Defence Labs at ST and collaborated with Dr Clemente to the development of novel FOPEN CFAR Detectors;
- Professor Chris Baker from the Ohio State University visited the group for two days in November 2014, discussing about joint collaboration on Automatic Target Recognition from SAR images and micro-Doppler;
- Future Experiments were discussed with Dr Anastasia Panoui and Anastasios Deligiannis during their visit at Strathclyde in December 2014. The discussion was focussed on identifying case studies to demonstrate the algorithms developed in L_WP2;
- The student Mustafa Bugra Ozcan from TOBB University of Ankara visited the Sensor Signal Processing & Defence Labs at ST and collaborated with Dr Clemente to the development of the SDR based MIMO radar sensor network for micro-Doppler analysis;
- Several meetings have taken place with the SELEX ES group led by Dr Anthony Kinghorn. Dr David Greig is the main contact for the technical interactions with L_WP4. SELEX ES is very supportive in terms of technical discussions and the provision of real data; Furthermore, George Matich and Stephen Clark from Selex in Basildon visited Strathclyde in October 2014.
- The construction of the LSSC Data Centre has continued and now different datasets are available: K and X-band micro-Doppler data, Gotcha Volumetric SAR Dataset, CCD Change Detection Challenge, MSTAR dataset, CARABASII FOPEN Data, MSAR data, SARvis Dataset.

Section 4.4 Plans for the third year

Realization of multi-carrier multi-angle MIMO micro-Doppler database

In order to provide data of interest useful to test algorithms a database of micro-Doppler data with multiple observation angle, carrier frequencies and MIMO configurations will be acquired using the USRP available and made available for the testing of algorithms.

Micro-Doppler enhanced Tracking

Exploiting micro-Doppler information, enhanced tracking techniques will be possible, for instance the case of manoeuvring targets is one of the cases where additional information provided by the micro-Doppler signatures can lead to enhanced tracking capabilities.

Investigation of solution for Enhanced Space Situation Awareness

The research topic of Space Situation Awareness will be opened during next year. In particular solutions able to provide enhanced capabilities for SSA will be investigated, including high-resolution imaging and enhanced sensor systems.

Investigation of novel signal processing techniques

Recently introduced signal processing techniques such as Partial Fast Fourier Transform, Dual Parameter Fractional Fourier transform, stochastic differential equation, and image moments appears to be very interesting and their potential in the network battlespace will be investigated.

References:

- [1] M. Asghari, C. Clemente, B. Jalali, J. Soraghan, "SAR Image Compression using DAST", Global- SIP2014, 2-3 December 2014, Atlanta, GE, USA
- [2] C. Clemente, T. Parry, G. Galston, P. Hammond, C. Berry, C. Ilioudis, D. Gaglione, J. Soraghan, "GNSS Based Passive Bistatic Radar for Micro-Doppler based Classification of Helicopters: Experimental Validation", IEEE International Radar Conference 2015, Arlington, USA, 11-15 May 2015
- [3] Zhuolin Jiang, Zhe Lin, Larry S. Davis. "Label Consistent K-SVD: Learning A Discriminative Dictionary for Recognition". IEEE Transactions on Pattern Analysis and Machine Intelligence, 2013, 35(11): 2651-2664
- [4] D. Gaglione, C. Clemente, L. Pallotta, A. De Maio, I. Proudler, J. Soraghan, "Krogager Decomposition and Pseudo-Zernike Moments for Polarimetric Distributed ATR", Sensor Signal Processing for Defence Conference 2014, 8-9 September 2014, Edinburgh, UK
- [5] C. Clemente, L. Pallotta, A. De Maio, I. Proudler, J. Soraghan, A. Farina, "Pseudo-Zernike Based Multi-Pass Automatic Target Recognition From Multi-Channel SAR", IET Radar Sonar and Navigation, Dec 2014.
- [6] C. Clemente, I. Shorokhov, I. Proudler, and J. Soraghan, "Radar Waveform Libraries Using Fractional Fourier Transform," in 2014 IEEE Radar Conference, Cincinnati, Ohio, 19-23 May 2014.

- [7] C. Clemente, C. Ilioudis, D. Gaglione, K. Thompson, S. Weiss, I. Proudler, and J. Soraghan, "Reuse of Fractional Waveform Libraries for MIMO Radar and Electronic Countermeasures," in 6th International Symposium on Communications, Control, and Signal Processing (ISCCSP 2014), Athens, Greece, 21-23 May 2014.
- [8] C.V. Ilioudis, C. Clemente, I. Proudler, and J. Soraghan, "Constant envelope fractional Fourier transform based radar waveforms detection and localization performance in DMR," in Sensor Signal Processing for Defence Conference 2014 (SSPD 2014), Edinburgh, UK, September 2014.
- [9] C.V. Ilioudis, C. Clemente, I. Proudler, and J. Soraghan, "Performance Analysis of Fractional Waveform Libraries in MIMO Radar Scenario," in 2015 IEEE Radar Conference, Arlington, Virginia, 11-15 May 2015.
- [10] C. Clemente, J. J. Soraghan, "GNSS Based Passive Bistatic Radar for micro-Doppler analysis of helicopter rotor blades", IEEE Transactions on Aerospace and Electronic Systems, Vol. 50, issue 1, January 2014.
- [11] C. Clemente, J. J. Soraghan, "Application of the singular spectrum analysis for extraction of micro-Doppler signature of helicopters" , IET Radar Conference 2012, 22-25 October 2012, Glasgow (UK)
- [12] E. Ertin, C. D. Austin, S. Sharma, O. L. Moses, and L. C. Potter, "Gotcha experience report: Three-dimensional SAR imaging with complete circular apertures," SPIE Proceedings, vol. 6568, 2007.
- [13] J. Misiurewicz, K. Kulpa, and Z. Czekala, "Analysis of recorded helicopter echo," in *Radar 97 (Conf. Publ. No. 449)*, Oct 1997, pp. 449–453.
- [14] J. Martin and B. Mulgrew, "Analysis of the theoretical radar return signal from aircraft propeller blades," in *Radar Conference, 1990., Record of the IEEE 1990 International*, May 1990, pp. 569–572.
- [15] G. Li and P. Varshney, "Micro-Doppler Parameter Estimation via Parametric Sparse Representation and Pruned Orthogonal Matching Pursuit," *Selected Topics in Applied Earth Observations and Remote Sensing, IEEE Journal of*, vol. 7, no. 12, pp. 4937–4948, Dec 2014.
- [16] M.H. Asghari and B. Jalali, "Discrete anamorphic transform for image compression," IEEE Signal Processing Letters, vol. 21, no. 7, pp. 829– 833, July 2014.
- [17] M.H. Asghari and B. Jalali, "Image compression using the anamorphic stretch transform," in 2013 IEEE International Symposium on Signal Processing and Information Technology (ISSPIT), Dec 2013, pp. 000233– 000236.
- [18] E.J. Candes and M.B. Wakin, "An introduction to compressive sampling," IEEE Signal Processing Magazine, vol. 25, no. 2, pp. 21–30, March 2008.
- [19] R.G. Baraniuk, "Compressive sensing [lecture notes]," IEEE Signal Processing Magazine, vol. 24, no. 4, pp. 118–121, July 2007.
- [20] M.H. Asghari and B. Jalali, "Anamorphic time stretch transform and its application to analog bandwidth compression," in Global Conference on Signal and Information Processing (GlobalSIP), 2013 IEEE, Dec 2013, pp. 1013–1016.
- [21] M.H. Asghari and B. Jalali, "Anamorphic transformation and its application to time-bandwidth compression," Applied Optics, vol. 52, pp. 6753–6743, 2013.
- [22] M.H. Asghari and B. Jalali, "The anamorphic stretch transform: Putting the squeeze on big data," Opt. Photon. News, vol. 25, pp. 24–31, 2014.
- [23] Mohammad H. Asghari and Bahram Jalali, "Experimental demonstration of optical real-time data compression)" Applied Physics Letters, vol.104, no. 11, pp. 111101–111101–4, Mar 2014.

- [24] S. M. Scarborough, L. Gorham, M. J. Minardi, U. K. Majumder, M. G. Judge, L. Moore, L. Novak, S. Jaroszewski, L. Spoldi, and A. Pieramico, "A challenge problem for SAR change detection and data compression," in Proc. SPIE, 2010, vol. 7699, pp. 76990U–76990U–5.
- [25] M. Lundberg; L. M. H. Ulander; W. E. Pierson ; A. Gustavsson; "A challenge problem for detection of targets in foliage". Proc. SPIE 6237, Algorithms for Synthetic Aperture Radar Imagery XIII, 62370K (May 17, 2006);
- [26] K. Conradsen, A. A. Nielsen, J. Schou, and H. Skriver, "A Test Statistic in the Complex Wishart Distribution and Its Application to Change Detection in Polarimetric SAR Data", IEEE Trans. Geosci. Remote Sens., vol. 41, no. 1, pp. 4-19, Jan. 2003.
- [27] L. M. Novak, "Change Detection for Multi-polarization, Multi-pass SAR", SPIE Conference on Algorithms for Synthetic Aperture Radar Imagery XII, Orlando, FL, pp. 234-246, Mar. 2005.
- [28] V. Carotenuto, A. De Maio, C. Clemente, J. Soraghan., "Invariant Rules for Multi-Polarization SAR Change Detection", IEEE Transactions on Geoscience and Remote Sensing, vol.53, no.6, pp.3294, 3311, June 2015
- [29] V. Carotenuto, A. De Maio, C. Clemente, J. Soraghan, "Multi-polarization SAR change detection with invariant decision rules", IEEE Radar Conference 2014, Cincinnati, USA, 19-23 May 2014
- [30] C. Clemente, L. Pallotta, A. De Maio, J. Soraghan, A. Farina, "A Novel Algorithm for Radar Classification based on Doppler Characteristics Exploiting Orthogonal Pseudo-Zernike Polynomials", IEEE Transactions on Aerospace and Electronic Systems (in Press).
- [31] L. Pallotta, C. Clemente, A. De Maio, J. Soraghan, A. Farina, "Pseudo-Zernike Moments Based Radar Micro-Doppler Classification", IEEE Radar Conference 2014, Cincinnati, USA, 19-23 May 2014
- [32] M. Stojanovic and J. Preisig, "Underwater acoustic communication channels: Propagation models and statistical characterization," *IEEE Commun. Mag.*, vol. 47, no. 1, pp. 84-89, Jan. 2009
- [33] Y. Li, X. Sha, F-C. Zheng and K. Wang, "Low Complexity Equalization of HCM Systems with DPFFT Demodulation over Doubly-Selective Channels," *IEEE Signal Processing Letters.*, vol. 21, no. 7, July 2014.
- [34] Y M. Aval, and M. Stojanovic, "Differentially Coherent Multichannel Detection of Acoustic OFDM Signals," *IEEE Journal of Oceanic Engineering.*
- [35] A. Solyman, S. Weiss and J.J. Soraghan, "Hybrid DFrFT and FFT based Multimode Transmission OFDM System." *presented at the ICEENG, 2012 Cairo, Egypt.*
- [36] D.C.-L. Fong and M. A. Saunders, "LSMR: An iterative algorithm for sparse least-squares problems," *SIAM Journal on Scientific Computing*, March 2011.
- [37] A. Solyman, S. Weiss and J.J. Soraghan, "Low-Complexity LSMR Equalization of FrFT-Based Multicarrier Systems in Doubly Dispersive Channels," *presented at the ISSPIT 2011, Bilbao Spain, 2011.*

Published Papers:

- 1- C. Clemente, J. J. Soraghan , "GNSS Based Passive Bistatic Radar for micro-Doppler analysis of helicopter rotor blades", IEEE Transactions on Aerospace and Electronic Systems, Vol. 50, issue 1, January 2014.
- 2- J.Zabalza, C. Clemente, G. Di Caterina, J.Ren, J.Soraghan,

- S.Marshall, "Robust Micro-Doppler Classification using SVM on Embedded Systems", IEEE Transactions on Aerospace and Electronic Systems, vol.50, no.3, pp.2304,2310, July 2014
- 3- C. Clemente, L. Pallotta, A. De Maio, J. Soraghan, A. Farina, "A Novel Algorithm for Radar Classification based on Doppler Characteristics Exploiting Orthogonal Pseudo-Zernike Polynomials", IEEE Transactions on Aerospace and Electronic Systems (in Press).
 - 4- C. Clemente, L. Pallotta, A. De Maio, I. Proudler, J. Soraghan, A. Farina, "Pseudo-Zernike Based Multi-Pass Automatic Target Recognition From Multi-Channel SAR", IET Radar Sonar and Navigation, Dec 2014.
 - 5- V. Carotenuto, A. De Maio, C. Clemente, J. Soraghan., "Invariant Rules for Multi-Polarization SAR Change Detection", IEEE Transactions on Geoscience and Remote Sensing, vol.53, no.6, pp.3294, 3311, June 2015
 - 6- C. Clemente, A. Balleri, K. Woodbridge, John Soraghan, "Developments in Radar Target Classification using Micro-Doppler Signatures", EURASIP Journal on Advances in Signal Processing 2013, 2013:47, 12 March 2013
 - 7- D. Gaglione, C. Clemente, F. Coutts, G. Li, J. Soraghan, "Model-Based Sparse Recovery Method for Automatic Classification of Helicopters", IEEE International Radar Conference 2015, Arlington, USA, 11-15 May 2015
 - 8- C. Clemente, T. Parry, G. Galston, P. Hammond, C. Berry, C. Ilioudis, D. Gaglione, J. Soraghan, "GNSS Based Passive Bistatic Radar for Micro-Doppler based Classification of Helicopters: Experimental Validation", IEEE International Radar Conference 2015, Arlington, USA, 11-15 May 2015
 - 9- C. Ilioudis, C. Clemente, I. Proudler, J. Soraghan, "Performance Analysis of Fractional Waveform Libraries in MIMO Radar Scenario", IEEE International Radar Conference 2015, Arlington, USA, 11-15 May 2015 - Invited Paper - Special Session on MIMO Radar
 - 10- V. Carotenuto, A. De Maio, C. Clemente, J. Soraghan, "Multi-polarization SAR change detection with invariant decision rules", IEEE Radar Conference 2014, Cincinnati, USA, 19-23 May 2014
 - 11- L. Pallotta, C. Clemente, A. De Maio, J. Soraghan, A. Farina, "Pseudo-Zernike Moments Based Radar Micro-Doppler Classification", IEEE Radar Conference 2014, Cincinnati, USA, 19-23 May 2014
 - 12- C. Clemente, I. Shorokhov, I. Proudler, J. Soraghan, "Radar Waveform Libraries Using Fractional Fourier Transform", IEEE Radar Conference 2014, Cincinnati, USA, 19-23 May 2014
 - 13- C. Clemente, C. Ilioudis, D. Gaglione, K. Thompson, S. Weiss, I. Proudler, J. Soraghan, "Reuse of Fractional Waveform Libraries for MIMO Radar and Electronic Countermeasures", 6th International Symposium on

Communications, Control, and Signal Processing (ISCCSP 2014), Athens, Greece, 21-23 May 2014

- 14-C. Clemente, L. Pallotta, I. Proudler, A. De Maio, J. Soraghan, A. Farina, "Multi-Sensor Full-Polarimetric SAR Automatic Target Recognition Using Pseudo-Zernike Moments", International Radar Conference 2014, Lille, France, 13-17 October 2014
- 15-V. Carotenuto, C. Clemente, A. De Maio, J. Soraghan, "GLRT Based Scale-Invariant Multipolarization SAR Change Detection", International Radar Conference 2014, Lille, France, 13-17 October 2014
- 16-C. Ilioudis, C. Clemente, I. Proudler, J. Soraghan, "Constant Envelope Fractional Fourier Transform based Waveform Libraries for MIMO Radar", Sensor Signal Processing for Defence Conference 2014, 8-9 September 2014, Edinburgh, UK.
- 17-D. Gaglione, C. Clemente, L. Pallotta, A. De Maio, I. Proudler, J. Soraghan, "Krogager Decomposition and Pseudo-Zernike Moments for Polarimetric Distributed ATR", Sensor Signal Processing for Defence Conference 2014, 8-9 September 2014, Edinburgh, UK.
- 18-V. Carotenuto, C. Clemente, A. De Maio, J. Soraghan, S. Iommelli, "Multi-Polarization SAR Change Detection: Unstructured Versus Structured GLRT", Sensor Signal Processing for Defence Conference 2014, 8-9 September 2014, Edinburgh, UK.
- 19-M. Asghari, C. Clemente, B. Jalali, J. Soraghan, "SAR Image Compression using DAST", Global- SIP2014, 2-3 December 2014, Atlanta, GE, USA
- 20-C. Clemente, A. Miller, J. J. Soraghan, "Robust Principal Component Analysis for micro-Doppler based automatic target recognition" , 3rd IMA conference on Mathematics in Defence, 24- October 2013, Malvern (UK)
- 21-A. Miller, C. Clemente, A. Robinson, D. Greig, T. M. Kinghorn, J. J. Soraghan, "Micro-Doppler based target classification using multi-feature integration" , Intelligent Signal Processing (ISP) Conference, 2-3 December 2013, London (UK)

Papers Under Review

- 22-V .Carotenuto, A. De Maio, C. Clemente, J. Soraghan , "Unstructured Versus Structured GLRTfor Multi-Polarization SAR Change Detection" , IEEE Geoscience and Remote Sensing Letters
- 23-V .Carotenuto, A. De Maio, C. Clemente, J. Soraghan, G. Alfano, "Forcing Scale-Invariance inMulti-Polarization SAR Change Detection" , IEEE Transactions on Geoscience and Remote Sensing.
- 24-Y. Chen, C. Clemente, S. Weiss, J. Soraghan, "Partial Fractional Fourier

Transform (PFRFT)-OFDM for Underwater Acoustic Communication”,
EUSIPCO 2015

25-J. Cao, C. Clemente, G. Mingotti, J. Soraghan, C. McInnes “A Novel
Approach for Earth Remote Sensing Using Femt-Satellites In Sun Synchronous
Orbit”, IAC 2015

PhD projects Titles:

Mr Domenico Gaglione (PS6- ST) -***Automatic Target Recognition and Tracking
from Radar***

Mr Christos Ilioudis (PS5- ST)– ***Distributed MIMO Radar Systems***

Mr Jianlin Cao (ST)-***Spacecraft-on-a-chip concepts with application to Earth
remote sensing***

Mr Yixin Chen (ST)-***Underwater acoustic Communication based on Multicarrier
Scenario***

Mr Adriano Rosario Persico (ST)-***Radar signal processing for defence against
airborne threats and space situation awareness***

L_WP5 (EI): Low Complexity Algorithms and Efficient Implementation

5.1 Staffing

Work Package Leaders:	Prof. Ian Proudler (LU), Dr. Stephan Weiss (ST)
Other Academics involved:	Prof. John McWhirter (CU)
Research Associate:	Dr. Keith Thompson (ST)
Other Research Associates:	Progressively all other PDRAs (LU, SU, CU and ST) will be involved.
Contributing PhD Students:	Jamie Corr (ST, affiliated 2013/14), Mohamed Alrmah (ST), and Jethro Dowell (ST)
Project Partners:	Mathworks and Texas Instruments,
Research Themes:	T8 and T9
[dstl] Contacts:	Dr David Nethercott, Dr George Jacob, and Dr Nick Goddard

5.2 Aims and the lists of the original L_WP5 in the case for support

To develop novel paradigms and implementation strategies for a range of complex signal processing algorithms operating in a networked environment. Links to L_WP1-L_WP4. (Relates to all themes)

Low complexity algorithms will be targeted by both generic efficient approaches to common themes across the consortium, such as high-dimensional array data, and application-specific low-cost implementations through collaborative research and active engagement with all other WPs.

L_WP5.1 Data reduction and distributed processing

Lower dimensional representation of data can lead to significant cost reduction, including data-independent techniques such as frequency domain, sub-band or subspace-based processing and thinning of sensor data. This work will exploit a combination of data dependent and independent techniques to achieve a significant data reduction, and will demonstrate how this can be exploited in low-cost algorithms. Due to operating in a networked environment, the efficient organisation of algorithms across a distributed processing platform will be considered. This work will explore algorithms and applications from across all work packages. Areas of study include (i) Polynomial decompositions leading to sparse representations through data-dependent optimal transformations (e.g. Karhunen-Loeve transform (KLT)), for dimensionality reduction in beamformers (ii) Parallel implementations of linear algebra functions and distributed processing methods (e.g. systolic array design, IP core implementations, vector-codebook methods) to minimise the communications bandwidth between processing nodes and (iii) Statistical signal processing problems will be utilised to map algorithms to distributed processors, whereby constraints on the communication bandwidth between nodes need to be set (e.g. Bayesian belief network (BBN) structures).

L_WP5.2 Hardware Realisations

Collaborating with Texas Instruments, PrismTech, and Steepest Ascent (now Mathworks), numerically efficient schemes are to be derived, with mappings onto suitable processing platforms to be investigated that demonstrate real-time algorithms in suitable test scenarios. Multi-core GPU-based platforms and

programming environments such as CUDA are an enabling technology for massively parallel processing of data (facilitating real-time applications at low cost, but potentially high power consumption). In contrast, micro-controllers, DSP and FPGA based processing platforms are perfect candidates for low power, inexpensive sensor processing units. In collaboration with industrial partners, state-of-the-art Multicore DSP/FPGA embedded solutions are to emerge that are capable of matching the power-performance-price constraints posed by the range of specific problems arising within all work packages of the consortium.

5.3 Progress made in the 2nd year in addressing the original objectives

In the 2nd year of the project our main focus in L_WP5.1 has been the further development of numerically efficient algorithms that address key areas of interest to the consortium. In particular, further development of efficient Polynomial Eigenvalue Decomposition (PEVD) algorithms has resulted in significant improvements and in-depth analysis in algorithm performance, supported by a number of academic outputs. In addition, a significant and very tangible output from WP5 has been the release of a publicly available PEVD Matlab toolbox. Further progress has also been made in addressing the distributed processing concepts outlined in the original objectives, where the use of Probabilistic Graphical Models for modelling distributed processing is being explored.

The work on L_WP5.2 (Hardware Realisations) has been performed with the view of developing the capability of implementing complex algorithms across a range of different computing platforms and devices. This has involved doing example implementations on DSP and FPGA platforms, and putting plans and resources in place to tackle the specific challenges and algorithm problems identified by the other work packages.

5.3.1 Progress of L_WP5.1 (Efficient Algorithms, Data Reduction and Distributed Processing)

In L_WP5.1 the focus of Keith Thompson has been leading the research into the use of statistical Probabilistic Graphical Models (PGMs) for the purposes of modeling distributed systems, and also mapping sequential algorithms to distributed processors. PGMs such as Bayesian Networks or Markov Random Fields, are powerful frameworks for representing probabilistic relationships between different variables and thus offer the potential to re-imagine algorithms in a compact probabilistic structure. As relationships between variables are captured by a graph structure (composed of nodes, edges), it is intuitive to re-imagine the variables, and relationships encoded, as a distributed system. Furthermore, in the established field of Distributed Algorithms various message-passing algorithms exist to share (traverse) information between processes across a communication graph, whereas for PGMs message-passing algorithms (such as Belief Propagation) update probabilities of individual nodes. Overall, there are overlaps between the two areas, but the overall utility of the methods are not directly comparable. As a result, research effort has been made to attempt to reconcile the two is producing interesting results. Keith is also involved in the ongoing development of PEVD algorithms through the co-supervision, with Dr. Stephan Weiss, of PhD student Jamie Corr and has provided support in organizing the release of the first PEVD

Matlab Toolbox. Keith has also shared his focus with developing capability for L_WP5.2 Hardware Realisations (see below).

Further in the context of L_WP5.1 the focus of Stephan Weiss has been to explore, characterise and apply polynomial matrix decomposition techniques. A new family of fast converging iterative PEVD algorithms called sequential matrix diagonalisation (SMD) has now been archived in IEEE Transactions on Signal Processing, published in January 2015, and the core algorithms have been packaged into the PEVD Matlab toolbox described further below. Through discussions with John McWhirter and Ian Proudler, two important improvements have been reached; firstly multiple-shift versions of SMD (and SBR2) have brought a further increase in convergence speed. Secondly, postprocessing of the paraunitary matrices that form a PEVD factorisation can lead to a significant order reduction, thus reducing the implementation cost of polynomial subspace methods such as used in broadband angle of arrival estimation. These algorithms have been demonstrated in a number of applications, including a new formulation of broadband minimum variance distortionless response beamforming using polynomial matrix techniques. Within the Strathclyde team, Jamie Corr has developed significant momentum and independence, and suggests and developed e.g. the Jacobi-sweep approach, mentioned below, entirely on his own.

5.3.2 Progress of L_WP5.2 (Hardware Implementations)

The focus of Dr. Keith Thompson has been on developing capability of implementing complex algorithms across a range of different computing platforms and devices. The three main families of devices are FPGAs, DSP processors, and Graphic Processing Units (GPUs). In the main this effort has involved doing some example implementations of systems and algorithms developed by colleagues in Strathclyde, including a SAR Coherent Change Detection algorithm from WP4 onto a DSP, and a wide-band Television White-Space (TVWS) transceiver design onto a FPGA based solution. This effort has been important to gain knowledge and experience in the development process of mapping of algorithms to hardware, and the use of the latest software tools. Further effort has been made in organizing resources to tackle the specific algorithms developed in L_WP4 and L_WP5 with the view to developing a capable technology demonstrator.

5.4. Technical Details

5.4.1 L_WP5.1 Polynomial EVD Theory, Implementations and Applications

Focus on Polynomial Matrix Techniques

During the 2nd quarterly meeting in Surrey in 2013, the consortium decided that L_WP5 should initially focus on one particular algorithm implementation. Due to its wide use across particularly L_WP3 and L_WP5, its degree of novelty and uniqueness to the consortium, and an encouraging application by Dstl in the sonar domain, much effort has therefore been dedicated to polynomial EVD (PEVD) algorithms. Our effort has however not just contributed to a direct implementation, but we have taken a more holistic approach to consider the theoretical foundations,

numerical efficiency, and a number of sample applications in addition to providing a stable implemented platform for others to use.

Sequential Matrix Diagonalisation

In addition to the “classical” solution of calculating a PEVD by means of the 2nd order sequential best rotation (SBR2) algorithm [McWhirter 2007], based on ideas by John McWhirter a sequential matrix diagonalisation (SMD) algorithm has been developed. The SMD algorithm is more complex to calculate than SBR2, but is capable of providing polynomial matrix factorisations that approximate a PEVD more accurately and with shorter paraunitary matrices than possible with SBR2. Thus, while in the calculation, SMD is more complex than SBR2, the application of the paraunitary matrices to data --- for applications such as subspace decomposition --- is significantly less expensive than with SBR2. This work was written up in 2013/14, and has now been archived in IEEE Transactions on Signal Processing [Redif 2015].

PEVD Implementations and Matlab Toolbox

With support from Mathworks, the industrial lead of L_WP5, we have released a first Matlab toolbox of PEVD algorithms [Weiss 2014] in late 2014 at <http://pevd-toolbox.eee.strath.ac.uk/> as shown in Figure 5.1 with a link from Mathworks Link Exchange. This PEVD toolbox at its core provides SBR2 and SMD algorithm implementations, and a number of demonstration files that highlight the differences between SMD and SBR2, and their use in applications such as subband coding. The toolbox algorithms come with a substantial HTML documentation. Both the toolbox files and the documentation are auto-generated, which will ease the future augmentation of the toolbox content to reflect our current algorithmic developments. The toolbox website requires registration for downloading, such that the uptake and utilisation of this toolbox can be monitored. To date, the toolbox has been downloaded by approximately 30 individuals.

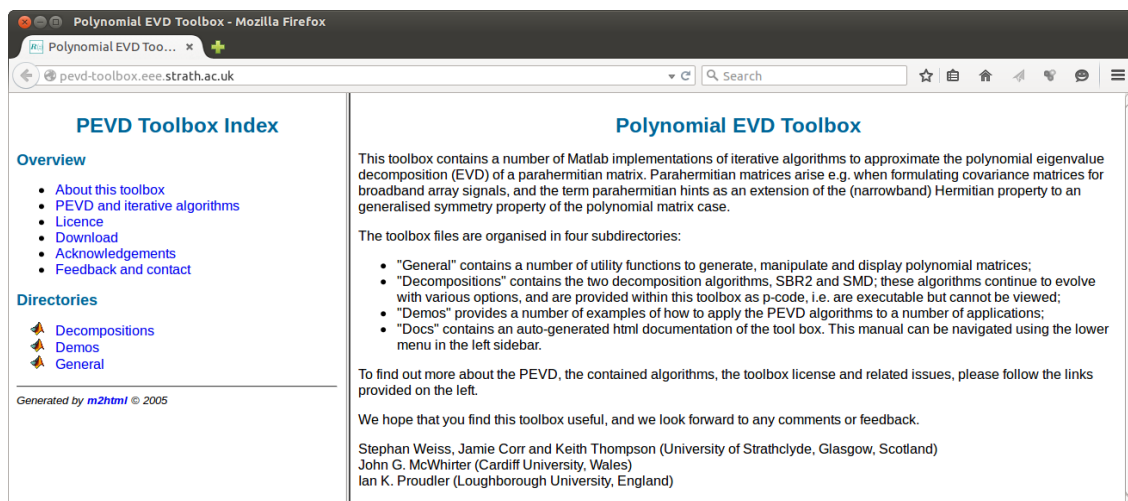


Figure 5.1 PEVD toolbox website.

Fast Converging PEVD Algorithms

The faster convergence of the SMD algorithm compared to SBR2 is due to a larger energy transfer from off-diagonal to diagonal elements per iteration step. Based on this, without much additional cost over SMD, a multiple-shift version has been created [Corr 2014a]. This multiple-shift (MS) SMD is capable of transferring more energy per step and has been shown to convergence even faster than SMD. The optimum energy transfer requires a very expensive exhaustive search across all possible shifts/delays within the parahermitian matrix, but suboptimal techniques still achieve around 90% of the energy transfer per step at an only insignificant increase in complexity compared to the standard SMD approach [Corr 2014b]. The algorithms can be modified to generate a paraunitary matrix from strictly causal components, a step that can be but is not necessarily guaranteed within the original SBR2 algorithm [Corr 2014c]. A similar step has been undertaken for the original SMR2 algorithm, where a multiple-shift SBR2 (MS-SBR2) algorithm [Wang 2015] combines the lower cost of the SMD family with the enhanced convergence properties of the multiple-shift approach.

Numerical Speed-up of SMD

To lower the implementation cost of particularly the SMD algorithm family, the EVD within these algorithms has been approximated by a Jacobi sweep; while in general an EVD would be iteratively calculated by a very large number of Given rotations, a limited number of such rotation steps might already suffice. In [Corr 2014d] a Jacobi sweep, i.e. a single iteration of Givens rotations over all off-diagonal elements, has been shown to yield no discernible degradation over the much costlier use of a full EVD, as shown in Figure 5.2.

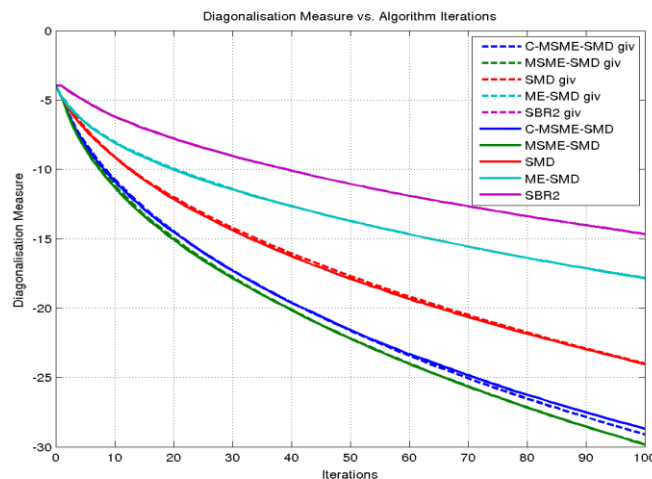


Figure 5.2: Comparison of methods using an exact EVD with an approximation by a Jacobi sweep with a single Givens rotation per off-diagonal element.

PEVD Applications and Linkages

In term of applications, work on broadband angle of arrival (AoA) estimation had been reported for the previous year [Alrmah 2013a; Weiss 2013], where a polynomial subspace implementation enables a broadband extension of the MUSIC algorithm. The enhanced performance of the SMD family of algorithms over SBR2 has been demonstrated to yield a higher accuracy when utilising the SMD instead of SBR2 for our proposed polynomial MUSIC algorithm [Alrmah 2014]. The formulation

of a broadband beamforming problem in the framework of polynomial matrices has led to interesting aspects [Weiss 2015]. Firstly, polynomial steering vectors as defined in e.g. [Alrmah 2013b; Alrmah 2013c] enable an easy definition of constraints off broadside, leading to a much lower distortion in look direction that achievable with standard time-domain broadband beamformer. Secondly, the use of a polynomial quiescent vector and blocking matrix in the Generalised Sidelobe Canceller algorithm decouples the complexity of this preprocessing step from a multichannel adaptive filter performing interference suppression, leading to a significant reduction in complexity for adaptive broadband beamformers with arbitrary look direction.

Multichannel Prediction, Complex Valued Processing and Non-Stationary / Non-Linear Methods

For a multichannel prediction problem involving complex-valued time series, we have previously reported a cyclo-stationary Wiener filter [Dowell 2014a; Dowell2014b]. The advanced version of this system benefitted from discussions that had taken place within the consortium, based on the expertise of Swati Chandna (PDRA SU). This work now also involves non-linear methods [Dowell 2013; Dowell 2014c; Dowell 2015], with a particularly beneficial impact of kernel methods on short-term prediction.

Algorithmic Links to Distributed Processing

Initial work in this area has concentrated on the interaction with two existing PhD projects. Firstly fractal arrays are attractive for large-scale beamformers [Karagiannakis 2013b; Karagiannakis 2013c; Punzo 2014], and the distributed calculation within such a beamformer has been proposed [Karagiannakis 2013a]. Local processing ensures that the processing in any one node does not exceed set limits, and that local calibration information about nodes is only required locally. Also, Pearl's algorithm has been implemented in a generic and scalable form, and used to optimise the station assignment in a heterogeneous network, where the Bayesian belief propagation idea with levels of uncertainty, e.g. for the gain of a link, can be taken into account and be replaced by concrete evidence if available [McGuire 2014]. The solution obtained with this approach has been confirmed and verified against a previous deterministic, exhaustive search optimisation [McGuire 2013].

Distributed Processing with Probabilistic Graphical Models

The concept explored in this work is to examine the potential use of statistical Probabilistic Graphical Models (PGMs) for the purposes of modeling distributed systems, and also mapping sequential algorithms to distributed processors. PGMs such as Bayesian Networks or Markov Random Fields are powerful frameworks for representing probabilistic relationships between variables and thus offer the potential to re-imagine algorithms in a compact probabilistic structure. PGMs are commonly applied to various machine learning problems and provide a framework to encode a complete probability distribution over multi-dimensional space (defined by a number of random variables). Such models are therefore useful for analyzing and discovering structure within complex distributions and have been used extensively in the fields of natural language processing, expert systems, fault diagnosis, and image analysis/segmentation, as described in [Koller 2009].

Given the graph structure composed of nodes (random variables) and directed/undirected edges, our concept has been to re-imagine this arrangement of random variables (nodes) and the relationships encoded, as a distributed algorithm/system. Furthermore, parallels with the established field of Distributed Algorithms exist where various message-passing algorithms exist to share (traverse) information between processes across a communication graph, see [Raynal 2013]. For PGMs, message-passing algorithms (such as Pearl’s Belief Propagation) are also widely employed to perform exact and approximate inference across the graph, updating probabilities given evidence (observed data). Therefore the work conducted has focused on reconciling these two different research areas to meet our specific research objectives. A notable closely-related body of work can be found in [Cetin 2006] and references therein, where wireless sensor network data fusion problems (self-localization, data-association in multi-object tracking) are re-cast as problems of inference in PGMs using Non-parametric Belief Propagation. Recent research involving a UDRC colleague [Üney 2014] (Dr. Murat Üney from Edinburgh Consortium) has employed Monte-Carlo techniques to address the problem of decentralized estimation of the random field, whilst retaining an overall message-passing approach.

At the moment our work has focused on investigating the use of PGMs to model beamforming implementations (not commonly considered as a sensor network or fusion problem, but rather as spatial array processing). Furthermore, we have investigated efficient methods for both approximating probability distributions (pdfs) and also estimating probability distributions. Recent work by colleagues at Strathclyde have utilized Pearl’s Belief Propagation algorithm to optimise station assignment in a heterogeneous communications network, where the Bayesian belief propagation idea with levels of uncertainty, e.g. for the gain of a link, can be taken into account and be replaced by concrete evidence if available [McGuire 2014]. A graph model for the application of the Bayesian belief network to the optimisation of the heterogeneous radio network is shown in Figure 5.3. This defined Bayesian (directed) network is being used as the basis for exploring the use of alternative probability representations (moving from histogram-based density estimation for discrete Conditional Probability Table representation, to continuous regression tree and Conditional Linear Gaussian representation).

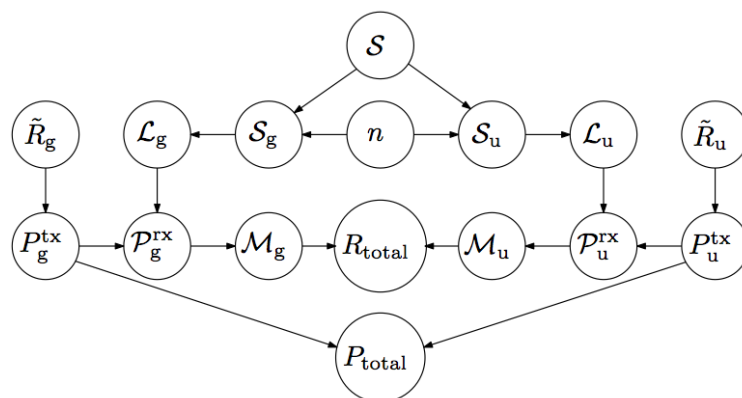


Figure 5.3: Probabilistic Graphical Model of multi-RAN (Radio Access Network) from [McGuire 2014] where P_{total} is the total base station power consumption, with dependencies between data rates, path loss, and distances from base station, encoded for a number of stations.

Also being further built upon is the prior work carried out by PI Prof. Ian Proudler [Proudler 2007], where approximations to probability distributions were identified that allowed some mathematical expressions with no closed form to be reconfigured as a directed tree graphical model that could be computed iteratively using Loopy Belief Propagation. A technical report addressing all these aspects is in preparation and will form the basis of submission to forthcoming conferences in the near future.

5.4.2 Technical Details for L_WP5.2

The overall goal of L_WP5.2 is to develop the capability of implementing complex algorithms across a range of different computing platforms and devices. In order to deliver this we have aimed to put together a capable suite of hardware devices, software development tools, and supporting materials that both ourselves and other students/researchers can use to implement their algorithms. As the implementation of algorithms remains an area where in-depth knowledge and experience of computer architecture, good practice and tacit knowledge play a significant role, suitable technical and training resources have also needed to be identified and studied closely.

The effort in L_WP5.2 has focused on developing some example implementations with which to gain knowledge and experience of the process and software tools involved for different device architectures. In particular we have focused on Texas Instruments DSP and Xilinx FPGA devices due to their prevalence in low-power solutions (c.f. GPU acceleration). For DSPs this has involved the conversion of algorithm code written in Matlab into more efficient C language code, and programming of the device through TI's propriety Code Composer Studio. For Xilinx FPGAs and the newer Xilinx System-on-Chip (SoC) Zync (FPGA + ARM Processor) platform, we have been using both Xilinx ISE and Xilinx Vivado development suites, with the accompanying Simulink based System Generator. For both DSP and FPGA-based development, we have also been exploring the use of Mathworks code-generation tools Matlab Coder (Matlab to C) and HDL Coder (Matlab to VHDL). Furthermore, the latest Vivado HLS software allows VHDL based IP blocks to be defined using higher-level C/C++ for algorithm elicitation.

Two main algorithm implementations that have been studied in recent months are the implementation of a SAR Coherent Change Detection (CCD) Matlab algorithm from WP4 [Carotenuto 2014] onto a OMAP L138 DSP development board (composed of a C674x DSP core and ARM926EJ RISC processor). The computations of the CCD Matlab algorithm were replicated on the embedded solution through partitioning of the large original complex image, with further effort earmarked to make this a better overall solution. Another case study targeting Xilinx FPGA-based devices has been the implementation of a wide-band Transceiver design to operate within the strict bandwidth requirements of the TV White-Space (TVWS) spectrum. This implementation is based on previous work [Elliot 2012] and has involved utilizing both a Xilinx Spartan6 FPGA and also the newer Xilinx Zync (FPGA + ARM Processor) device.

The TVWS system is composed of a multi-stage filter bank transceiver that has the capability to simultaneously up and down convert the whole TVWS range (40 Channels, each 8MHz wide), taking advantage of proposed fast ADC/DAC components that operate at a sampling rate of 1.92GHz. The system, as shown in Figure 5.4, aims to down-convert all 40 channels within the TVWS spectrum of 470MHz to 790MHz, to the baseband with all 8Mhz channels from DC to 320MHz, utilizing necessary spectral masks. The spectra in the UHF range and in baseband are depicted in Figure 5.5.

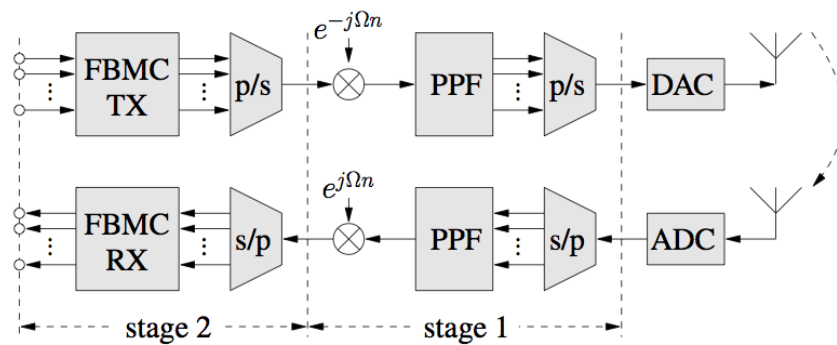


Figure 5.4: Multi-stage TVWS Filterbank Transmitter (above) and receiver (below) with Polyphase filter (PPF) in stage 1 and Filter Bank Multi-Carrier modulator (FBMC) in stage 2.

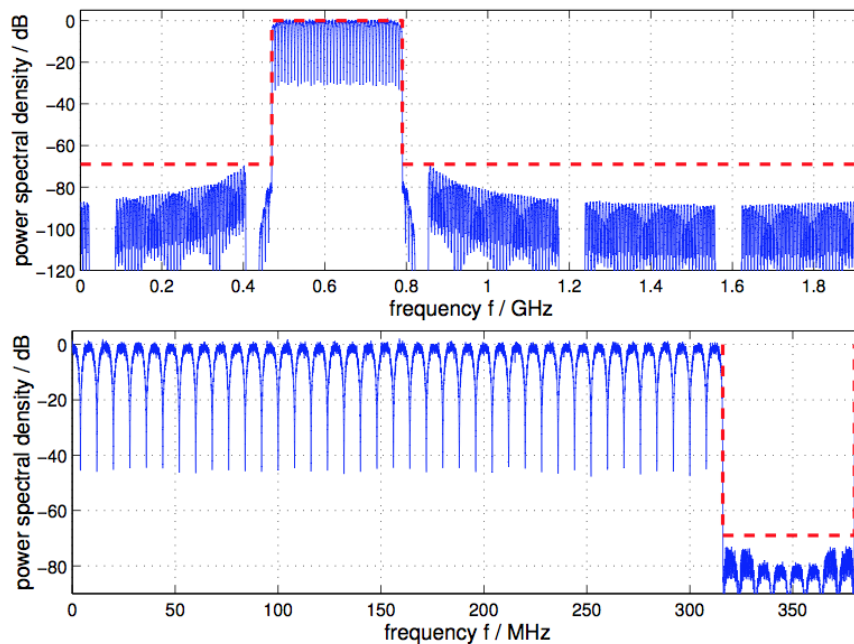


Figure 5.5: Power Spectral Densities of Stage (1) and Stage (2) Signals with spectral masks indicated as dashed lines.

A filterbank approach rather than OFDM approach has been adopted due to the restrictions imposed by permitted interference levels outlined by industry/regulators. As most filterbank transceivers operate in the baseband, the design is novel in that it

aims to operate a filterbank receiver up to radio frequency, thus the flexible design is an interesting case of converting to and from RF. As a result, this is of potential cross-over interest in our defence realm given the shared frequency spectrum and competing users of the 'Network Battlespace'. Results from simulation show that design trade-offs exist when considering the level of decimation in stage 1 and the length of the stage 2 filters, impacting on the overall complexity in the former, and latency in the latter. This implementation is in progress and shall be the topic of a paper submitted for consideration into a SDR focused edition of the IEEE Transactions on Circuits and Systems.

In addition, we have been defining plans to tackle the specific algorithms of interest to WP5 and also WP4. In this first period of the WP5 project we have been utilizing development kits sourced from the university programs of technology partners (Texas Instruments, Xilinx). Such devices are ideal for education purposes, smaller (limited memory requirements) solutions and proof of concept designs, but our intention is to implement algorithms using more capable hardware utilizing the most recent hardware improvements. Therefore our upcoming program for implementation in L_WP5.2 is the following:

Radar algorithms from WP4:

- Sparse/Dictionary Learning
- Template-Based Classification
- Pseudo-Zernike Feature Extraction

Explore the implementation of these multiple feature extraction algorithms on the same processing device, along with the potential for fusion. Objective is to employ the latest Texas instruments Keystone II (Multicore DSP + ARM) Device, along with OpenMP API to fully leverage latest multicore DSP architecture.

FPGA Implementation of PEVD algorithms

To accompany the PEVD Toolbox, algorithms including SBR2, SMD, and latest improvements are to be implemented onto FPGA devices from Xilinx. A more capable Xilinx Virtex5 device has been obtained from Strathclyde colleagues, but a newer series-7 logic Xilinx Kintex 7 has been identified as the ideal future target solution.

GPU and National Instruments USRPs

Together with Dr. Clemente (WP4), we are putting in place a GPU enabled workstation in the laboratory with which to employ CUDA and facilitate parallelized algorithm acceleration. Furthermore, the use of USRP devices procured in WP4 will also be explored to meet any WP5 objectives.

5.5. Linkages with Dstl and Industry

Regular contact has been maintained with our designated contacts from [dstl], David Nethercott and George Jacob. In particular we were supplied with a table outlining the intersection of various techniques with applications of interest to [dstl], with the

broad objective of examining the complexity of various methods and potential for approximation. We have since discussed this task as the focus of a 'campaign effort' to take place over the coming year, and will be finalising the requirements of this work in the coming weeks and starting soon (upon completion of outstanding objectives).

Our contact at Mathworks, Dr Marc Willerton, has provided excellent support and feedback during the first two years. He delivered a presentation during the 2014 UDRC Summer School Industry Day, where he demonstrated the Mathworks Parallel Processing Toolbox. He has also encouraged the now published PEVD Matlab toolbox, and provided us with best practise insights into its publications and linkage to Mathworks own material via the Matlab Link Exchange. Dr Marc Willerton kindly tested the toolbox for us, and has provided guidance for its further development --- this includes the addition of extra functionality for beamforming and angle of arrival estimation, but also the use of GitHub as Mathworks' preferred platform for external 3rd party toolboxes. GitHub will be able to support a number of copyright models, which can help to address the fact that the original algorithm in the toolbox, SBR2, is currently under patent by QinetiQ. Our contact at QinetiQ, Prof Malcolm Macleod, has kindly arranged for QinetiQ to allow the utilisation of SBR2 for academic output by any third parties.

Through our work on polynomial matrix decompositions, we have held discussions with Dr Nick Goddard at Dstl in the context of sonar applications. Following a condensed meeting on advanced processing in sonar organised by Dr Nick Goddard on 13/11/14, a proposal on signal processing techniques, including polynomial matrix methods, has been submitted to Dstl by Jonathon Chambers, Ian Proudler, and Stephan Weiss. This proposal aims to supplement ongoing work within the consortium and within a MarCE project on sparse processing of flank arrays led by Wenwu Wang and Jonathon Chambers with Atlas Elektronik.

With regard to Texas Instruments, Prof Soraghan, Dr. Carmine Clemente, and Dr.Keith Thompson were involved in the organisation and smooth delivery of the Texas Instruments sponsored EDERC 2014 conference where researchers from across Europe were invited to present their latest research into embedded systems development. The organisation of this event allowed us at Strathclyde greater opportunity to strengthen our relationships with TI's University Program. This relationship is important in the process of collaborating to deliver on-going hardware-based projects.

5.6. Future Plans

Plans for 3rd Year

Low Order Polynomial Matrix Techniques

Even if a PEVD exists with a unique diagonal parahermitian matrix, we now know that the paraunitary matrices performing this decomposition are not unique [Corr 2015; independently recognise by John McWhirter previously]. Since the order of the paraunitary matrix is vital for e.g. low-cost implementations of polynomial subspace decompositions, we will aim to reduce the order of the paraunitary matrices. An initial investigation applied to the MSME-SMD and SMD algorithms in [Corr 2015] will be

extended to the SBR2 family. This is expected to impact on a number of application areas.

Polynomial Subspace Metrics and Manipulation

Different iterative PEVD algorithms return different paraunitary matrices. It is not clear what impact this will have on, for example, subspace decompositions; also, for algorithm development reasons, we would like to assess the difference between the estimated paraunitary matrix and the exact decomposition (many of our test use a source model with known ground truth). A suitable metric may be subspace angle or correlations, which will gain a frequency dependency in the polynomial case. Difference between single vectors can be easily established, but subspaces spanned by several such vectors appear to be more difficult to assess. The narrowband equivalent relies heavily on the SVD, which in the polynomial case is subject to exactly those variabilities that we are trying to assess. There are some initial ideas for a polynomial Gram-Schmidt orthogonalisation, which relies heavily on detecting common roots across several polynomials. For large polynomials, robust root estimation will be vital.

Broadband Beamforming

We will extend the work initiated in [Weiss 2015]. The subspace reduction is expected to lead to smaller blocking matrices in case of a polynomial generalised sidelobe canceller, for which a paraunitary matrix completion is required; one way to accomplish this is via polynomial Gram-Schmidt. Techniques developed for broadband polynomial beamforming will have wider impact for polynomial subspace methods.

PEVD Toolbox Evolution

Include multiple-shift algorithms once properly archived (IEEE TSP etc); include polynomial SVD [McWhirter 2007] and polynomial QR [Foster 2010] Aim to wider publicise PEVD algorithms to enhance their uptake in the signal processing community. Stephan Weiss and John McWhirter have submitted a tutorial session proposal to EUSIPCO 2015.

Distributed Processing

Following in-depth research into the variety of potential methods of employing probabilistic graphical models towards distributed processing, our intention is to complete initial studies based on existing communications based Bayesian Belief Network configurations in collaboration with Dr. Colin McGuire (Mathworks Glasgow). This existing network is being used as a test case to explore the impact of using approximate methods of representing probability density functions, and the utility of approximate inference message-passing algorithms (Belief Propagation, Nonparametric Belief Propagation, Survey Propagation, Expectation Propagation etc.). Going further, we are to continue to consider the use of such methods to describe distributed beamforming implementations, and look at how the methods may be extended to a temporally varying case.

Hardware Implementations

As outlined in the previous Section 4.2, our immediate objective is to complete the implementation of the TVWS transceiver using both a Xilinx Spartan6 FPGA and Xilinx ZynqSoC devices. The recently released Xilinx Zynq family combines an

application-capable ARM processor with the latest series-7 programmable logic in same silicon. Although both devices are composed of programmable logic resources, the SoC device has a greater number of DSP blocks available, and we are investigating the impact of how the additional resources of the dual-core ARM processor (that also includes a NEON SIMD engine) can be used effectively.

Also outlined in Section 4.2 are our plans to complete the implementation of the latest PEVD algorithm research onto more capable FPGA devices (Xilinx Virtex 6 and Kintex 7) to offer a further level of analysis into the applicability of the underlying research. Similarly we are to move from individual example implementations of given algorithms on DSP devices into investigating the use of Multicore DSP (TI Keystone II) devices to combine a number of feature extraction algorithms developed in WP4. Further plans are to deploy a GPU enabled workstation for algorithm acceleration in the coming months. Feedback from the Cardiff CMT meeting (January 2015) indicated that some collaboration with Ioannis Kaloskampisi from Cardiff University on accelerating anomaly detection algorithms would be worthwhile.

[dstl] Campaign

The campaign proposed by [dstl] (previously mentioned in Section 5.5) into examining the complexity and potential methods of approximation of various techniques of interest will be a feature of the coming year. Our industrial partner Mathworks has also indicated to us that they would be interested in examining the outcome of this work.

5.7. Academic Outputs

UDRC Output with Dstl Clearance: Journal and Conference Publications

[Alrmah 2014] M. Alrmah, J. Corr, A. Alzin, K. Thompson, and S. Weiss. Polynomial subspace decomposition for broadband angle of arrival estimation. In *Sensor Signal Processing for Defence*, pages 1–5, Edinburgh, Scotland, Sept. 2014.

[Corr 2014a] J. Corr, K. Thompson, S. Weiss, J. McWhirter, S. Redif, and I. Proudler. Multiple shift maximum element sequential matrix diagonalisation for parahermitian matrices. In *IEEE Workshop on Statistical Signal Processing*, pages 312–315, Gold Coast, Australia, June 2014.

[Corr 2014b] J. Corr, K. Thompson, S. Weiss, J.G. McWhirter, and I.K. Proudler. Maximum energy sequential matrix diagonalisation for parahermitian matrices. In *48th Asilomar Conference on Signals, Systems and Computers*, Pacific Grove, CA, USA, November 2014.

[Corr 2014d] J. Corr, K. Thompson, S. Weiss, J. McWhirter, and I. Proudler. Cyclic-by-row approximation of iterative polynomial EVD algorithms. In *Sensor Signal Processing for Defence*, pages 1–5, Edinburgh, Scotland, Sept. 2014.

[Corr 2015] J. Corr, K. Thompson, S. Weiss, I. Proudler, and J. McWhirter. Row-shift corrected truncation of paraunitary matrices for PEVD algorithms. Submitted to *European Signal Processing Conference*, Nice, France, September 2015.

[Dowell 2014a] J. Dowell, S. Weiss, D. Infield, and S. Chandna. A widely linear multi-channel Wiener filter for wind prediction. In *IEEE Workshop on Statistical Signal Processing*, pages 29–32, Gold Coast, Australia, June 2014.

[Redif 2015] S. Redif, S. Weiss, and J. McWhirter. Sequential matrix diagonalization algorithms for polynomial EVD of parahermitian matrices. *IEEE Transactions on Signal Processing*, 63(1):81–89, January 2015.

[Wang 2015] Z. Wang, J.G. McWhirter, J. Corr, and S. Weiss. Multiple shift second order sequential best rotation algorithm for polynomial matrix EVD. Submitted to *European Signal Processing Conference*, Nice, France, September 2015.

[Weiss 2013] S. Weiss, M. Alrmah, S. Lambbotharan, J. McWhirter, and M. Kaveh. Broadband angle of arrival estimation methods in a polynomial matrix decomposition framework. In *IEEE 5th International Workshop on Computational Advances in Multi-Sensor Adaptive Processing*, pages 109–112, Dec. 2013.

[Weiss 2015] S. Weiss, S. Bendoukha, A. Alzin, F. Coutts, I.K. Proudler, and J.A. Chambers. MVDR broadband beamforming using polynomial matrix techniques. Submitted to *European Signal Processing Conference*, Nice, France, September 2015.

Software Output:

[Weiss 2014] S. Weiss, J. Corr, K. Thompson, J.G. McWhirter, and I.K. Proudler: PEVD Toolbox. Published online at pevd-toolbox.eee.strath.ac.uk, last updated December 2014.

Related Output (without Dstl Clearance):

[Alrmah 2013a] M. Alrmah, S. Weiss, S. Redif, S. Lambbotharan, and J. McWhirter. Angle of arrival estimation for broadband signals: A comparison. In *IET Intelligent Signal Processing*, London, UK, December 2013.

[Alrmah 2013b] M. Alrmah and S. Weiss. Filter bank based fractional delay filter implementation for widely accurate broadband steering vectors. In *5th IEEE International Workshop on Computational Advances in Multi-Sensor Adaptive Processing*, Saint Martin, December 2013.

[Alrmah 2013c] M. Alrmah, S. Weiss, and J.G. McWhirter. Implementation of accurate broadband steering vectors for broadband angle of arrival estimation. In *IET Intelligent Signal Processing*, London, UK, December 2013.

[Corr 2014c] J. Corr, K. Thompson, S. Weiss, J. G. McWhirter, and I. K. Proudler. Causality-Constrained multiple shift sequential matrix diagonalisation for parahermitian matrices. In 22nd European Signal Processing Conference, pages 1277–1281, Lisbon, Portugal, September 2014.

[Dowell 2013] J. Dowell, S. Weiss, Short-term prediction using an ensemble of particle swarm optimised FIR filters, *IET Conference on Intelligent Signal Processing*, London, 2013.

[Dowell 2014b] J. Dowell, S. Weiss, D. Hill, and D. Infield. Short-term spatio-temporal prediction of wind speed and direction. *Wind Energy*, 17(12):1945–1955, December 2014.

[Dowell 2014c] J. Dowell, S. Weiss, and D. Infield. Spatio-temporal prediction of wind speed and direction by continuous directional regime. In *13th International Conference on Probabilistic Methods Applied to Power Systems*, Durham, UK, July 2014. (Best student paper award)

[Dowell 2015] J. Dowell, S. Weiss, D. Infield, Kernel Methods for Short-term Spatio-Temporal Wind Prediction. *IEEE PES General Meeting*, Denver, CO, 2015.

[Karagiannakis 2013a] P. Karagiannakis, K. Thompson, J. Corr, S. Weiss, and I. K. Proudler. Distributed processing of a fractal array beamformer. In *IET Intelligent Signal Processing*, London, UK, December 2013.

[Karagiannakis 2013b] P. Karagiannakis and S. Weiss. Analysis of a purina fractal beamformer. In *Asilomar Conference on Signals, Systems and Computers*, pages 466–470, November 2013.

[Karagiannakis 2013c] P. Karagiannakis, S. Weiss, G. Punzo, M. Macdonald, J. Bowman, and R. Stewart. Impact of a Purina fractal array geometry on beamforming performance and complexity. In *21st European Signal Processing Conference*, pages 1–5, Marrakech, Morocco, September 2013.

[McGuire 2013] C. McGuire and S. Weiss. Power-optimised multi-radio network under varying throughput constraints for rural broadband access. In *21st European Signal Processing Conference*, Marrakech, Morocco, September 2013.

[McGuire 2014] C. McGuire and S. Weiss. Multi-radio network optimisation using Bayesian belief propagation. In *22nd European Signal Processing Conference*, pages 421–425, Lisbon, Portugal, September 2014.

[Punzo 2014] G. Punzo, P. Karagiannakis, D. Bennet, M. Macdonald, and S. Weiss. Enabling and exploiting self-similar central symmetry formations. *IEEE Transaction on Aerospace and Electronic Systems*, 50(1):789–803, January 2014.

5.8. References

[Alrmah 2013a] M. Alrmah, S. Weiss, S. Redif, S. Lambotharan, and J. McWhirter. Angle of arrival estimation for broadband signals: A comparison. In *IET Intelligent Signal Processing*, London, UK, December 2013.

[Alrmah 2013b] M. Alrmah and S. Weiss. Filter bank based fractional delay filter implementation for widely accurate broadband steering vectors. In *5th IEEE International Workshop on Computational Advances in Multi-Sensor Adaptive Processing*, Saint Martin, December 2013.

[Alrmah 2013c] M. Alrmah, S. Weiss, and J.G. McWhirter. Implementation of accurate broadband steering vectors for broadband angle of arrival estimation. In *IET Intelligent Signal Processing*, London, UK, December 2013.

[Alrmah 2014] M. Alrmah, J. Corr, A. Alzin, K. Thompson, and S. Weiss. Polynomial subspace decomposition for broadband angle of arrival estimation. In *Sensor Signal Processing for Defence*, pages 1–5, Edinburgh, Scotland, Sept. 2014.

[Carotenuto 2014] V. Carotenuto, A. De Maio, C. Clemente, J. Soraghan. “Multi-Polarization SAR Change Detection with Invariant Decision Rules”. In IEEE Radar Conference 2014.

[Cetin 2006] M. Cetin, L. Chen, J.W. Fisher III, A.T. Ihler, R.L. Moses, M.J. Wainwright, and A.S. Willsky. “Distributed Fusion in Sensor Networks”, In IEEE Signal Processing Magazine, (Volume:23 ,Issue: 4), 2006.

[Corr 2014a] J. Corr, K. Thompson, S. Weiss, J. McWhirter, S. Redif, and I. Proudler. Multiple shift maximum element sequential matrix diagonalisation for parahermitian matrices. In *IEEE Workshop on Statistical Signal Processing*, pages 312–315, Gold Coast, Australia, June 2014.

[Corr 2014b] J. Corr, K. Thompson, S. Weiss, J.G. McWhirter, and I.K. Proudler. Maximum energy sequential matrix diagonalisation for parahermitian matrices. In *48th Asilomar Conference on Signals, Systems and Computers*, Pacific Grove, CA, USA, November 2014.

[Corr 2014c] J. Corr, K. Thompson, S. Weiss, J. G. McWhirter, and I. K. Proudler. Causality-Constrained multiple shift sequential matrix diagonalisation for parahermitian matrices. In 22nd European Signal Processing Conference, pages 1277–1281, Lisbon, Portugal, September 2014.

[Corr 2014d] J. Corr, K. Thompson, S. Weiss, J. McWhirter, and I. Proudler. Cyclic-by-row approximation of iterative polynomial EVD algorithms. In *Sensor Signal Processing for Defence*, pages 1–5, Edinburgh, Scotland, Sept. 2014.

[Corr 2015] J. Corr, K. Thompson, S. Weiss, I. Proudler, and J. McWhirter. Row-shift corrected truncation of paraunitary matrices for PEVD algorithms. Submitted to *European Signal Processing Conference*, Nice, France, September 2015.

[Dowell 2013] J. Dowell, S. Weiss, Short-term prediction using an ensemble of particle swarm optimised FIR filters, *IET Conference on Intelligent Signal Processing*, London, 2013.

[Dowell 2014a] J. Dowell, S. Weiss, D. Infield, and S. Chandna. A widely linear multi-channel Wiener filter for wind prediction. In *IEEE Workshop on Statistical Signal Processing*, pages 29–32, Gold Coast, Australia, June 2014.

[Dowell 2014b] J. Dowell, S. Weiss, D. Hill, and D. Infield. Short-term spatio-temporal prediction of wind speed and direction. *Wind Energy*, 17(12):1945–1955, December 2014.

- [Dowell 2014c] J. Dowell, S. Weiss, and D. Infield. Spatio-temporal prediction of wind speed and direction by continuous directional regime. In *13th International Conference on Probabilistic Methods Applied to Power Systems*, Durham, UK, July 2014. (Best student paper award)
- [Dowell 2015] J. Dowell, S. Weiss, D. Infield, Kernel Methods for Short-term Spatio-Temporal Wind Prediction. *IEEE PES General Meeting*, Denver, CO, 2015.
- [Elliot 2012] R. Elliot, M.A. Enderwitz, L.H. Crockett, S. Weiss, and R.W. Stewart. “Efficient TV White Space Filter Bank Transceiver”. In *20th European Signal Processing Conference*, Bucharest, Romania, September 2012.
- [Foster 2010] Foster JA, McWhirter J, Davies MR, Chambers JA, An algorithm for calculating the QR and singular value decompositions of polynomial matrices, *IEEE Transactions on Signal Processing* , 58(3):1263-1274, March 2010.
- [Karagiannakis 2013a] P. Karagiannakis, K. Thompson, J. Corr, S. Weiss, and I. K. Proudler. Distributed processing of a fractal array beamformer. In *IET Intelligent Signal Processing*, London, UK, December 2013.
- [Karagiannakis 2013b] P. Karagiannakis and S. Weiss. Analysis of a purina fractal beamformer. In *Asilomar Conference on Signals, Systems and Computers*, pages 466–470, November 2013.
- [Karagiannakis 2013c] P. Karagiannakis, S. Weiss, G. Punzo, M. Macdonald, J. Bowman, and R. Stewart. Impact of a Purina fractal array geometry on beamforming performance and complexity. In *21st European Signal Processing Conference*, pages 1–5, Marrakech, Morocco, September 2013.
- [Koller 2009] D. Koller and N. Friedman. “Probabilistic Graphical Models - Principles and Techniques”, MIT Press, 2009
- [McEliece 1998] R.J. McEliece, D.J.C. Mackay, and J-F. Cheng: “ Turbo Decoding as an Instance of Pearl’s ‘Belief Propagation’ Algorithm,” *IEEE Journal on Selected Areas in Communications*, 16(2):140-152, 1998.
- [McGuire 2013] C. McGuire and S. Weiss. Power-optimised multi-radio network under varying throughput constraints for rural broadband access. In *21st European Signal Processing Conference*, Marrakech, Morocco, September 2013.
- [McGuire 2014] C. McGuire and S. Weiss. Multi-radio network optimisation using Bayesian belief propagation. In *22nd European Signal Processing Conference*, pages 421–425, Lisbon, Portugal, September 2014.
- [McWhirter 2007] J.G. McWhirter, P.D. Baxter, T. Cooper, S. Redif, and J. Foster: “An EVD Algorithm for Para-Hermitian Polynomial Matrices,” *IEEE Transactions on Signal Processing*, 55(5):2158-2169, 2007.

[Proudler 2007] I.K. Proudler, S. Roberts, S. Reece, and I. Rezek: “An Iterative Signal Detection Algorithm Based on Bayesian Belief Propagation Ideas,” 15th International Conference on Signal Processing, 2007.

[Raynal 2013] M. Raynal. “Distributed Algorithms for Message-Passing Systems”, Springer-Verlag, 2013.

[Punzo 2014] G. Punzo, P. Karagiannakis, D. Bennet, M. Macdonald, and S. Weiss. Enabling and exploiting self-similar central symmetry formations. *IEEE Transaction on Aerospace and Electronic Systems*, 50(1):789–803, January 2014.

[Redif 2015] S. Redif, S. Weiss, and J. McWhirter. Sequential matrix diagonalization algorithms for polynomial EVD of parahermitian matrices. *IEEE Transactions on Signal Processing*, 63(1):81–89, January 2015.

[Üney 2014] M. Üney and M. Cetin. “Optimization of decentralized random field estimation networks under communication constraints through Monte Carlo methods”, In *Digital Signal Processing* 34, 16–28, 2014.

[Wang 2015] Z. Wang, J.G. McWhirter, J. Corr, and S. Weiss. Multiple shift second order sequential best rotation algorithm for polynomial matrix EVD. Submitted to *European Signal Processing Conference*, Nice, France, September 2015.

[Weiss 2013] S. Weiss, M. Alrmah, S. Lambotharan, J. McWhirter, and M. Kaveh. Broadband angle of arrival estimation methods in a polynomial matrix decomposition framework. In *IEEE 5th International Workshop on Computational Advances in Multi-Sensor Adaptive Processing*, pages 109–112, Dec. 2013.

[Weiss 2015] S. Weiss, S. Bendoukha, A. Alzin, F. Coutts, I.K. Proudler, and J.A. Chambers. MVDR broadband beamforming using polynomial matrix techniques. Submitted to *European Signal Processing Conference*, Nice, France, September 2015.